Current advances in the Chemical functionalization and Potential applications of Guar gum and its derivatives

Le, Trung-Anh; Huynh, Tan-Phat

Published in:
European Polymer Journal

DOI:
10.1016/j.eurpolymj.2023.111852

Published: 07/02/2023

Document Version
Final published version

European Polymer Journal 184 (2023) 111852

Contents lists available at ScienceDirect

European Polymer Journal

journal homepage: www.elsevier.com/locate/europolj

Current advances in the chemical functionalization and potential applications of guar gum and its derivatives

Trung-Anh Le *, Tan-Phat Huynh *

Laboratory of Molecular Sciences and Engineering, Åbo Akademi University, Henrikinkatu 2, 20500 Turku, Finland

ARTICLE INFO

Keywords:
Chemical functionalization
Cross-linking
Graft polymerization
Guar gum
Nucleophilic reaction
Partial oxidation

ABSTRACT

Guar gum (GG) from seeds of cluster bean *(Cyamopsis tetragonolobus)* contains mainly non-ionic galactomannan polysaccharide. Due to fascinating properties, great natural abundancy, low cost, biocompatibility and biodegradability, natural GG polysaccharide has been studied and employed in various research fields and industries. To explore and extend full potentials of GG, further chemical functionalization of the material is essential. This review highlights recent progress in the chemical modification of GG and its derivatives based on nucleophilic reactions, partial oxidation, graft polymerization and cross-linking with diverse chemical reagents and reaction pathways. Moreover, further insights into structure–property relationships as well as potential applications of the materials are also provided and discussed.

Abbreviations: AA, acrylic acid; $AA^{\bullet-}$, ascorbic acid radical anions; AAm, acrylamide; AAPBA, 3-acrylamidophenylboronic acid; AcOH, acetic acid; ACN, acetonitrile; Ag NPs, Ag nanoparticles; Ag NPs@MIL-100(Fe), Ag NPs dispersed in porous iron(III) carboxylate of MIL; AGA, 2-acrylamidoglycolic acid; AGG, acryloyl GG; AGU, anhydroglucose unit; Ala, L-alanine; Ala-cl-GG-g-PAA, Ala-cross-linked GG-g-PAA; AmB, amphotericin B; AMPS, 2-acrylamido-2-methyl-1-propane sulfonic acid; AN, acrylonitrile; APGG, 3-aminopropyl GG; APTES, (3-aminopropyl)triethoxysilane; APTMS, (3-aminopropyl)trimethoxysilane; ARX, arabinoxylan; ASA, 5-aminosalicylic acid; AX, amoxicillin; *B. subtilis*, *Bacillus subtilis*; $B(OH)_3$,H_3BO_3, boric acid; $[B(OH)_4]^-$, tetrahydroxyborate; $[B_4O_5(OH)_4]^{2-}$, hydrated tetraborate; BA, benzoic acid; BDO, 1,4-butanediol; BMBA, 4-(bromomethyl)benzoic acid; BNI-PGG, N-(propyl GG)-4-bromonaphthalimide; borax-cl-GG, borax-cross-linked GG; borax-cl-GG/Cur-Ag NPs, borax-cross-linked GG/Cur-Ag NPs; borax-cl-GG/MnO_2, borax-cl-GG/MnO_2 nanocomposite; borax-cl-GG-*N*-GO, borax-cross-linked GG-*N*-GO; borax-cl-GG-GelG, borax-cross-linked GG-GelG; borax-cl-GG-g-PAAm, borax-cross-linked GG-g-PAAm; borax-cl-GG-SAP, borax-cross-linked GG-SAP; borax, Fe^{3+}-cl-HPGG-PDA-rGO, borax, Fe^{3+}-cross-linked HPGG-PDA-rGO; boric acid-cl-HPGG, boric acid-cross-linked HPGG; BrB, bromophenol blue; *C. albicans*, *Candida albicans*; CA, citric acid; CA-cl-CMGG, CA-cross-linked CMGG; β-CD, β-cyclodextrin; β-CD/FU, β-CD/FU complex; CED, cephradine; $[Ce(NO_3)_6]^{2-}$, hexanitratocerate (IV); $[Ce^{IV}\text{-}O\text{-}Ce^{IV}]^{6+}$, oxo-bridged dinuclear cerium(IV) complexes; CGG, cationic GG; CHPTAC, N-(3-chloro-2-hydroxypropyl)-trimethyl ammonium chloride; ε-CL, ε-caprolactone; cl-DAGG, cross-linked-DAGG; cl-DAGG-CMCS, cross-linked DAGG-CMCS; cl-DAGG-CMCS/DOX, DOX-encapsulated cl-DAGG-CMCS; cl-DAGG-CS/PPE, cross-linked DAGG-CS/PPE; cl-DAGG-SF/Cur-zein NPs, cross-linked DAGG-SF/Cur-zein NPs; cl-DAGG-gelatin, cross-linked DAGG-gelatin; cl-DAGG-gelatin/GTE, GTE-encapsulated cl-DAGG-gelatin; cl-GG-MA-CS-g-PCL, cross-linked GG-MA-CS-g-PCL; cl-GG-MA-CS-g-PCL/rifampicin, rifampicin-encapsulated cl-GG-MA-CS-g-PCL; cl-OCGG-CS, cross-linked OCGG-CS; CMCS, carboxymethyl CS; CMGG, carboxymethyl GG; CNC, cellulose nanocrystal; CNC/Pd NPs, CNC/Pd NPs nanocomposite; -CO_2H, carboxylic acid; CPA, 3-chloropropylamine; CS, chitosan; CS_2, carbon disulfide; CS-g-PCL, poly(ε-caprolactone) grafted chitosan; CTAB, hexadecyl trimethyl ammonium bromide; CTAB-cl-CGG-g-P(AA-*co*-SMA), CTAB-cross-linked AA-*co*-SMA grafted CGG; $Cu(OAc)_2$, copper(II) acetate; CuS, copper sulfide covellite; Cur, curcumin; Cur-Ag NPs, Cur-stabilized Ag NPs; Cur-zein NPs, Cur-loaded zein nanoparticles; DA, dopamine; DAGG, dialdehyde GG; DBSA, dodecylbenzenesulfonic acid; DBTDL, dibutyltin dilaurate; DCC, N,N'-dicyclohexylcarbodiimide; DCGG, dicarboxylic acid GG; DCM, dichloromethane; DDSA, dodecenyl succinic anhydride; DFT, density functional theory; DLS, dynamic light scattering; DMAAm, N,*N*-dimethylacrylamide; DMAP, 4-dimethylaminopyridine; DMBA, 2,2-dimethylolbutyric acid; DMF, N,*N*-Dimethylformamide; DMSO, dimethyl sulfoxide; DOX, doxorubicin; DS, degree of substitution; *E. coli*, *Escherichia coli*; EA, ethyl acrylate; EC, ethyl cellulose; ECH, epichlorohydrin; ECH-cl-GG-P-CS/Fe_3O_4, ECH-cross-linked GG-P-CS/Fe_3O_4; EDC, 1-ethyl-3-(3-dimethylaminopropyl)carbodiimide; EGG, erucic guar gum; EPTAC, 2,3-epoxypropyltrimethylammonium chloride; ESR, electron spin resonance; Et_3N, triethylamine; EtOH, ethanol; Eu, eudragit L30D; Eu-coated-HDGG/AmB, Eu-coated AmB-encapsulated HDGG; Eu-coated-HDGG/AmB/Pip, Eu-coated AmB and Pip-encapsulated HDGG; FA, Folic acid; FA-GG, FA-conjugated GG; FA-GG-SA, FA-GG-succinic acid; FDA, food and drug administration; Fe^0, zero-valent iron; Fe^{2+}-cl-DCGG, Fe^{2+}-cross-linked DCGG; Fe_3O_4 NPs, iron oxide nanoparticles; FFR, furfural; FITC, fluorescein isothiocyanate; FITC-SiO_2@Au-LCME, fluorescein isothiocyanate-SiO_2 core-Au shell-L-cysteine methyl ester; FRGP, free-radical graft polymerization; FU, 5-fluorouracil; GA, glutaraldehyde; GA-cl-GG-RDA-PVA, GA-cross-linked GG-RDA-PVA; GA-cl-GG-RDA-PVA/AX, AX-encapsulated GA-cl-GG-RDA-PVA; GA-cl-GG-RDA-PVA/GS, GS-encapsulated GA-cl-GG-RDA-PVA.

* Corresponding authors.
E-mail addresses: trle@abo.fi (T.-A. Le), tan.huynh@abo.fi (T.-P. Huynh).

https://doi.org/10.1016/j.eurpolymj.2023.111852
Received 7 December 2022; Accepted 20 January 2023
Available online 27 January 2023

1. Introduction

Recently, dramatic climate changes have reached to the critical point globally and drastic actions are urgently demanded. To overcome these challenges, holistic effort and strategies have been considered such as reducing greenhouse gases [1,2], preventing pollution in different forms [3,4], replacing fossil fuels by renewable fuels [5,6], practicing more sustainable and productive agriculture [7,8], etc. Since natural photosynthesis can utilize solar energy and reduce carbon dioxide green-house gas in the atmosphere to produce useful polysaccharide products, promoting the use of polysaccharides as materials, food and medicine has been one of the most sustainable approaches to cope with climate changes and to ensure sustainable human activities.

Over the years, great attention has been drawn to novel materials research of guar gum (GG) in various fields (Fig. 1), due to GG's natural abundancy, low cost, biocompatibility, biodegradability, and accessible

; GA-cl-GG-IA-keratin, GA-cross-linked GG-IA-keratin; GA, Fe^{3+}-cl-GG/SAL/DA-STMS/GA, GA, Fe^{3+}-cross-linked GG/SAL/DA-STMS/GA; Gal, galactose; GE, grafting efficiency; GelG, gellan gum; GG, guar gum; GG-APSi, GG-(3-aminopropyl)silane; GG-APSi-FFR, GG-APSi-furfural; GG-APSi-FFR-Pd, GG-APSi-FFR-Pd2+; GG-APSi-SAAL, GG-APSi-salicylaldehyde; GG-APSi-SAAL-Cu, GG-APSi-SAAL-Cu2+; GG-BA, GG-benzoic acid; GG-C, GG cinnamate; GG-C-N, GG-C nanoparticles; GG-g-LPEI, LPEI grafted GG; GG-g-LPEI/pDNA, GG-g-LPEI/pDNA coacervate; GG-GMA, glycidyl methacrylate guar gum; GG-GMA-g-P(AA-*co*-DMAAm), AA-*co*-DMAAm grafted GG-GMA; GG-GMA-g-P(AA-*co*-DMAAm)/HCS, HCS-encapsulated GG-GMA-g-P(AA-*co*-DMAAm); GG-g-PAA, acrylic acid grafted guar gum; GG-g-PAAm, AAm grafted GG; GG-g-PAGA, AGA grafted GG; GG-g-PCL, PCL grafted GG; GG-g-PEA, EA grafted GG; GG-g-PHEMA, HEMA grafted GG; GG-g-PHEMA/ASA, ASA-encapsulated GG-g-PHEMA; GGH, GG hydrolysate; GGH-DDSA, GGH-dodecenyl succinic acid; GGH-OSA, GGH-*n*-octenyl succinic acid; GGH-S-L, GGH-sulfonic acid by Larm method; GGH-S-O, GGH-sulfonic acid by O'Neill method; GG-IA, GG indole acetate; GG-MA, GG-maleic acid; GG-N, aminated GG-NH_2; GG-O-Sn(C≡CPh)$_3$, alkoxy-tin(IV) of GG; GG-P, GG-phosphonic acid; GG-PU, GG-based polyurethanes; GG-RDA, GG-ricinoleic dimer acid; GG-SL, guar gum-soya lecithin; GG-S-L, GG-sulfonic acid by Larm method; GG-S-O, GG-sulfonic acid by O'Neill method; GG-X, GG xanthate; GG-X/CuS, GG-X/CuS nanocomposite; GH, galacylhydrazine; glyoxal-cl-GG/activated C, glyoxal-cross-linked GG/activated C; GMA, glycidyl methacrylate; GMS, gentamicin sulphate; GO, graphene oxide; GS, gentamicin sulfate; GTE, green tea extract; GTMAC, glycidyltrimethylammonium chloride; GY, grafting yield; h, hour; H^+, proton; H_2AA, ascorbic acid; HCS, hydrocortisone; HDGG, 6-O-(3-hexadecyloxy-2-hydroxypropyl)-GG; HDGG/AmB, AmB-encapsulated HDGG; HDGG/AmB/Pip, AmB and Pip-encapsulated HDGG; HEK-293, human embryonic kidney 293; HEMA, 2-hydroxyl ethyl methacrylate; ^1H NMR, proton nuclear magnetic resonance; $HO^•$, hydroxyl radicals; HOMO, highest occupied molecular orbital; HOS, human osteosarcoma; HPGG, hydroxypropyl GG; $HSO_3^•$, S-centered bisulfite free radicals; HSO_3^-, bisulfite; HSO_4^-, bisulfate; HTPB, hydroxyl-terminated polybutadiene; hydrazine-cl-DAGG-MBAAm-cl-P(AA-*co*-MMA), hydrazine-cross-linked DAGG-MBAAm-cl-P(AA-*co*-MMA); I2959, Irgacure 2959; IO_4^-, periodate; IPA, isopropyl alcohol; IPDI, isophorone diisocyanate; *K. pneumonia*, *Klebsiella pneumonia*; $K_2S_2O_8$ or KPS, potassium persulfate; KSPA, potassium 3-sulfopropyl acrylate; LCME, L-cysteine methyl ester; LGG, linoleic guar gum; LiCl, lithium chloride; LPEI, low-molecular-weight polyethylenimine; LUMO, lowest unoccupied molecular orbital; MA, maleic anhydride; Man, mannose; MB, methylene blue; MBAAm, N,N'-methylenebisacrylamide; MBAAm-cl-AGG-g-P(AA-*co*-KSPA), MBAAm-cross-linked AA-*co*-KSPA grafted AGG; MBAAm-cl-AGG-g-P(AA-*co*-KSPA)/GMS, GMS-encapsulated MBAAm-cl-AGG-g-P(AA-*co*-KSPA); MBAAm-cl-CMGG-g-PAA, MBAAm-cross-linked AA grafted CMGG; MBAAm-cl-CMGG-g-P(AA-*co*-AAm), MBAAm-cross-linked AA-*co*-AAm grafted CMGG; MBAAm-cl-CMGG-g-PAAm, MBAAm-cross-linked AAm grafted CMGG; MBAAm-cl-CMGG-g-PAAm/*meta*-BPDM, *meta*-BPDM-embedded MBAAm-cl-CMGG-g-PAAm; MBAAm-cl-GG-g-PAA, MBAAm-cross-linked GG-g-PAA; MBAAm-cl-GG-g-PAA/Ag NPs, MBAAm-cl-GG-g-PAA/Ag NPs nanocomposite; MBAAm-cl-GG-g-P(AA-*co*-AAm), MBAAm-cross-linked AA-*co*-AAm grafted GG; MBAAm-cl-GG-g-P(AA-*co*-AN), MBAAm-cross-linked AA-*co*-AN grafted GG; MBAAm-cl-GG-g-P(AA-*co*-AN)/TQ, TQ-encapsulated MBAAm-cl-GG-g-P(AA-*co*-AN); MBAAm-cl-GG-g-P(AA-*co*-NIPAAm), MBAAm-cross-linked AA-*co*-NIPAAm grafted GG; MBAAm-cl-GG-g-P(AA-*co*-NIPAAm-*co*-NIPAAmPA), MBAAm-cross-linked AA-*co*-NIPAAm-*co*-NIPAAmPA grafted GG; MBAAm-cl-GG-g-P(AAm-*co*-AMPS), MBAAm-cross-linked AAm-*co*-AMPS grafted GG; MBAAm-cl-GG-g-P(AAm-*co*-AGA)/Ag NPs, MBAAm-cross-linked AAm-*co*-AGA grafted GG/Ag NPs nanocomposite; MBAAm-cl-GG-g-PAMPS, MBAAm-cross-linked AMPS grafted GG; MBAAm-cl-P(AA-*co*-MMA), MBAAm cross-linked copolymer of acrylic acid and methyl methacrylate; MBAAm-cl-GG-SL/Fe^0, MBAAm-cross-linked GG-SL/Fe^0; MBAAm-cl-GG/SLS-g-PAA, MBAAm-cross-linked AA grafted GG/SLS; MBAAm, Fe^{3+}-cl-CMGG-g-PAA, MBAAm, Fe^{3+}-cross-linked CMGG-g-PAA; MCA, monochloroacetic acid; MDCK, Madin-Darby canine kidney; MeO, methyl orange; MeOH, methanol; *meta*-BPDM, *meta*-benziporphodimethene; MG, malachite green; MGG, methylated GG; MGG/nanoclays, MGG/nanoclays nanocomposite; MIL, Materials of Institute Lavoisier; MnO_2, manganese dioxide; MnO_4^-, permanganate(VII); MnO_4^{2-}, manganate(VI); MS, degree of molar substitution; MW, microwave; $NaBH_4$, sodium borohydride; $NaBH_4$-cl-GG-g-PAGA/Ag NPs, $NaBH_4$-cross-linked GG-g-PAGA/Ag NPs; $NaBH_4$-cl-GG/CNC/Pd NPs, $NaBH_4$-cross-linked GG/CNC/Pd NPs nanocomposite; $NaBH_4$-cl-GG-PVA/Ag NPs, $NaBH_4$-cross-linked GG-PVA/Ag NPs; $NaBO_2$, sodium metaborate; $Na_2B_4O_7$, anhydrous sodium tetraborate; $Na_2B_4O_7{\cdot}5H_2O$, sodium tetraborate pentahydrate; $Na_2B_4O_7{\cdot}10H_2O$ or $Na_2[B_4O_5(OH)_4]{\cdot}8H_2O$, sodium tetraborate decahydrate; NaBr, sodium bromide; $NaClO_2$, sodium chlorite; $NaIO_4$, sodium periodate; NaOCl, sodium hypochlorite; NaOH, sodium hydroxide; $Na_2S_2O_8$ or SPS, sodium persulfate; NBA, 4-bromo-1,8-naphthalic anhydride; -NCO, isocyanate; NHS, *N*-hydroxysuccinimide; -NH_2, amino; NH_2-C_2H_4-NH_2, ethylenediamine; $(NH_4)_2[Ce(NO_3)_6]$ or CAN, ceric(IV) ammonium nitrate; $(NH_4)_2S_2O_8$ or APS, ammonium persulfate; NIPAAm, *N*-isopropylacrylamide; NIPAAmPA, 3-(*N*-isopropylacrylamido) propanoic acid; NTP, non-thermal plasma; OCGG, oxidized CGG; OGG, oxidized guar gum; -OH, hydroxyl; OH-, hydroxide; OlGG, oleic guar gum; O/N, overnight; O-O, peroxide bond; OSA, *n*-octenyl succinic anhydride; PAA, poly(acrylic acid); P(AA-*co*-AN), poly(AA-*co*-acrylonitrile); PAAm, polyacrylamide; *P. aeruginosa*, *Pseudomonas aeruginosa*; PBA, phenylboronic acid; PBA-cl-HPGG-g-P(AAm-*co*-AAPBA), PBA-cross-linked AAm-*co*-AAPBA grafted HPGG; PBS, phosphate-buffered saline; PCL, poly(ε-caprolactone); PCLD, poly(ε-caprolactone) diol; PDA, polydopamine; PDA-rGO, polydopamine-coated reduced graphene oxide; PDA-STMS/GA, PDA-coated GA-loaded STMS; PDI, polydispersity index; pDNA, EGFP-N1 plasmid DNA; Pd NPs, Pd nanoparticles; PEG, polyethylene glycol; PHGG, partially hydrolyzed GG; Pip, piperine; PO, propylene oxide; P_2O_5, phosphorus pentoxide; $POCl_3$, phosphorus oxychloride; PPE, pomegranate peel extract; PVA, polyvinyl alcohol; PVP, polyvinylpyrrolidone; py, pyridine; QGG, quaternized GG; RB19, reactive blue 19; RDA, ricinoleic dimer acid; RhB, rhodamine B; ROP, ring-opening polymerization; rt, room temperature; s, second; SA, succinic acid; SAAL, salicylaldehyde; *S. aureus*, *Staphylococcus aureus*; SAP, self-assembly peptide; SAL, sodium alginate; SBS, sodium bisulfite; SF, silk fibroin; SGP, step-growth polymerization; SH, salicylhydrazine; SIF, simulated intestinal fluid; SiO_2, silicon dioxide; SiO_2@Au, SiO_2 core-Au shell; SL, soya lecithin; SLS, sodium lignosulfonate; SMA, stearyl methacrylate; S_N, nucleophilic substitution; S_N2, bimolecular nucleophilic substitution; Sn(C≡CPh)$_4$ or SnAK, tetra(phenylethynyl)tin; SO_3, sulfur trioxide; $SO_3^{•-}$, S-centered sulfite radical anions; $SO_4^{•-}$, sulfate radical anions; SO_4^{2-}, sulfate; $SO_5^{•-}$, peroxymonosulfate radical anions; $S_2O_5^{•-}$, S-centered metabisulfite radical anions; $S_2O_5^{2-}$, metabisulfite; $S_2O_8^{2-}$, peroxydisulfate or persulfate; SSD, silver sulfadiazine; STMP, sodium trimetaphosphate; STMP-cl-GG/orange oil, STMP-cross-linked orange oil-incorporated GG/orange oil; STMS, stellate mesoporous silica; STPP, sodium tripolyphosphate; TBHP, *tert*-butyl hydroperoxide; TEGDA, tetra(ethyleneglycol)diacrylate; TEGDA-cl-GG-g-PAAm, TEGDA-cross-linked GG-g-PAAm; TEMPO, 2,2,6,6-tetramethylpiperidine-1-oxyl radical; TEMPO+, 2,2,6,6-tetramethylpiperidine-1-oxoammonium; TEMPOH, 1-Hydroxy-2,2,6,6-tetramethylpiperidine; TEOS, tetraethyl orthosilicate; TEOS-cl-CMGG-CS, TEOS-cross-linked CMGG-CS; TEOS-cl-CMGG-CS@, NTP-treated TEOS-cross-linked CMGG-CS; TEOS-cl-CMGG-CS@Ar, Ar NTP-treated TEOS-cross-linked CMGG-CS; TEOS-cl-CMGG-CS@O_2, O_2 NTP-treated TEOS-cross-linked CMGG-CS; TEOS-cl-CMGG-CS@O_2+Ar, O_2 and Ar NTP-treated TEOS-cross-linked CMGG-CS; TEOS-cl-CMGG-PVA, TEOS-cross-linked CMGG-PVA; TEOS-cl-CMGG-PVA@/chrysin, chrysin-encapsulated NTP-treated TEOS-cl-CMGG-PVA; TEOS-cl-GG-ARX, TEOS-cross-linked GG-ARX; TEOS-cl-GG-ARX/SSD, SSD-encapsulated TEOS-cl-GG-ARX; TEOS-cl-GG-CS-PEG/CED, TEOS-cross-linked CED-encapsulated GG-CS-PEG/CED; TEOS-cl-GG-CS-PVA, TEOS-cross-linked GG-CS-PVA; TEOS-cl-GG-CS-PVA/paracetamol, paracetamol-loaded TEOS-cl-GG-CS-PVA; TEOS-cl-GG-g-PNIPAAm, TEOS-cross-linked NIPAAm grafted GG; TEOS-cl-GG-g-PNIPAAm/β-CD/FU, β-CD/FU-loaded TEOS-cl-GG-g-PNIPAAm; THF, tetrahydrofuran; TMEDA or TEMED, N,N,N',N'-tetramethylethylenediamine; TNBC, triple negative breast cancer; TOC, total organic carbon; TQ, thymoquinone; TsOH, tosylic acid; UO_2^{2+}, uranyl ions; v/v, volume by volume; wt%, weight percentage; w/v, weight by volume; w/w, weight by weight; Zr^{4+}-cl-HPGG, Zr^{4+}-cross-linked HPGG.

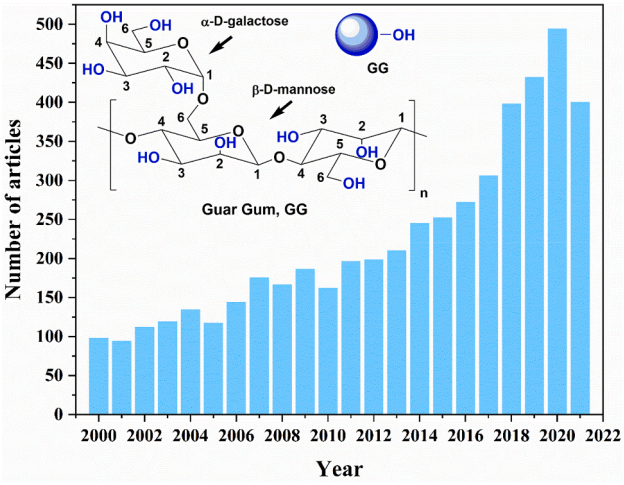

Fig. 1. Published articles per year based on "guar gum" keyword from Web of Science search engine on June 5, 2022 and chemical structure of GG repeating unit.

chemical synthetic techniques [9–21]. GG is obtained naturally from seeds of cluster bean *(Cyamopsis tetragonolobus)*. Endosperm of guar seed contains more than 80 % of non-ionic galactomannan polysaccharide, as well as some amount of water, protein, ash, and fat [22]. GG has been widely used as stabilizers for soil treatment,[23–25] concrete additives [26], corrosion inhibitors in metal protection [27,28], promoters for tetrahydrofuran (THF) hydrate formation [29], inhibitors for methane hydrate formation [30,31], precursors in carbon dot synthesis and single-atom catalysts [32,33], binders for Li-ion batteries [34–36], electrolytes in zinc-ion batteries [37,38], perovskite-based zinc-air batteries [39], and dye-sensitized solar cells [40], biomaterials in food industry [41–47], bio-ink in 3D printing [48], as well as components in photocatalysts [49–51], wound dressing, healing and drug delivery [52–60]. Besides numerous fascinating properties of pristine GG, in order to extend its applicability and overcome remaining limitations, namely, uncontrollable swelling, susceptibility to bacterial contamination and rapid biodegradation, etc. further studies on chemical modification of GG are highly motivated [10].

Herein, latest approaches in the chemical functionalization and potential applications of GG and its derivatives are discussed and highlighted. Even though polymer blending offers great simplicity to modify properties of materials including GG [61–63], this approach, however, is not covered in detail here since direct chemical modifications of GG are rarely performed. In addition, partial hydrolysis of native GG can also be carried out to depolymerize the polysaccharide chain, hence, decreasing the molecular weight and viscosity of GG [64,65]. In this review, chemical modifications on partially hydrolyzed GG (PHGG) or GG hydrolysate (GGH) are also covered and treated equivalently to GG due to their similar repeating units in the polymer structure.

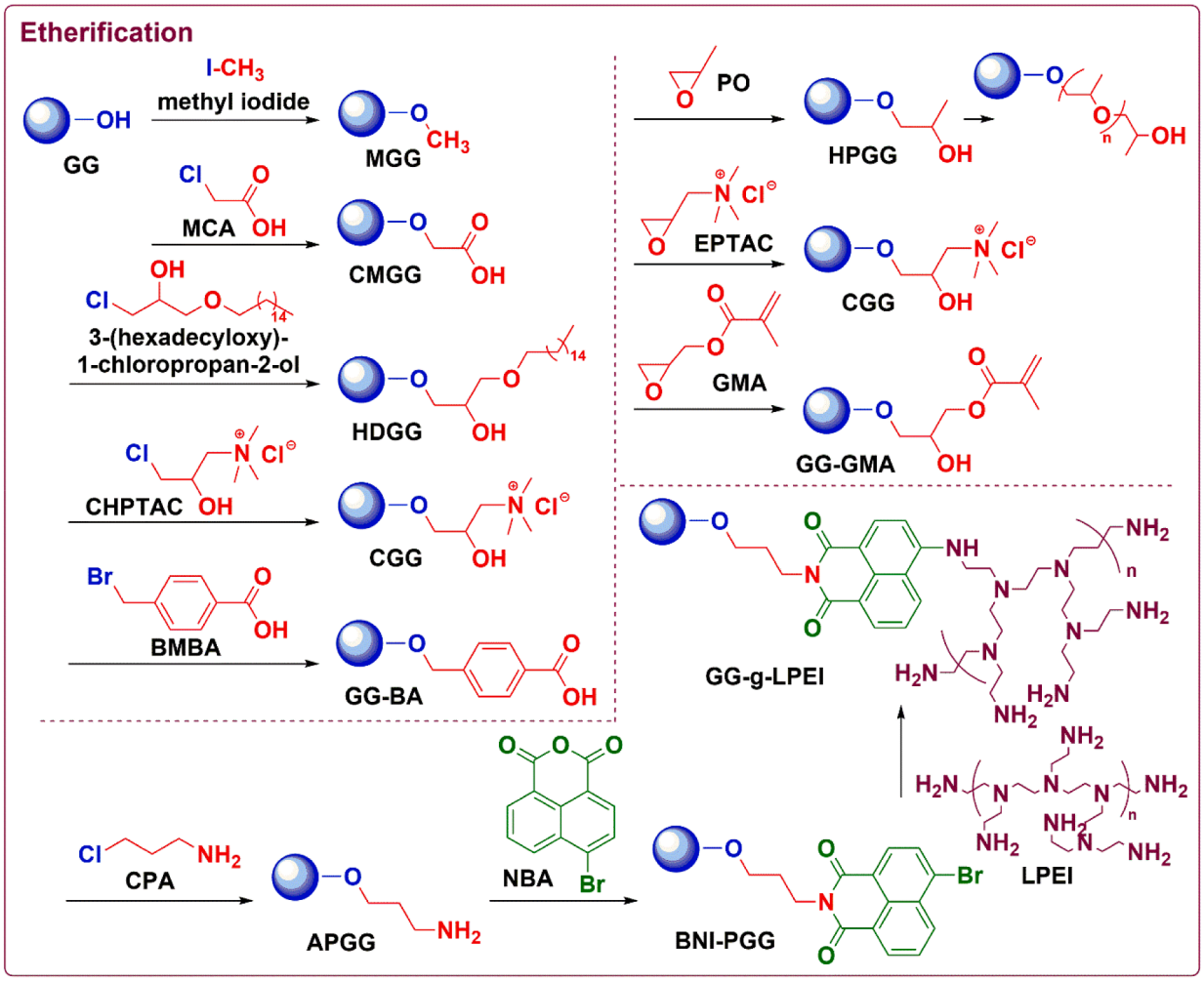

Fig. 2. Etherification of GG by different alkylating agents.

Table 1
Reaction conditions for graft polymerization of GG and its derivatives.

Entry	Reaction condition								Product			Ref.
	Polymer	Monomer	Cross-linker	Initiator	Atm[a]	Solvent	T [°C]	t[b]	Abbreviation	GE	GY [%]	
Acrylic acid (AA) monomer												
54	GG	AA	Ala	APS	N_2	H_2O	rt	15 *m*	Ala-cl-GG-g-PAA	N/A	N/A	[256]
55	GG	AA	MBAAm	APS	N/A	H_2O	30	N/A	MBAAm-cl-GG-g-PAA	N/A	N/A	[258]
56	GG	AA	MBAAm	APS	N_2	H_2O	60–70	3 h	MBAAm-cl-GG-g-PAA	N/A	N/A	[259]
57	GG	AA	None	APS	N/A	H_2O	50	N/A	GG-g-PAA	N/A	N/A	[260]
58	GG, SLS	AA	MBAAm	APS	N/A	H_2O	60–80	1 h	MBAAm-cl-GG/SLS-g-PAA	N/A	N/A	[261]
59	GG	AA, AN	MBAAm	MW	N/A	H_2O	N/A	90 s	MBAAm-cl-GG-g-P(AA-*co*-AN)	N/A	50–86.6	[262]
60	GG	AA, AAm	MBAAm	APS	N_2	H_2O	68–70	3–4 h	MBAAm-cl-GG-g-P(AA-*co*-AAm)	N/A	N/A	[263]
61	GG	AA, AAm	None	MW	N/A	H_2O	N/A	120 s	GG-g-P(AA-*co*-AAm)	N/A	N/A	[264]
62	GG	AA, NIPAAm	MBAAm	KPS, SBS	amb	H_2O	25	34 *m*	MBAAm-cl-GG-g-P(AA-*co*-NIPAAm), MBAAm-cl-GG-g-P(AA-*co*-NIPAAm-*co*-NIPAAmPA)	N/A	76	[265]
2	CMGG	AA and/or AAm	MBAAm	KPS	N/A	H_2O	60–65	2.5 h	MBAAm-cl-CMGG-g-PAA, MBAAm-cl-CMGG-g-PAAm, MBAAm-cl-CMGG-g-P(AA-*co*-AAm)	N/A	N/A	[82]
4	CMGG	AA	MBAAm, Fe^{3+}	KPS, TEMED	N_2	H_2O	50	12 h	MBAAm, Fe^{3+}-cl-CMGG-g-PAA	N/A	N/A	[84]
15	CGG	AA, SMA	CTAB	APS	inert	H_2O	60	7 h	CTAB-cl-CGG-g-P(AA-*co*-SMA)	N/A	N/A	[121]
20	GG-GMA	AA	DMAAm	SPS	N/A	H_2O	50, rt	30 *m*	GG-GMA-g-P(AA-*co*-DMAAm)	N/A	N/A	[132]
29	AGG	AA, KSPA	MBAAm	APS	N/A	H_2O	60	3 h	MBAAm-cl-AGG-g-P(AA-*co*-KSPA)	N/A	N/A	[150]
Acrylamide (AAm) monomer												
63	GG	AAm	TEGDA	KPS	N_2	H_2O	65	4 h	TEGDA-cl-GG-g-PAAm	N/A	91	[269]
64	GG	AAm	Borax	CAN, MW	N/A	H_2O	N/A	30 s × 3	borax-cl-GG-g-PAAm	79.5	795.6	[270]
65	GG	AAm, AMPS	MBAAm	KPS	N_2	H_2O	70	3 h	MBAAm-cl-GG-g-P(AAm-*co*-AMPS)	N/A	N/A	[271]
66	GG	AAm, AGA	MBAAm	APS	N/A	H_2O	60	10 *m*	MBAAm-cl-GG-g-P(AAm-*co*-AGA)	N/A	N/A	[272]
3	CMGG	AAm	MBAAm	KPS	N/A	H_2O, acetone	60	N/A	MBAAm-cl-CMGG-g-PAAm	N/A	N/A	[83]
9	HPGG	AAm	AAPBA	I2959 (UV at 360 nm)	N/A	H_2O	rt	3 h	PBA-cl-HPGG-g-P(AAm-*co*-AAPBA)	N/A	N/A	[97]
Other monomers												
67	GG	NIPAAm	TEOS	APS, TEMED	N_2	H_2O	rt	N/A	TEOS-cl-GG-g-PNIPAAm	N/A	N/A	[273]
68	GG	AGA	$NaBH_4$	APS	N_2	H_2O	60	2 h	$NaBH_4$-cl-GG-g-PAGA	N/A	N/A	[274]
69	GG	AMPS	MBAAm	KPS	N_2	H_2O	70	3 h	MBAAm-cl-GG-g-PAMPS	N/A	N/A	[276]
70	GG	EA	None	KPS, H_2AA	N/A	H_2O	35	1 h	GG-g-PEA	N/A	N/A	[277]
71	GG	HEMA	None	CAN, MW	amb	H_2O		40 s × 3	GG-g-PHEMA	114.22	1142	[278]

[a] Atm: atmosphere, amb: ambient, N/A: not available.
[b] m: minute.

2. Chemical structure and properties of GG

Galactomannan polysaccharide of GG is composed of mannose (Man) backbones and galactose (Gal) side chains with an average Man: Gal ratio varying between 1.8:1 and 2:1. Natural GG exhibits a significantly high molecular weight, which can be found up to millions of Da [66]. While Man moieties are linked via β-1,4-glycosidc bonds to establish the polymer backbone, Gal side chains are connected to the Man backbones by α-1,6-glycosidic bonds (insert of Fig. 1). Due to the unique structure of galactomannan chain and numerous remaining hydroxyl (-OH) functional groups, hydrophilic GG has high solubility even in cold water even though it is least hygroscopic among different types of gums [67–69]. Moreover, because of the rich chemistry of these -OH functional groups, further chemical functionalization and derivatization of original GG can be easily performed [70–72]. On an average, each GG monomer contains three anhydroglucose units (AGU), while each AGU contains approximately three -OH groups, and therefore, the degree of derivatization or substitution (DS) for each AGU might be up to three. Additionally, the nucleophilicity of these -OH groups vary, i.e., less bulky primary -OH groups are more nucleophilic than secondary -OH groups [73].

3. Chemical functionalization and potential applications of GG and its derivatives

3.1. Nucleophilic reactions

3.1.1. Etherification (GG-O-)

Etherification is one of the most common synthetic routes to chemically modify GG due to its synthetic simplicity. Typically, GG is activated in N_2-purged alkaline solutions, followed by an addition of electrophilic alkylating agents to carry out nucleophilic substitution (S_N) reactions. A summary of reported etherification reactions on GG can be found in Fig. 2 and Table 2.

3.1.1.1. Carboxymethyl GG (CMGG) and its derivatives. Carboxymethylation of GG has been reported via S_N of GG with monochloroacetic acid (MCA) or sodium chloroacetate in aqueous solutions [70,74], lithium chloride/dimethylsulfoxide (LiCl/DMSO) solvent system [75], or using dry method.[76] Carboxymethyl GG (CMGG) products can be found as valuable starting materials to develop novel hydrogels and coacervates for drug delivery [77–80].

In the recent past, Dalei et al. reported a similar procedure for the carboxymethylation of GG using MCA in a solvent mixture of isopropyl

Table 2
Reaction conditions for chemical modifications of GG and its derivatives.

Entry	Reaction	Reaction condition						Product			Ref.
		Reactant	Catalyst	Atm	Solvent	T [°C]	t	Abbreviation	DS	Yield [%]	
Nucleophilic reactions											
Etherfication											
Carboxymethyl GG (CMGG) and its derivatives											
1	Carboxymethylation	(1) GG, NaOH	None	N/A	IPA, H_2O	rt	2 h	CMGG	N/A	N/A	[81]
		(2) MCA	None	N/A	IPA, H_2O	60	8 h		N/A	N/A	
	Cross-linking	CMGG, CS, TEOS	None	N/A	H_2O	rt	brief	TEOS-cl-CMGG-CS	–	N/A	
	NTP treatment	CMGG-TEOS-cl-CS, O_2 and/or Ar	None	0.5 mbar	None	N/A	30 s	TEOS-cl-CMGG-CS@O_2, TEOS-cl-CMGG-CS@Ar, TEOS-cl-CMGG-CS@O_2 + Ar	–	N/A	
	Drug encapsulation	CMGG-TEOS-cl-CS or CMGG-TEOS-cl-CS@, diclofenac sodium	None	N/A (dark)	EtOH	N/A	48 h	–	–	N/A	
2	Carboxymethylation	(1) GG, NaOH	None	inert	H_2O	rt	15 *m*	CMGG	N/A	N/A	[82]
		(2) MCA	None	inert	H_2O	50	4 h		N/A	N/A	
	FRGP and cross-linking	(1) CMGG, NaOH, AA and/or AAm, KPS	None	N/A	H_2O	60	30 *m*	MBAAm-cl-CMGG-g-PAA, MBAAm-cl-CMGG-g-PAAm, MBAAm-cl-CMGG-g-P(AA-*co*-AAm)	–	N/A	
		(2) MBAAm	None	N/A	H_2O	65	2 h		–	N/A	
3	FRGP and cross-linking	CMGG, AAm, MBAAm, *meta*-BPDM, KPS	None	N/A	H_2O, acetone	60	N/A	MBAAm-cl-CMGG-g-PAAm/*meta*-BPDM	–	N/A	[83]
4	FRGP and cross-linking	CMGG, AA, MBAAm, $FeCl_3{\cdot}6H_2O$, KPS, TEMED	None	N_2	H_2O	50	12 h	MBAAm, Fe^{3+}-cl-CMGG-g-PAA	–	N/A	[84]
5	Cross-linking	CMGG, CA	None	N/A	None	140	5 *m*	CA-cl-CMGG	–	N/A	[85]
6	Cross-linking	CMGG, PVA, TEOS	None	N/A	H_2O	N/A	brief	TEOS-cl-CMGG-PVA	–	N/A	[86]
	NTP treatment	TEOS-cl-CMGG-PVA, N_2 or N_2 + NH_3	None	0.5 mbar	None	N/A	30 s	TEOS-cl-CMGG-PVA@N_2, TEOS-cl-CMGG-PVA@N_2 + NH_3	–	N/A	
	Drug encapsulation	TEOS-cl-CMGG-PVA@, chrysin	None	N/A	EtOH	37	24 h	TEOS-cl-CMGG-PVA@/chrysin	–	N/A	
Hydroxypropyl GG (HPGG) and its derivatives											
7	Hydroxypropylation	(1) GG, NaOH	None	N_2	H_2O	rt	0.5 h	HPGG		N/A	[95]
		(2) PO	None	N_2	H_2O	rt	0–30 h		0–1.2[c]		
	Cross-linking	(1) HPGG, $Na_2S_2O_3$, Na_2CO_3	None	N/A	H_2O	25	N/A	boric acid-cl-HPGG, Zr^{4+}-cl-HPGG	–	N/A	
		(2) H_3BO_3 or sodium zirconium lactate	None	N/A	H_2O	25	N/A				
8	Hydroxypropylation	(1) GG, NaOH	None	N/A	H_2O	25	15 *m*	HDGG	N/A	N/A	[96]
		(2) 3-(hexadecyloxy)-1-chloropropan-2-ol (THF)	None	N/A	H_2O, THF	50	24 h		N/A	N/A	
	Drug encapsulation	HDGG, AmB (DMSO)	None	N/A (dark)	H_2O, DMSO	25	16 h	HDGG/AmB	–	92	
	Drug encapsulation	HDGG, AmB, Pip (DMSO)	None	N/A (dark)	H_2O, DMSO	25	16 h	HDGG/AmB/Pip	–	54	
	Drug encapsulation and coating	HDGG, AmB (DMSO), Eu	None	N/A (dark)	H_2O, DMSO	25	16 h	Eu-coated-HDGG/AmB	–	87	
	Drug encapsulation and coating	HDGG, AmB, Pip (DMSO), Eu	None	N/A (dark)	H_2O, DMSO	25	16 h	Eu-coated-HDGG/AmB/Pip	–	80	
9	FRGP and cross-linking	HPGG, AAm, AAPBA	I2959 (UV at 360 nm)	N/A	H_2O	rt	3 h	PBA-cl-HPGG-g-P(AAm-*co*-AAPBA)	–	N/A	[97]

(*continued on next page*)

Table 2 (*continued*)

Entry	Reaction	Reaction condition						Product			Ref.
		Reactant	Catalyst	Atm	Solvent	T [° C]	t	Abbreviation	DS	Yield [%]	
10	Cross-linking	(1) HPGG, PDA-rGO, $FeCl_3{\cdot}6H_2O$	None	N/A	H_2O, glycerol	rt	N/A	borax, Fe^{3+}-cl-HPGG-PDA-rGO	–	N/A	[98]
		(2) borax	None	N/A	H_2O	45	N/A		–	N/A	
Methylated GG (MGG) and its derivatives											
11	Methylation	GG, NaOH, CH_3I	None	N_2	H_2O	25	2.5	MGG	0.4	94	[100]
12	Methylation	GG, NaOH, CH_3I	None	N_2	H_2O	25	2.5	MGG	0.4	94	[101]
	Nanocomposite	MGG, nanoclays, glycerol	None	N/A	H_2O	N/A	O/N	MGG/nanoclays	–	N/A	
Cationic GG (CGG) and its derivatives											
13	Quaternization	(1) GG, NaOH	None	N/A	H_2O, EtOH	N/A	N/A	CGG	0.158	N/A	[118]
		(2) EPTAC	None	N/A	H_2O, EtOH	55	3 h				
14	Quaternization	(1) GG, NaOH	None	N/A	H_2O, MeOH	rt	15 *m*	CGG	0.49	N/A	[119]
		(2)CHPTAC	None	N/A	H_2O, MeOH	30	2 h				
15	FRGP and cross-linking	CGG, AA, SMA, CTAB, APS	None	inert	H_2O	60	7 h	CTAB-cl-CGG-g-P(AA-*co*-SMA)	–	N/A	[121]
16	Partial oxidation and cross-linking	CGG, CS, $NaIO_4$	None	N/A (dark)	H_2O	rt	24 h	cl-OCGG-CS	–	N/A	[122]
17	Quaternization	GG, CHPTAC, NaOH	None	N/A	H_2O	50	3 h	CGG	0.21	N/A	[123]
	Partial oxidation	CGG, $NaIO_4$	None	N/A (dark)	H_2O	rt	24 h	OCGG	4.8[d]	N/A	
	Cross-linking	OCGG, CMCS	None	N/A	H_2O	rt	N/A	cl-OCGG-CMCS		N/A	
Other GG derivatives											
18	Nucleophilic substitution	(1) GG, NaOH	None	N/A	H_2O, IPA	50	1 h	APGG	N/A	N/A	[130]
		(2) CPA(IPA)	None	N/A	H_2O, IPA	50	4.5 h				
	Condensation	APGG, NBA	None	N_2	DMSO	80	3 h	BNI-PGG	N/A	N/A	
	Nucleophilic substitution	BNI-PGG, LPEI	None	N_2	H_2O	80	3 h	GG-g-LPEI	42.9–56.6 % [e]	N/A	
	Complex coacervation	GG-g-LPEI (acetate buffer), pDNA (sodium sulfate solution)	None	N/A	H_2O	55	10 *m*	GG-g-LPEI/ pDNA		N/A	
19	Nucleophilic substitution	(1) GG, NaOH	None	N_2	H_2O	rt	30 *m*	GG-BA	0.164	83.1	[131]
		(2) 4-(bromomethyl) benzoic acid	None	N_2	H_2O	rt	O/N				
20	Nucleophilic substitution	GG, NaOH, GMA	None	N/A	H_2O	60	24 h	GG-GMA	N/A	N/A	[132]
	FRGP and cross-linking	GG-GMA, sodium acrylate, DMAAm, SPS	None	N/A	H_2O	50, rt	30 *m*	GG-GMA-g-P(AA-*co*-DMAAm)	N/A	N/A	
	Drug loading	GG-GMA-g-P(AA-*co*-DMAAm), HCS	None	N/A	H_2O	rt	20 h	GG-GMA-g-P(AA-*co*-DMAAm)/HCS	–	N/A	
Esterification											
21	Esterification (microwave)	GG, DA, NaOH, DBSA	TsOH	N/A	None (Solvent free)	N/A	N/A	GG-RDA	N/A	N/A	[136,137]
	Cross-linking and drug loading	GG-RDA, PVA, GA, glycerol, GS or AX	HCl	N/A	H_2O	60	5 h	GA-cl-GG-RDA-PVA/GS or AX	–	N/A	
22	Steglich esterification	GG, FA, DCC	DMAP	N/A (dark)	DMSO	rt	48 h	FA-GG	N/A	N/A	[138]
	Esterification	FA-GG, succinic anhydride	DMAP	N/A	H_2O	rt	24 h	FA-GG-SA	N/A	N/A	
	Condensation	(1) FITC-SiO_2@Au, LCME	None	N/A	DMSO	rt	12 h	FA-GG-SA-FITC-SiO_2@Au-DOX	N/A	N/A	
		(2) FA-GG-SA, EDC	NHS	N/A	DMSO	rt	12 h				
		(3) hydrazine	None	N/A	DMSO	rt	3 h				
		(4) DOX	None	N/A	DMSO	rt	24 h				
23	Esterification	GGH, DDSA	$NaHCO_3$	N/A	H_2O, EtOH	45	2 h	GGH-DDSA	0.029	N/A	[140]
	Esterification	GGH, OSA	$NaHCO_3$	N/A	H_2O, EtOH	85	2 h	GGH-OSA	0.07	N/A	
24	Esterification	GG, MA	Et_3N	N/A	DCM	40	3–4 h	GG-MA	N/A	N/A	[141]
25	Esterification	GG, MA	DMAP	N/A	ACN	25	12 h	GG-MA	N/A	N/A	[142]

(*continued on next page*)

Table 2 (*continued*)

Entry	Reaction	Reaction condition						Product			Ref.
		Reactant	Catalyst	Atm	Solvent	T [° C]	t	Abbreviation	DS	Yield [%]	
	aza-Michael addition	GG-MA, CS-g-PCL	None	N/A	H_2O	60	24 h	cl-GG-MA-CS-g-PCL	N/A	N/A	
	Drug encapsulation	(1) GG-MA/CS-g-PCL, rifampicin	None	N/A	H_2O, DMSO	rt	30 *m*	cl-GG-MA-CS-g-PCL/ rifampicin	–	N/A	
		(2) ultrasonication	None	N/A	H_2O, DMSO	~ 0	5 *m*				
26	Esterification	GG, oleic/ linoleic/ erucic acyl chlorides, NaOH	None	N/A	acetone	50	12 h	OGG, LGG, EGG	0.01–0.08	90.2–94.4	[143]
27	Esterification	GG, cinnamoyl chloride	DMAP	N_2	LiCl/ DMSO	30	4 h	GG-C	0.79–1.40	N/A	[144]
	Ouzo nanoprecipitation (nanonization)	GG-C (DMSO)	None	N/A	H_2O, DMSO	rt	30 h	GG-C-N	–	N/A	
28	Esterification	GG, 2-(1H-indol-3-yl)acetyl chloride	DMAP	N_2	LiCl/ DMSO	30	3 h	GG-IA	0.61	N/A	[149]
	Cross-linking and solvent-casting	GG-IA, keratin, GA, glycerol	None	inert	H_2O	42	18 h	GA-cl-GG-IA-keratin	–	N/A	
29	Esterification	(1) GG, NaOH	None	N/A	H_2O	N/A	N/A	AGG	N/A	N/A	[150]
		(2)acryloyl chloride	None	N/A	N/A	ice	N/A				
	FRGP and cross-linking	AGG, AA, KSPA, MBAAm, APS	None	N/A	H_2O	60	3 h	MBAAm-cl-AGG-g-P(AA-*co*-KSPA)	–	N/A	
	Drug loading	MBAAm-cl-AGG-g-P(AA-*co*-KSPA), GMS	None	N/A	H_2O	37	8 h	MBAAm-cl-AGG-g-P(AA-*co*-KSPA)/GMS	–	N/A	
Xanthation											
30	Xanthation	(1) GG, NaOH	None	N_2	H_2O	rt	30 *m*	GG-X	0.132	87.23	[161]
		(2)CS_2	None	N_2	H_2O	rt	2.5 h				
	Surfactant-assisted precipitation	GG-X, $CuCl_2$, Na_2S	None	N_2	H_2O	85	2 h	GG-X/CuS	–	N/A	
Silanization/ Silylation											
31	Silylation	GG, APTES	None	N/A	toluene	100	48 h	GG-APS	N/A	N/A	[169]
	Schiff-base condensation	GG-APS, FFR	None	N/A	MeOH	reflux	72 h	GG-APS-FFR	N/A	N/A	
	Metal complexation	GG-APS-FFR, Na_2PdCl_4	None	N/A	H_2O	rt	5 h	GG-APS-FFR-Pd	–	N/A	
32	Silylation	GG, APTMS	None	N_2	H_2O	100	24 h	GG-APS	N/A	N/A	[170]
	Schiff-base condensation	GG-APS, SA	None	N_2	EtOH	80	24 h	GG-APS-SA	N/A	N/A	
	Metal complexation	GG-APS-SA, Cu $(OAc)_2$	None	N/A	EtOH	80	24 h	GG-APS-SA-Cu	–	N/A	
Phosphorylation											
33	Phosphorylation, metal dispersion and cross-linking	GG, SL, DCC, Fe (0), MBAAm	None	N/A	$CHCl_3$	60	3 h	MBAAm-cl-GG-SL/Fe^0	N/A	78	[178]
34	Phosphorylation	(1) GG, urea	None	N/A	DMF	110	1 h	GG-P	N/A	95	[180]
		(2) H_3PO_4	None	N/A	DMF	150	3 h				
	Cross-linking	(1) GG-P, CS, Fe_3O_4	None	N/A	H_2O	50	1 h	ECH-cl-GG-P-CS/Fe_3O_4	–	N/A	
		(2) ECH(dioxane)	None	N/A	H_2O, 1,4-dioxane	60	3 h				
Sulfation											
35	Sulfation (O'Neill method)	GG or GGH, py, chlorosulfonic acid	None	N/A	HCHO	0 40	1 h 6 h	GG-S-O, GGH-S-O	1.26, 1.21	N/A	[184]
	Sulfation (Larm method)	GG or GGH, SO_3·py	None	N/A	DMF	25	6 h	GG-S-L, GGH-S-L	0.38, 1.91	N/A	
36	Sulfation	GG, chlorosulfonic acid	None	N/A	1,4-dioxane	60	2.9 h	GG-S	0.91	N/A	[185]
37	Sulfation	GG, urea, sulfamic acid	None	N/A	1,4-dioxane	80	3 h	GG-S	0.78	N/A	[186]
Amination											
38	Amination	(1) GG, ethylenediamine	None	N/A	H_2O	rt	O/N	GG-N	N/A	N/A	[190]
		(2) HCl	None	N/A	H_2O	rt	30 *m*				
	Cross-linking	GG-N, GO, borax	None	N/A	H_2O	rt	3 h	borax-cl-GG-*N*-GO	–	N/A	
Partial oxidation											
TEMPO-mediated oxidation											

(*continued on next page*)

Table 2 (*continued*)

Entry	Reaction	Reaction condition						Product			Ref.
		Reactant	Catalyst	Atm	Solvent	T [° C]	t	Abbreviation	DS	Yield [%]	
39	TEMPO oxidation	GG, NaOCl	NaBr, TEMPO	N_2	H_2O	3	N/A	OGG	1.2[d]	71	[199]
40	Enzymatic TEMPO oxidation and self-cross-linking	GG, O_2	Laccase, TEMPO	N/A	H_2O	35 rt	3 h 24 h	OGG	N/A	N/A	[200]
Periodate-mediated oxidation											
41	Periodate oxidation and self-cross-linking	GG, $NaIO_4$	None	N/A	H_2O	N/A	N/A	cl-DAGG	N/A	N/A	[208]
42	Periodate oxidation, self-cross-linking and nanocomposite	GG, Ag NPs@MIL-100(Fe), $NaIO_4$	None	N/A	H_2O	rt	N/A	cl-DAGG/Ag NPs@MIL-100 (Fe)	N/A	N/A	[209]
43	Periodate oxidation	GG, $NaIO_4$	None	N/A (dark)	H_2O	rt	6 h	DAGG	78 %	N/A	[210]
	Cross-linking and incorporation	DAGG, gelatin, GTE, ethylene glycol	None	N/A	H_2O	40 rt	45 *m* 24 h	cl-DAGG-gelatin/GTE	–	N/A	
44	Periodate oxidation	GG, $NaIO_4$	None	N/A (dark)	H_2O	rt	6 h	DAGG	72 %	N/A	[211]
	Cross-linking and incorporation	DAGG, CS, PPE	None	N/A	H_2O	rt	24 h	cl-DAGG-CS/PPE	–	N/A	
45	Periodate oxidation	GG, $NaIO_4$	None	N/A (dark)	H_2O	25	24 h	DAGG	56.3 %	N/A	[212]
	Cross-linking	DAGG, CMCS	None	N/A	H_2O	37	30 *m*	cl-DAGG-CMCS	–	N/A	
	Drug loading	cl-DAGG-CMCS, DOX	None	N/A	H_2O	N/A	48 h	cl-DAGG-CMCS/DOX	–	N/A	
46	Periodate oxidation	GG, $NaIO_4$	None	N/A (dark)	H_2O	N/A	2 h	DAGG	N/A	N/A	[213]
	Cross-linking and drug loading	DAGG, Cur-zein NPs, SF	None	N/A	H_2O	N/A	N/A	cl-DAGG-SF/Cur-zein NPs	–	N/A	
47	Periodate oxidation	GG, $NaIO_4$	None	N/A	H_2O	40	4 h	DAGG	N/A	N/A	[218]
	Schiff-base condensation	DAGG, GH	None	N/A	EtOH	45	72 h	DAGG-GH	N/A	N/A	
48	Schiff-base condensation	DAGG, SH	TsOH	N/A	EtOH	45	72 h	DAGG-SH	N/A	N/A	[219]
49	Periodate oxidation	GG, $NaIO_4$	None	N/A (dark)	H_2O	40	8 h	DAGG	67.6 %	N/A	[220]
	Nucleophilic acyl substitution	MBAAm-cl-P(AA-*co*-MMA), hydrazine·H_2O	None	N/A	H_2O	80	3 h	MBAAm-cl-P(AA-*co*-MMASH)	N/A	N/A	
	Cross-linking	DAGG, MBAAm-cl-P(AA-*co*-MMASH)	AcOH	N/A	EtOH	85	4 h	hydrazine-cl-DAGG MBAAm-cl-P(AA-*co*-MMA)	–	N/A	
50	Periodate oxidation	GG, $NaIO_4$	None	N/A (dark)	H_2O	40	24 h	DAGG	0.59–1.79[d] (30.12–60.63 %)	77.5	[221]
	Chlorite oxidation	DAGG, $NaClO_2$	AcOH	N/A	H_2O	30	48 h	DCGG	0.49–1.62[d]	82	
	Cross-linking	DCGG, $FeSO_4$,	None	N_2	H_2O	30	24 h	Fe^{2+}-cl-DCGG	None	64	
Graft polymerization											
51	SGP	GG, HTPB, IPDI, BDO	DBTDL	N_2	None	90	N/A	GG-PU	–	N/A	[225]
52	SGP	(1) PCLD, DMBA, IPDI	None	N_2	None	80	2 h	GG-PU	–	N/A	[226]
		(2) GG, TEA	None	N_2	None	80	1 h				
		(3) BD	None	N_2	None	80	1 h				
53	ROP	GG, ε-cL	SnAK	amb	None	rt 120	2 h 15–20 *m*	GG-g-PCL	–	92–94 %	[232,233]
54	FRGP	GG, AA, Ala, APS	None	N_2	H_2O	rt	15 *m*	Ala-cl-GG-g-PAA	–	N/A	[256]
	Drug loading	GG-g-PAA, levofloxacin (PBS)	None	N/A	H_2O	N/A	2 h	Ala-cl-GG-g-PAA/levofloxacin	–	65–75 %	
55	FRGP	GG, AA, MBAAm, APS	None	N/A	H_2O	30	N/A	MBAAm-cl-GG-g-PAA	–	N/A	[258]
	Drug loading	MBAAm-cl-GG-g-PAA, vitamin B6	None	N/A	H_2O	37	48 h	MBAAm-cl-GG-g-PAA/vitamin B6	–	94 %	
57	FRGP	GG, AA, APS	None	N/A	H_2O	50	N/A	GG-g-PAA	–	N/A	[260]
	Nanocomposite	GG-g-PAA, $AgNO_3$, $NaBH_4$, MBAAm	None	N/A	H_2O	N/A	10 *m*	MBAAm-cl-GG-g-PAA/Ag NPs	–	N/A	

(*continued on next page*)

Table 2 (*continued*)

Entry	Reaction	Reaction condition						Product			Ref.
		Reactant	Catalyst	Atm	Solvent	T [° C]	t	Abbreviation	DS	Yield [%]	
59	FRGP	GG, AA, AN, MBAAm, MW	None	N/A	H_2O	N/A	90 s	MBAAm-cl-GG-g-P(AA-*co*-AN)	–	50–86.6 %	[262]
	Drug encapsulation	MBAAm-cl-GG-g-P(AA-*co*-AN), TQ	None	N/A	H_2O	25	60 *m*	MBAAm-cl-GG-g-P(AA-*co*-AN)/TQ	–	N/A	
66	FRGP	GG, AAm, AGA, MBAAm, APS	None	N/A	H_2O	60	10 *m*	MBAAm-cl-GG-g-P(AAm-*co*-AGA)	–	N/A	[272]
	Incorporation	(1) MBAAm-cl-GG-g-P(AAm-*co*-AGA), $AgNO_3$	None	N/A	H_2O	25	24 h	MBAAm-cl-GG-g-P(AAm-*co*-AGA)/Ag NPs	–	N/A	
		(2) rhubarb extract	None	N/A (dark)	H_2O	25	12 h				
67	Hot-guess complexation	(1) β-CD, FU (1:1)	None	N/A	H_2O	N/A	24 h	β-CD/FU	–	N/A	[273]
		(2) freeze-drying	None	N/A	N/A	−55	48 h				
	FRGP, cross-linking and drug loading	(1) GG, NIPAAm, APS, TEMED	None	N_2	H_2O	rt	N/A	TEOS-cl-GG-g-PNIPAAm-FU or TEOS-cl-GG-g-PNIPAAm-β-CD/FU	–	N/A	
		(2) TEOS	None	N_2	H_2O	rt	24 h				
		(3) FU or β-CD/FU	None	N_2	H_2O	rt	brief				
68	FRGP	GG, AGA, APS	None	N_2	H_2O	60	2 h	GG-g-PAGA	–	N/A	[274]
	Nanocomposite and cross-linking	GG-g-PAGA, $AgNO_3$, $NaBH_4$	None	N/A	H_2O	N/A	N/A	$NaBH_4$-cl-GG-g-PAGA/Ag NPs	–	N/A	
71	FRGP	GG, HEMA, CAN (MW)	None	N/A	H_2O	N/A	40 s × 3	GG-g-PHEMA	–	N/A	[278]
	Drug loading	(1) GG-g-PHEMA, PVP, ASA	None	N/A	EtOH	50	N/A	GG-g-PHEMA/ASA	–	N/A	
		(2) magnesium stearate, SiO_2	None	N/A	None	N/A	N/A				
Cross-linking											
B-O-											
72	Cross-linking	GG, peptide, borax	None	N/A	H_2O	rt	15 *m*	borax-cl-GG-SAP	–	N/A	[288]
73	Cross-linking	GG, GelG, borax	None	N/A	H_2O	80	1 h	borax-cl-GG-GelG	–	N/A	[289]
74	Cross-linking	GG, borax	None	N/A	H_2O	rt	4.5 h	borax-cl-GG	–	N/A	[290]
	Nanocomposite	$KMnO_4$, NaOH, borax-cl-GG	None	N/A	H_2O	rt	O/N	borax-cl-GG/MnO_2	–	N/A	
75	Nanocomposite	CNC, $PdCl_2$, $NaBH_4$	None	N/A	H_2O	rt	2 h	CNC/Pd NPs	–	N/A	[291]
	Cross-linking	GG, CNC/Pd, $NaBH_4$	None	N/A	H_2O	N/A	N/A	$NaBH_4$-cl-GG/CNC/Pd NPs	–	N/A	
76	Nanocomposite	Cur (DMSO), K_2CO_3, $AgNO_3$	None	N/A	H_2O	100	1 h	Cur-Ag NPs	–	N/A	[292]
	Cross-linking	GG, Cur-Ag NPs, NaOH, borax	None	N/A	H_2O	N/A	N/A	borax-cl-GG/Cur-Ag NPs	–	N/A	
77	Cross-linking	GG, PVA, $AgNO_3$, $NaBH_4$	None	N/A	H_2O	rt	48 h	$NaBH_4$-cl-GG-PVA/Ag NPs	–	N/A	[293]
C-O-											
78	Coprecipitation	(1) $FeCl_3$, $FeCl_2$, NH_3	None	N_2	H_2O	70	15 *m*	Fe_3O_4 NPs	–	N/A	[295]
		(2) CA	None	N_2	H_2O	70	1 h				
	Cross-linking	GG, Fe_3O_4 NPs, GA, NaOH	None	N_2	IPA	60	3 h	GA-cl-GG/Fe_3O_4 NPs	–	N/A	
79	Encapsulation	(1) STMS, GA	None	N/A	EtOH	rt	48 h	PDA-STMS/GA	–	N/A	[296]
		(2) DA·HCl, Tris·HCl	None	N/A	EtOH	rt	36 h				
	Cross-linking and nanocomposite	PDA-STMS/GA, Fe^{3+}, GG, SAL	None	N/A	H_2O	rt	2 h	GA, Fe^{3+}-cl-GG/SAL/DA-STMS/GA	–	N/A	
80	Cross-linking and nanocomposite	GG, activated C, glyoxal	None	N/A	H_2O	60	24 h	glyoxal-cl-GG/activated C	–	N/A	[297]
Si-O-											
81	Drug loading and cross-linking	GG, CS, PEG, CED, TEOS	None	N/A	H_2O	60	2 h	TEOS-cl-GG-CS-PEG/CED	–	N/A	[298]
82	Drug loading and cross-linking	GG, ARX, SSD (MeOH), TEOS	None	N/A	H_2O	60	3 h	TEOS-cl-GG-ARX/SSD	–	N/A	[299]

(*continued on next page*)

Table 2 (*continued*)

Entry	Reaction	Reaction condition						Product			Ref.
		Reactant	Catalyst	Atm	Solvent	T [° C]	t	Abbreviation	DS	Yield [%]	
83	Drug loading and cross-linking	GG, CS, PVA, paracetamol, TEOS	None	N/A	H_2O	55	3 h	TEOS-cl-GG-CS-PVA/ paracetamol	–	N/A	[300]
P-O-84	Cross-linking	GG, SL, glycerol, orange oil, NaOH, STMP	None	N/A	H_2O	N/A	2 h	STMP-cl-GG/ orange oil	–	N/A	[301]

[c] degree of molar substitution (MS).
[d] mmol g^{-1}.
[e] degree of amination.

alcohol (IPA) and water [81]. The obtained CMGG product was then cross-linked with chitosan (CS) using tetraethyl orthosilicate (TEOS) to give TEOS-cl-CMGG-CS hydrogels. Due to the presence of carboxylic acid (-CO_2H) and amino (-NH_2) functional groups from CMGG and CS respectively, TEOS-cl-CMGG-CS hydrogels are responsive to a wide range of pH values, which plays an important role in swelling and drug delivery properties of hydrogels. Further surface modification of the hydrogels was then performed in a direct current glow discharge plasma reactor, using Ar, O_2 or a mixture of Ar and O_2 gases. The non-thermal plasma (NTP)-treated TEOS-cl-CMGG-CS (TEOS-cl-CMGG-CS@) hydrogels show a significant decrease in contact angles with water, hence, a significant increase in wettability of the hydrogel surface. The TEOS-cl-CMGG-CS@ hydrogels are promising candidates for the delivery of diclofenac sodium non-steroidal anti-inflammatory medication to human colon. They also possess good biocompatibility to human blood cells, as well as excellent biodegradability.

In order to study surface topography, roughness and swelling properties of CMGG by atomic force microscopy, Hasan and coworkers also used MCA in an aqueous alkaline solution to modify GG (see Table 1) [82]. Free-radical graft polymerization (FRGP) was then employed on CMGG with pH-responsive acrylic acid (AA) and/or thermo-responsive acrylamide (AAm) monomers, potassium persulfate (KPS) free-radical initiator, N,N'-methylenebis(acrylamide) (MBAAm) cross-linker to prepare MBAAm-cross-linked AA grafted CMGG (MBAAm-cl-CMGG-g-PAA), MBAAm-cross-linked AAm grafted CMGG (MBAAm-cl-CMGG-g-PAAm) and MBAAm-cross-linked AA-*co*-AAm grafted CMGG [MBAAm-cl-CMGG-g-P(AA-*co*-AAm)] hydrogels.

In addition, FRGP of CMGG with AAm monomer and MBAAm cross-linker was reported by Chauhan et al. to fabricate a hydrophilic polymeric platform with embedded hydrophobic *meta*-benziporphodimethene (*meta*-BPDM), namely, MBAAm-cl-CMGG-g-PAAm/*meta*-BPDM [83]. The newly fabricated hydrogel can be employed in colorimetric sensing of aqueous d^{10}-metal ions such as Zn^{2+}, Cd^{2+} and Hg^{2+}. Upon the exposure to these ions, metal complexation with embedded *meta*-BPDM in the hydrogel allows a color change from red to blue-green, while no color change is observed with other interfering alkali, alkaline and transition metal ions such as Na^{+}, K^{+}, Ca^{2+}, Mg^{2+}, Cr^{3+}, Fe^{3+}, Fe^{2+}, Mn^{2+}, Co^{2+}, Ni^{2+}, Cu^{2+} and Pb^{2+}.

Moreover, CMGG-based hydrogels can be prepared by combining FRGP of AA monomers and Fe^{3+} cross-linking process in an aqueous solution of CMGG as reported by Chen and coworkers [84]. N,N,N',N'-tetramethylethylenediamine (TMEDA or TEMED) was chosen to initiate KPS for the grafting reaction. The obtained MBAAm, Fe^{3+}-cross-linked CMGG-g-PAA (MBAAm, Fe^{3+}-cl-CMGG-g-PAA) hydrogels possess dynamic, reversible hydrogen bonding and coordinate covalent bonding between -CO_2H groups from CMGG and PAA, resulting in strong, stretchable and self-healing ionic conductive hydrogels. These hydrogels can also be fabricated into strain sensors to monitor human body motions e.g. joint bending, swallowing and speaking, with great sensitivity and repeatability.

Citric acid (CA) was chosen by Orsu and Matta to cross-link CMGG at high temperature through several continuous steps of forming cyclic carboxylic acid anhydride, followed by esterification reactions with remaining -OH groups on CMGG [85]. The prepared CA-cross-linked CMGG (CA-cl-CMGG) scaffold films show good hemocompatibility to human blood and great potential for wound healing and drug release of ciprofloxacin up to 60 % over 60 min under physiological pH and temperature.

Dalei et al. incorporated pH-responsive CMGG and polyvinyl alcohol (PVA) due to its good capacity in forming films, stability towards pH and temperature [86]. The two polymers were cross-linked by TEOS to obtain TEOS-cross-linked CMGG-PVA (TEOS-cl-CMGG-PVA) hydrogels with good mechanical integrity and pH-responsivity. Surface properties of the TEOS-cl-CMGG-PVA hydrogels such as wettability, energy, topography were of great interest to enhance their biocompatibility. NTP modification was also carried out using N_2 or a mixture of N_2 and NH_3 to improve surface wettability and to induce topographical changes of hydrogels. NTP-treated TEOS-cl-CMGG-PVA (TEOS-cl-CMGG-PVA@) hydrogels show good antibacterial activity against *Escherichia coli* (*E. coli*), hemocompatibility, biodegradability, as well as great potential for the delivery of chrysin (5,7-dihydroxyflavone) as a natural anticancer bioflavonoid to colon.

3.1.1.2. Hydroxypropyl GG (HPGG) and its derivatives. Over the years, hydroxypropyl GG (HPGG) has been well-known as a more hydrophobic derivative of native GG [87]. HPGG and its similar compounds can be found in fracturing fluids [88–90], fragile surface cleaning [91], stabilization of fly ash suspensions [92], as a binder in lithium-ion batteries [93], detection of NH_3 [94], etc.

In order to modify the hydrophilicity, water dissolution and temperature resistance of native GG, Gao and Grady recently studied in detail the kinetics of hydroxypropylation of GG in aqueous solution [95]. After the activation of GG by sodium hydroxide (NaOH), propylene oxide (PO) was used to carry out nucleophilic reaction in a polymerization reaction manner to obtain oligomeric PO chains linked to GG. Under the chosen reaction conditions, the reaction was found to be first and zeroth order with respect to the concentration of GG and PO respectively. Proton nuclear magnetic resonance (^{1}H NMR) was employed to quantify the amount of PO repeating units on GG. However, because different oligomeric chains of PO units might be attached onto each AGU of GG, the degree of molar substitution (MS) based on the average number of moles was reported instead. The reported MS values of HPGG vary from 0 to 1.2, depending on the reaction time. In addition, boric acid (H_3BO_3) and Zr^{4+} ions were used to create boric acid-cross-linked HPGG and Zr^{4+}-cross-linked HPGG (boric acid-cl-HPGG and Zr^{4+}-cl-HPGG respectively) to get viscoelastic gels. Rheological studies

suggest that Zr^{4+} ions can provide much better cross-linking than borates in the same concentration range between 20 and 200 ppm at pH above 9.5.

To further explore the drug delivery behavior of HPGG, Ray et al. employed the hydroxypropylation of GG using 3-(hexadecyloxy)-1-chloropropan-2-ol electrophiles to prepare a new derivative of GG, namely 6-O-(3-hexadecyloxy-2-hydroxypropyl)-GG (HDGG) [96]. HDGG was used to encapsulate polyene antibiotic amphotericin B (AmB) and piperine (Pip) due to their potential antileishmanial activity and ability to enhance the bioavailability of various drugs respectively. In addition, the encapsulated HDGG nanoparticles were also coated with eudragit L30D (Eu) for oral medication administration. In vitro and in vivo studies of the final nanoparticle products were performed to show good controlled drug release at the designated organs, great drug bioavailability, antileishmanial activity and non-nephrotoxic nature.

From HPGG starting material, Lu et al. recently reported a novel FRGP of GG using AAm, 3-acrylamidophenylboronic acid (AAPBA) monomers and Irgacure 2959 (I2959) photo-initiator [97]. The AAPBA monomers offer both double bonds for copolymerization and boric acid moieties for cross-linking with remaining hydroxyl groups on HPGG via phenylboronic acid (PBA)-diol ester bonds. These ester bonds are responsive to pH changes and therefore, acid-base chemistry can be employed to tune mechanical properties of the self-healing PBA-cross-linked AAm-*co*-AAPBA grafted HPGG [PBA-cl-HPGG-g-P(AAm-*co*-AAPBA)] hydrogel products. Rheological results indicate a significant improvement in mechanical behaviors of the hydrogels when pH varies from acidic to neutral and alkaline conditions (4.00, 7.00, 8.15 and 9.00).

Besides taking advantage of hydrogen bonding and boron-based cross-linkers, Sun and coworkers also explored the mussel-inspired chemistry of catechol and Fe^{3+} to form hydrogels between HPGG and polydopamine-coated reduced graphene oxide (PDA-rGO) [98]. The obtained borax, Fe^{3+}-cross-linked HPGG-PDA-rGO (borax, Fe^{3+}-cl-HPGG-PDA-rGO) hydrogels possess numerous dynamic, reversible and pH-sensitive cross-linkers between hydroxyl groups on HPGG and catechol groups from PDA-rGO through boron and Fe^{3+}, resulting in good self-healing and mechanical properties. While PDA-rGO offers more flexibility and electrical conductivity to the hydrogel, glycerol also enhances the freeze resistance and moisture retention of the material. Borax, Fe^{3+}-cl-HPGG-PDA-rGO hydrogels might be employed to fabricate flexible sensors, which can detect different types of human motion over a wide temperature range (-20 to 30 °C) with good stability and repeatability.

3.1.1.3. Methylated GG (MGG) and its derivatives. Methylation of GG can be carried out to decrease the hydrophilicity of GG, hence, enhancing barrier and mechanical properties, as well as sealability against humidity of GG-based biodegradable films [99].

Recently, Tripathi et al. carried out the methylation of GG using methyl iodide in an aqueous solution of NaOH to yield methylated GG (MGG) [100]. The obtained product shows improvements in crystallinity, hydrophobicity, thermal stability, mechanical and barrier properties to water vapor transmission, hence, the MGG product can be used as biodegradable food packaging films. In addition, the mechanical and barrier properties against humidity transmission can be further enhanced by incorporating nanoclays, e.g. inorganic bentonite nanofil 116 and organically modified bentonite cloisite 20A, into MGG to create nanocomposite films [101]. Beneficial effects of these nanoclays were observed as the concentration of nanoclays increased up to 20 % w/w, while no significant change in the opacity of the nanocomposite films was reported.

3.1.1.4. Quaternized/ cationic GG (QGG/CGG) and its derivatives. The introduction of quaternary ammonium groups (quaternization) to GG is one of the most common approaches to obtain cationic GG (CGG) [102]. In the past, nucleophilic reactions between GG and etherifying reagents such as N-(3-chloro-2-hydroxypropyl)-trimethyl ammonium chloride (CHPTAC) in aqueous medium [103,104], aqueous IPA solution [105], 2,3-epoxypropyltrimethylammonium chloride (EPTAC, glycidyltrimethylammonium chloride, GTMAC) in aqueous EtOH medium [106], etc. were reported. Since CGG shows no harmful effect on natural environment or human health, it has been found in cosmetic products [107,108], protein drug release [109], and liposome encapsulation [110]. Moreover, CGG can also be employed in developing complex membranes and films for oil/water separation [111], antibacterial packaging [112–114], as depressants in flotation separation,[115] and stabilizers for zirconia suspensions as well as plasma emulsion [116,117].

In the recent time, Nakamura and coworkers used EPTAC (GTMAC) cationizing reagent in an aqueous EtOH solution to introduce positive charge to non-ionic GG [118]. The CGG product was used as a flocculant for negatively charged bentonite aqueous suspensions. In order to optimize the reaction conditions for the quaternization of GG, Tyagi et al. recently employed the well-known Taguchi's statistical methodology in designing and optimizing experimental conditions [119,120]. Due to the instability, toxicity, and high cost of EPTAC, CHPTAC was used to quaternize GG instead. Under alkaline condition, CHPTAC might easily be converted into EPTAC in situ, followed by nucleophilic reaction with activated GG. Several reaction factors were tested, namely, concentration of alkali and cationizing reagent, reaction time and temperature, using Taguchi L_{16} orthogonal array (4^5). The optimized experimental condition was reported that GG was dispersed in aqueous MeOH (80 % v/v) with a GG:solvent ratio of 1:20, together with 3.24 mol of NaOH and 2.04 mol of CHPTAC per each mole of GG AGU for 2 h at 30 °C. Among different experimental factors, the reaction time and amount of NaOH play a crucial role in the quaternization of GG.

FRGP was employed by Jing et al. to develop ultra-stretchable, self-healing hydrogels based on hexadecyl trimethyl ammonium bromide (CTAB)-cross-linked AA-*co*-stearyl methacrylate (SMA) grafted CGG [CTAB-cl-CGG-g-P(AA-*co*-SMA)] [121]. The quaternary amine groups in CGG offer hydrogen bonding and ionic interaction with carboxylate moieties in AA, hence, enhancing the mechanical strength of the hydrogel product. In addition, CTAB cross-linker was chosen to reinforce physical intermolecular interaction of the hydrogel by ionic attraction between positively charged ammonium groups and carboxylate groups from AA, as well as hydrophobic dispersion force between aliphatic hexadecyl chains and stearyl chains from SMA. Due to the presence of various dynamic intermolecular interaction in CTAB-cl-CGG-g-P(AA-*co*-SMA), the hydrogel shows self-healing capacity, ionic conductivity and can be used to develop strain electronic sensors.

Besides the quaternization of GG, partial oxidation of CGG has also been considered to broaden the applicability of CGG. Dai et al. reported a simple procedure to cross-link oxidized CGG (OCGG) and CS without employing extraneous cross-linking agents [122]. Several hydroxyl groups on CGG and CS were partially oxidized by sodium periodate ($NaIO_4$) first to yield aldehyde functional groups. These aldehyde groups subsequently reacted with remaining -OH groups on OCGG, -OH and/or $-NH_2$ groups from CS to form a cross-linked hydrogel via acetal and imine chemical bonds. The received cross-linked OCGG-CS (cl-OCGG-CS) hydrogel responds to pH changes due to the chemistry of acetal and imine bonds. In addition, cl-OCGG-CS possesses thermal responsiveness within the temperature range between 25 and 80 °C, and adhesiveness towards various surfaces e.g. metal, glass, plastic, wood and human skin. The gel is also an efficient adsorbent for the removal of phosphate in wastewater treatment and the obtained phosphate-adsorbed hydrogel can be utilized to fabricate N,P-doped carbon aerogel electrodes in supercapacitors.

Moreover, Yu et al. proposed an idea of cross-linking OCGG and carboxymethyl CS (CMCS) to create hydrogels for wound dressing [123]. Criteria for hydrogel properties in wound dressing can be found from some of these excellent reviews [124–128]. While CGG can offer

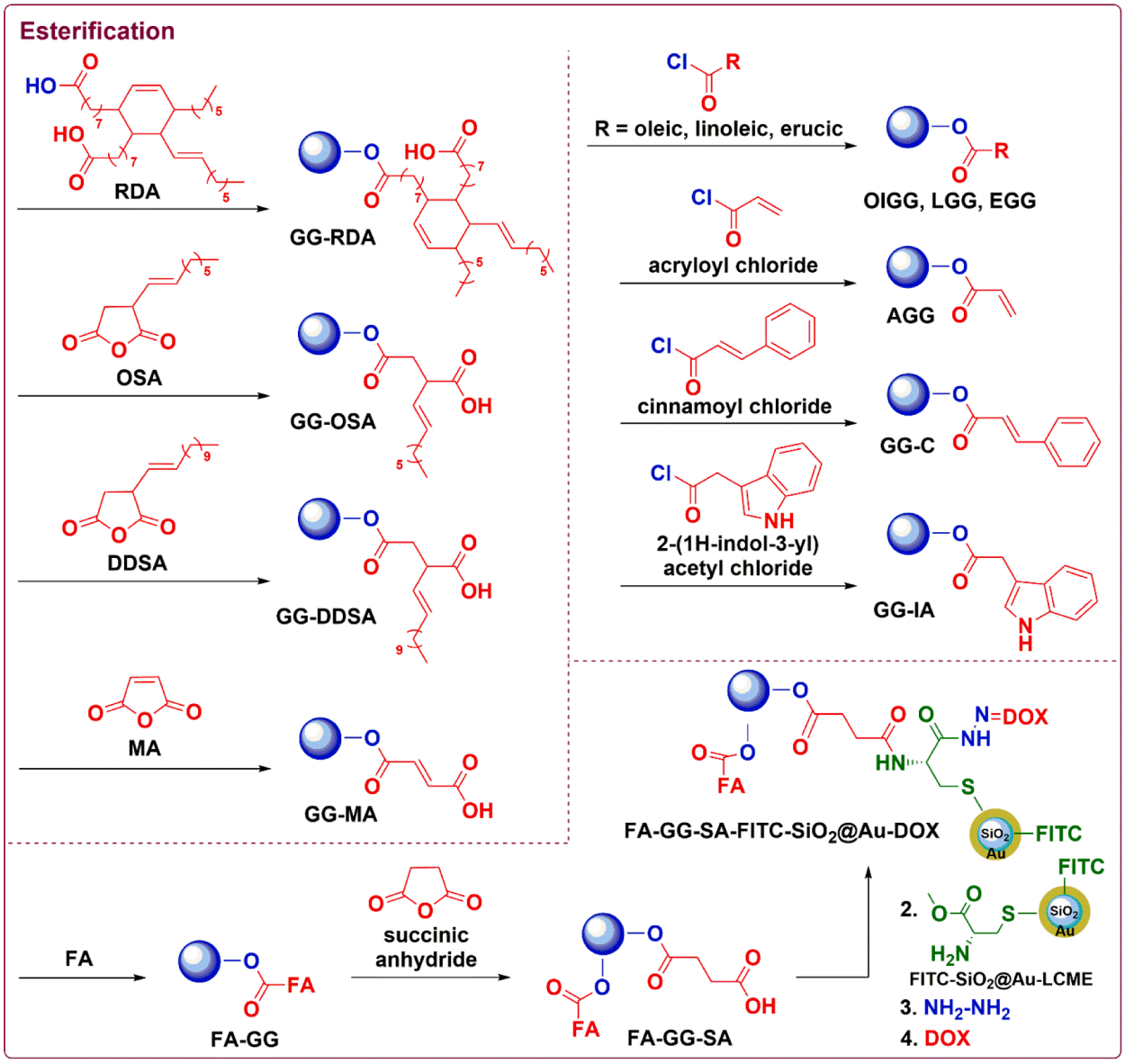

Fig. 3. Esterification of GG by carboxylic acids, acid anhydrides and acyl halides.

antibacterial activity due to the presence of quaternary ammonium groups [129], remaining -OH groups of CGG can also be partially oxidized to yield aldehyde groups for further cross-linking with CMCS. The cross-linked OCGG-CMCS (cl-OCGG-CMCS) hydrogel product has excellent antibacterial activity against *E. coli* and *Staphylococcus aureus* (*S. aureus*), hemostatic, cytocompatible, self-healing, injectable properties and great potential in wound dressing and healing.

3.1.1.5. Other derivatives of GG. Etherification remains as one of the most convenient approaches to modify GG. To create a novel non-viral, receptor-targeted gene delivery vector system for gene therapy against triple negative breast cancer (TNBC), Jana et al. performed several consecutive chemical transformations on GG [130]. GG was conjugated with low-molecular-weight polyethylenimine (LPEI), which has been reported as a non-viral carrier due to its high transfection efficiency, by using 4-bromo-1,8-naphthalic anhydride coupling agent. In the first step, S_N reaction was carried out between GG and 3-chloropropylamine (CPA) to form 3-aminopropyl GG (APGG). LPEI was then grafted to APGG via naphthalimide moieties to yield the final cationic LPEI grafted GG (GG-g-LPEI) product. Finally, complex coacervation between cationic GG-g-LPEI and anionic EGFP-N1 plasmid DNA (pDNA) was performed to form GG-g-LPEI/pDNA final coacervate product. The synthesized GG-g-LPEI has excellent blood and cyto-compatibility towards cervical HeLa and triple negative breast MDA-MB-231 cancer cells. GG-g-LPEI with 10 % the concentration of LPEI shows the highest in vitro transfection efficiency in TNBC, comparing to other concentrations of LPEI. Higher transfection efficiency in MDA-MB 231 cell line comparing to HeLa cell line has been reported and suggested due to the overexpression of mannose receptors in MDA-MB-231 cells.

Recently, Le and coworkers introduced benzoic acid (BA) moieties onto GG to yield GG-benzoic acid (GG-BA) [131]. After activating GG by NaOH in aqueous solution, 4-(bromomethyl)benzoic acid (BMBA) was used to provide BA moieties to the S_N reaction on GG. BA can offer rich coordination chemistry due to the presence of carboxylic acid functional groups, as well as hydrophobicity and π stacking intermolecular interaction from aromatic rings. Density functional theory (DFT) was employed to study electronic properties and visualize molecular orbitals of GG-BA. GG-BA with the concentration up to 4000 μg mL^{-1} shows good biocompatibility to mouse embryonic fibroblasts, human mammary epithelial cells and can potentially be used to develop novel

biomaterials such as bioadhesives, hydrogels, and coacervates.

In addition, Reis and coworkers also chemically introduced vinyl moieties onto GG via etherification reaction with epoxide groups from glycidyl methacrylate (GMA) [132]. The obtained glycidyl methacrylate guar gum (GG-GMA) was grafted with AA (in the sodium acrylate salt form) and N,*N*-dimethylacrylamide (DMAAm) spacer to yield AA-*co*-DMAAm grafted GG-GMA [GG-GMA-g-P(AA-*co*-DMAAm)] hydrogels as colon-targeting drug carriers. The obtained GG-GMA-g-P(AA-*co*-DMAAm) hydrogels show pH-responsiveness and swelling at intestinal pH 6.8 comparing to gastric pH 1.2, due to the presence of carboxylic acid functional groups. The hydrogel possesses low cytotoxicity to 3T3 cells line murine with hydrogel concentration up to 1000 μg mL^{-1} and can be used for the controlled release of hydrocortisone (HCS) model drug.

3.1.2. Esterification (GG-O-CO-)

Esterification of -OH groups on GG can be carried out using carboxylic acids and their reactive derivatives such as carboxylic acid anhydrides and acyl halides (Fig. 3, Table 2) [133–135].

To increase the hydrophobicity of GG, Bajpai and Raj used ricinoleic dimer acid (RDA) to esterify GG in the presence of dodecylbenzenesulfonic acid (DBSA) and catalytic amount of tosylic acid (TsOH), under microwave (MW) irradiation condition [136,137]. GG-ricinoleic dimer acid (GG-RDA) ester product is less susceptible to microbial growth than original GG and can be cross-linked with PVA by glutaraldehyde (GA) to form GA-cross-linked GG-RDA-PVA (GA-cl-GG-RDA-PVA) biofilms. Hydrophilic antibiotic gentamicin sulfate (GS) and hydrophobic amoxicillin (AX) medications were successfully loaded into GA-cl-GG-RDA-PVA films for wound dressing and drug delivery applications. These films show good biodegradability, resistance toward microbial growth of *E. coli*, *S. aureus* and *Candida albicans* (*C. albicans*), moisture-retention, wound exudate absorption capacity and wound healing properties.

Recently, Rajkumar and Prabaharan have reported complex chemical transformations of GG to prepare muti-functional nanoparticles for simultaneous cancer imaging and therapy [138]. Folic acid (FA) was first conjugated to GG as a tumor-targeting ligand to assist the drug delivery process to tumor sites, i.e. better cellular uptake and cytotoxicity for cancer cells via folate receptor-mediated endocytosis [139]. Steglich esterification with N,N'-dicyclohexylcarbodiimide (DCC) and 4-dimethylaminopyridine (DMAP) catalyst was chosen to provide a mild reaction condition for FA and GG at room temperature in DMSO. FA-conjugated GG (FA-GG) product was further esterified with succinic anhydride to introduce succinic acid (SA) moieties onto FA-GG to yield FA-GG-succinic acid (FA-GG-SA). Meanwhile, fluorescein isothiocyanate-SiO_2 core-Au shell-L-cysteine methyl ester (FITC-SiO_2@Au-LCME) nanoparticles were synthesized for fluorescence-computed tomography of cancer cells. SiO_2 core-Au shell (SiO_2@Au) nanoparticles offer good mesoporous structure, large surface area, biocompatibility and photostability. While conjugated fluorescein isothiocyanate (FITC) can exhibit emission spectrum peak wavelengths of around 490 nm corresponding to green fluorescence, L-cysteine methyl ester (LCME) linkers can connect FITC-SiO_2@Au via Au-S bonds, FA-GG-SA via amide bonds based on remaining SA moieties, and doxorubicin (DOX) chemotherapy medication via acid-cleavable hydrazone bonds. The acid-sensitive hydrazone bonds allow the controlled release of DOX at pH 5.6 inside Hela cancer cells, while remain stable at physiological pH 7.4. EDC/NHS coupling chemistry based on 1-ethyl-3-(3-dimethylaminopropyl)carbodiimide (EDC) and *N*-hydroxysuccinimide (NHS) was employed to form amide bonds between FA-GG-SA and FITC-SiO_2@Au-LCME, resulting in FA-GG-SA-FITC-SiO_2@Au-DOX final product.

In addition, Soni et al. carried out esterification of GGH by hydrophobic carboxylic acid anhydrides to enhance emulsifying and microencapsulation properties of GGH [140]. GGH and $NaHCO_3$ were dispersed in aqueous EtOH (95 % v/v) solutions of dodecenyl succinic anhydride (DDSA) or *n*-octenyl succinic anhydride (OSA). 45 °C and 2 h were reported as the optimized reaction temperature and time to obtain DS of 0.029 for GGH-dodecenyl succinic acid (GGH-DDSA) product. Meanwhile, GGH-*n*-octenyl succinic acid (GGH-OSA) product was obtained with DS of 0.07. GGH-DDSA was reported as a promising alternative to gum arabic for the emulsification and microencapsulation of soybean oil in food engineering.

Besides, Zhang and coworkers employed maleic anhydride (MA) to prepare anionic GG [141]. GG was dispersed in a dichloromethane (DCM) solution of maleic anhydride and triethylamine (Et_3N) catalyst to yield GG-maleic acid (GG-MA). The obtained GG-MA product has better water solubility, elasticity and great potential as a fracturing fluid with good temperature resistance between 120 and 150 °C, as indicated by rheology. Moreover, Yuan et al. has used maleic anhydride to cross-link GG and poly(ε-caprolactone) (PCL) grafted chitosan (CS-g-PCL) to form hydrogels for drug delivery [142]. Acetonitrile (ACN) solvent was chosen to disperse GG in the presence of DMAP catalyst for esterification reaction between GG and MA to yield GG-MA. Then, aza-Michael addition was allowed between double bonds on maleic acid moieties of GG-MA and free amine groups from CS-g-PCL to yield cross-linked cl-GG-MA-CS-g-PCL hydrogels. Noncytotoxic cl-GG-MA-CS-g-PCL shows anti-microbial activity against *S. aureus* (ATCC 27661), *Klebsiella pnumoniae* (*K. pnumoniae*) (ATCC 13883) and can be used to develop micelles for the delivery of rifampicin medication, which has low water solubility, in tuberculosis treatment.

A wide range of acyl halides has also been employed for esterification of GG. Zhang et al. has prepared acyl chlorides from oleic, linoleic, erucic acids and phosphorous trichloride [143]. These hydrophobic unsaturated acyl chlorides were then added to dispersions of GG and NaOH in acetone to yield new derivatives of GG, namely oleic guar gum (OlGG), linoleic guar gum (LGG) and erucic guar gum (EGG). Rheological studies indicate that aqueous solutions of these GG derivatives are non-Newtonian shear-thinning fluids and possess hydrophobic interaction.

Recently, Das and coworkers reported an esterification of GG using cinnamoyl chloride to modify the hydrophobicity and antibacterial activity of GG [144]. LiCl/DMSO solvent system was used as a medium for this reaction with catalytic amount of DMAP to yield GG cinnamate (GG-C). Beneficial effects of LiCl in polar aprotic solvents such as DMSO have been well-known for the dissolution of polysaccharides due to its ability to disrupt and prevent the reformation of hydrogen bonds [145–147]. Nanoprecipitation based on ouzo effects of GG-C hydrophobic solute, DMSO polar organic solvent and water non-solvent, was employed to yield GG-C nanoparticles (GG-C-N) [148]. The obtained GG-C-N have hydrodynamic size of around 289 nm and polydispersity index (PDI) of 0.43 from dynamic light scattering (DLS) measurements. Antibacterial activity of GG-C and GG-C-N was studied on E. coli (MTCC 44) and S. aureus (MTCC 160) strains to show that GG-C has better activity comparing to ciprofloxacin antibiotic control. Moreover, GG-C-N exhibit nearly-two times higher the antibacterial activity of GG-C and this was attributed to strong hydrophobic, aromatic interaction and high surface area of GG-C-N, resulting in better cell membrane perforations and cell death.

Similarly, Das and coworkers carried out esterification of GG with 2-(1H-indol-3-yl)acetyl chloride also in the LiCl/DMSO solvent system to form GG indole acetate (GG-IA) [149]. GA was then chosen to cross-link GG-IA and hydrolyzed fibrous keratin protein, which was extracted from chicken feather wastes, and subsequently solvent-casted into GA-cross-linked GG-IA-keratin (GA-cl-GG-IA-keratin) film scaffolds. These scaffolds are noncytotoxic and biocompatible to human dermal fibroblast cells. Both GG-IA and GA-cl-GG-IA-keratin films possess antimicrobial activity against gram-positive (*S. aureus* MTCC160), gram-negative (*E. coli* MTCC44) bacteria and show great potentials in skin tissue engineering.

Additionally, Bhattacharyya and Chowdhury introduced vinyl moieties to GG via esterification of NaOH-activated GG and acryloyl chloride, resulting in acryloyl GG (AGG) [150]. AGG was then grafted with AA and potassium 3-sulfopropyl acrylate (KSPA) to develop a novel pH-

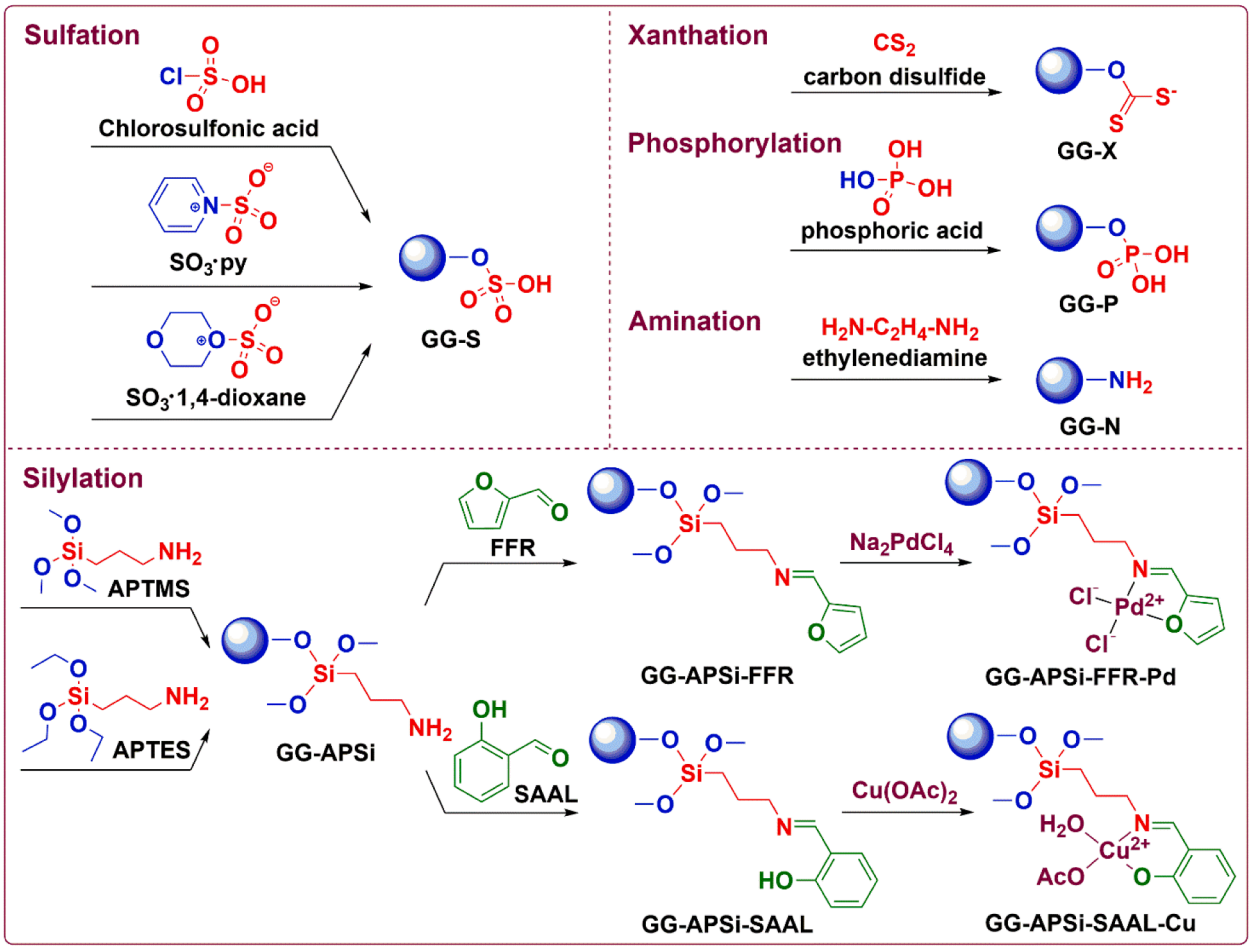

Fig. 4. Xanthation, silylation, phosphorylation, sulfation and amination of GG.

responsive MBAAm-cross-linked AA-*co*-KSPA grafted AGG [MBAAm-cl-AGG-g-P(AA-*co*-KSPA)] drug delivery system. Gentamicin sulphate (GMS) medication, which is used for the treatment of colorectal and anal fistula surgical site infections, can be adsorbed or desorbed from MBAAm-cl-AGG-g-P(AA-*co*-KSPA) hydrogels via reversible hydrogen bonding. Under physiological pH, deprotonation of carboxylic acid groups in the hydrogels increases the electrostatic repulsion between the polymer chains, hence, enhancing the release of GMS.

3.1.3. *Xanthation (GG-O-CS$_2^-$)*

According hard-soft acid-base (HSAB) theory, hydroxyl functional groups of native GG are considered as hard bases and possess strong affinity towards hard acids [151]. The coordination chemistry of -OH groups on GG, therefore, remains limited mainly to hard metal ions. Meanwhile, a wide range of transition and heavy metal ions is soft acids and tend to interact more strongly with soft bases such as S-containing thiol, sulfide, xanthate and dithiocarbamate functional groups [152–154]. While dithiocarbamate can be easily introduced onto polysaccharides that contain amino groups such as chitosan [155–158], xanthate functional groups are of great interest to polysaccharides possessing hydroxyl groups [159,160].

To broaden coordination chemistry of GG to a wider range of metal ions, especially heavy metal ions, Le and coworkers have reported a facile aqueous xanthation protocol (Fig. 4) [161]. Nucleophilic hydroxyl groups on GG were first activated by NaOH, followed by an addition of electrophilic carbon disulfide (CS_2) to yield GG xanthate (GG-X) product. N_2 purging to remove dissolved O_2 was found crucial to avoid further oxidation of xanthate groups. Under alkaline condition, while hard -OH groups of GG have good coordinating capacity towards hard metal ions, e.g. Al^{3+}, GG-X with soft xanthate moieties can easily form gels with various borderline and soft metal ions, e.g. Co^{2+}, Fe^{2+}, Cu^{2+}, Ni^{2+}, Pb^{2+}, Pt^{2+} and Cd^{2+}. GG-X, therefore, exhibits great potentials for heavy metal ion extraction, removal, and hydrogel formation. In addition, GG-X was employed to fabricate nanocomposites with CuS covellite (GG-X/CuS). GG-X not only can act as a capping agent for the aqueous dispersion of CuS nanoparticles, but also provides beneficial effects on the crystallite size of CuS. The application of GG-X/CuS nanocomposite in humidity sensing was also explored, in which hydrophilic GG-X matrix allows the interaction with humidity while CuS semiconductor contributes the electrical sensitivity to the nanocomposite. As a result, reversible linear responses of GG-X/CuS to relative humidity changes between 10 and 80 % were recorded.

3.1.4. *Silylation/ Silanization (GG-O-Si-)*

Over the years, silylation has been a popular process to covalently modify hydroxyl functional groups of chemical molecules or on different surfaces for various applications [162–167]. Si has high affinity towards O and Si-O bonds are particularly stable, hence the silylation of -OH groups can be carried out readily [168].

To construct Pd-based catalytic sites onto GG, Baran and coworkers have carried out several chemical modification steps on GG (Fig. 4) [169]. (3-aminopropyl)triethoxysilane (APTES) was first used to silylate hydroxyl groups and introduce free -NH_2 groups on GG. Schiff-base condensation between amino groups of GG-(3-aminopropyl)silane (GG-APSi) product and aldehyde groups from furfural (FFR) was then performed with refluxing MeOH to yield GG-APSi-furfural (GG-APSi-FFR). Finally, metal complexation between FFR, aldimine moieties on GG-APSi-FFR and Pd^{2+} metal cations were carried out to complete GG-

APSi-FFR-Pd catalytic sites for Suzuki solvent-free cross-coupling reactions between phenylboronic acid and different aryl halides under green reaction conditions (microwave radiation in 5 min and ambient atmosphere). The newly developed GG-APSi-FFR-Pd heterogeneous catalyst shows good catalytic activity and recyclability.

Moreover, (3-aminopropyl)trimethoxysilane (APTMS) was employed by Kumari et al. to also silylate and introduce amino groups on GG for developing a new Cu-based heterogeneous catalyst [170]. Silylated GG-APSi product was then refluxed with salicylaldehyde (SAAL) in EtOH to receive GG-APSi-salicylaldehyde (GG-APSi-SAAL) via Schiff-base condensation reaction. Final GG-APSi-SAAL-Cu heterogeneous catalyst was then obtained by metal complexation of GG-APSi-SAAL and copper(II) acetate [$Cu(OAc)_2$]. Catalytic activity of GG-APSi-SAAL-Cu was demonstrated based on selective oxidation reactions of diarylmethanes, resulting in different benzophenone derivatives. ACN solvent and *tert*-butyl hydroperoxide (TBHP) oxidant at 70 °C were found as the best condition for this catalytic reaction to give a reaction yield up to 90 % with good turnover number and frequency.

3.1.5. Phosphorylation (GG-O-P-)

Mimicking nature in developing new materials has been one of the most sustainable approaches in modern materials science. While discussions on the reasons why nature chooses phosphate and similar derivatives have long been of great interest to the science community [171–173], much effort has also been devoted to introducing phosphate moieties onto various materials to explore their properties and potential applications [174–176]. Over the years, phosphorylation of polysaccharides using phosphorylating agents such as phosphorus oxychloride ($POCl_3$), phosphorus pentoxide (P_2O_5), sodium trimetaphosphate (STMP), sodium tripolyphosphate (STPP), phosphoric acid and its anhydride, has been reported as a convenient chemical modification pathway to alter biological activities of natural polysaccharides [177].

In order to enhance hydrophobicity, emulsifying properties and homogenization of GG, Sharma and coworkers linked GG and soya lecithin (SL) via C-O-P bonds [178]. DCC was used to couple phosphate ester groups of SL and hydroxyl groups from GG, resulting in guar gum-soya lecithin (GG-SL). Then, MBAAm-cross-linked GG-SL/Fe^0 (MBAAm-cl-GG-SL/Fe^0) nanocomposites were prepared from GG-SL and zero-valent iron (Fe^0) in the presence of MBAAm cross-linker for the photocatalytic degradation of methyl violet dye. The Fe^0 photocatalyst can absorb solar energy to yield photogenerated electrons and holes, followed by the formation of reactive oxygen species and the degradation, mineralization of organic dyes. Detailed studies on the degradation of methyl violet, total organic carbon (TOC) removal efficiency and reusability of MBAAm-cl-GG-SL/Fe^0, have also been performed to show that MBAAm-cl-GG-SL/Fe^0 is an efficient photocatalytic system.

Phosphate and its derivatives are ones of the most commonly used coordinating functional groups in U(VI) removal due to their high affinity towards uranyl (UO_2^{2+}) ions [179]. In an effort of developing new materials for the removal of U(VI) in wastewater treatment, Hamza et al. have performed phosphorylation of GG to introduce phosphonic acid (or phosphonate groups) onto GG (Fig. 4) [180]. The phosphorylation of GG was carried out by using urea and H_3PO_4 reactants in 1,4-dioxane solvent at high temperature. New insights into the phosphorylation reaction mechanism by urea and H_3PO_4 have been presented recently [181]. Urea was suggested as a chemical source for the in-situ generation of NH_3 real catalyst, while phosphoramidate was proposed as the reaction intermediate. The obtained GG-phosphonic acid (GG-P) was then cross-linked with CS via epichlorohydrin (ECH), while magnetic Fe_3O_4 could also be added to the mixture to introduce magnetic properties for better separation and recovery of ECH-cross-linked GG-P-CS/Fe_3O_4 (ECH-cl-GG-P-CS/Fe_3O_4) nanocomposite product. The ECH-cl-GG-P-CS/Fe_3O_4 nanocomposite is pH-responsive due to the presence of both amino and phosphonate groups, resulting in the pH-dependence of metal cation sorption and desorption. This nanocomposite also possesses good selectivity towards UO_2^{2+} and Nd^{3+} comparing to other tested alkali-earth metals ions (e.g. Ca^{2+} and Mg^{2+}). In addition, ECH-cl-GG-P-CS/Fe_3O_4 can also offer antibacterial activity towards gram-positive [*Bacillus subtilis* (*B. subtilis*), *S. aureus*] and -negative [*E. coli, Pseudomonas aeruginosa* (*P. aeruginosa*)] bacteria.

3.1.6. Sulfation (GG-O-S-)

Recently, the introduction of sulfate functional groups to polysaccharides has drawn much attention as a convenient and efficient approach to alter the physicochemical properties of polysaccharides, especially their antioxidant, anticoagulant and antitumor activity [182,183].

To explore anticoagulant and antithrombotic effects of GG derivatives, de Oliveira Barddal and coworkers have carried out sulfation reactions on GG and GGH (Fig. 4) [184]. Chlorosulfonic acid-pyridine (py) (O'Neill method) and sulfur trioxide (SO_3)-pyridine (Larm method) sulfating reagents were employed to yield GG-sulfonic acid (GG-S-O, GG-S-L) and GGH-sulfonic acid (GGH-S-O, GGH-S-L respectively) with good DS. Further hydrolysis of GG products was also noticed and suggested due to the acidic reaction media. Degradation of GG-S-O and GGH-S-O was observed over the time while GG-S-L and GGH-S-L remained more stable. In vitro anticoagulant activity studies were performed to correlate the anticoagulant activity to the presence of sulfate groups and also indicate that GGH-S-L is a promising alternative to heparin, which is a glycosaminoglycan anticoagulant and antithrombotic medication. In addition, GGH-S-L has good antithrombotic activity from in vivo studies on male Wistar rats and good bioavailability when administered subcutaneously.

Kazachenko et al. combined chlorosulfonic acid and 1,4-dioxane at 20 °C to prepare SO_3·1,4-dioxane sulfating complex for the sulfation of GG [185]. GG-S product with DS of 0.91 was obtained after dispersing GG with SO_3·1,4-dioxane complex in 1,4-dioxane solvent at 60 °C for 2.9 h. Gel permeation chromatography has indicated a decrease in the molecular weight from 600 to 176 kDa after the sulfation. Moreover, computational chemistry was also carried out by DFT using Gaussian 09W software with B3PW91/6-31 + G(d, p) basis set to provide insights into electronic properties of GG-S.

Besides traditional sulfating agents, e.g. chlorosulfonic acid-pyridine, sulfur trioxide-pyridine and concentrated sulfuric acid-*n*-butanol, Kazachenko and coworkers have explored a novel milder sulfation pathway on GG using sulfamic acid and urea-based activators in 1,4-dioxane solvent [186]. It was suggested that urea and its similar compounds could activate sulfamic acid by creating Lewis acid-base complexes with S atom, hence, weakening S-N bonds in sulfamic acid to yield SO_3. Urea appears to be the best activator comparing to thiourea, methyl urea, ethyl urea, hydroxyethylurea and biuret. Among the tested polar aprotic solvents, namely, diglyme, 1,4-dioxane, DMF, piperidine, py and morpholine, 1,4-dioxane was also reported as the best solvent in terms of sulfur content for this bimolecular nucleophilic substitution (S_N2) sulfation reaction. While the experimental optimal reaction condition was obtained at 80 °C in 3 h using 25 mmol sulfamic acid per 1 g GG, the calculated optimal condition was suggested at 85 °C in 2.6 h with 34 mmol sulfamic acid for every 1 g of GG. In addition, depolymerization of GG chain was also observed, resulting in a molecular weight reduction by a factor of 2.7.

3.1.7. Amination (GG-NH_2)

Amino groups can be introduced to pristine polysaccharides via several pathways, resulting in chemical and biological property changes of polysaccharides [187]. For instance, polyamines have been conjugated to polysaccharide chains via condensation reaction with carboxylic acids [188], naphthalic anhydride coupling chemistry [130], and aza-Michael addition with oxidized polysaccharides [189].

In addition, direct replacement of hydroxyl groups on polysaccharides by amino groups is also another alternative and was recently performed on GG by Gopi et al. to prepare cross-linked hydrogels with

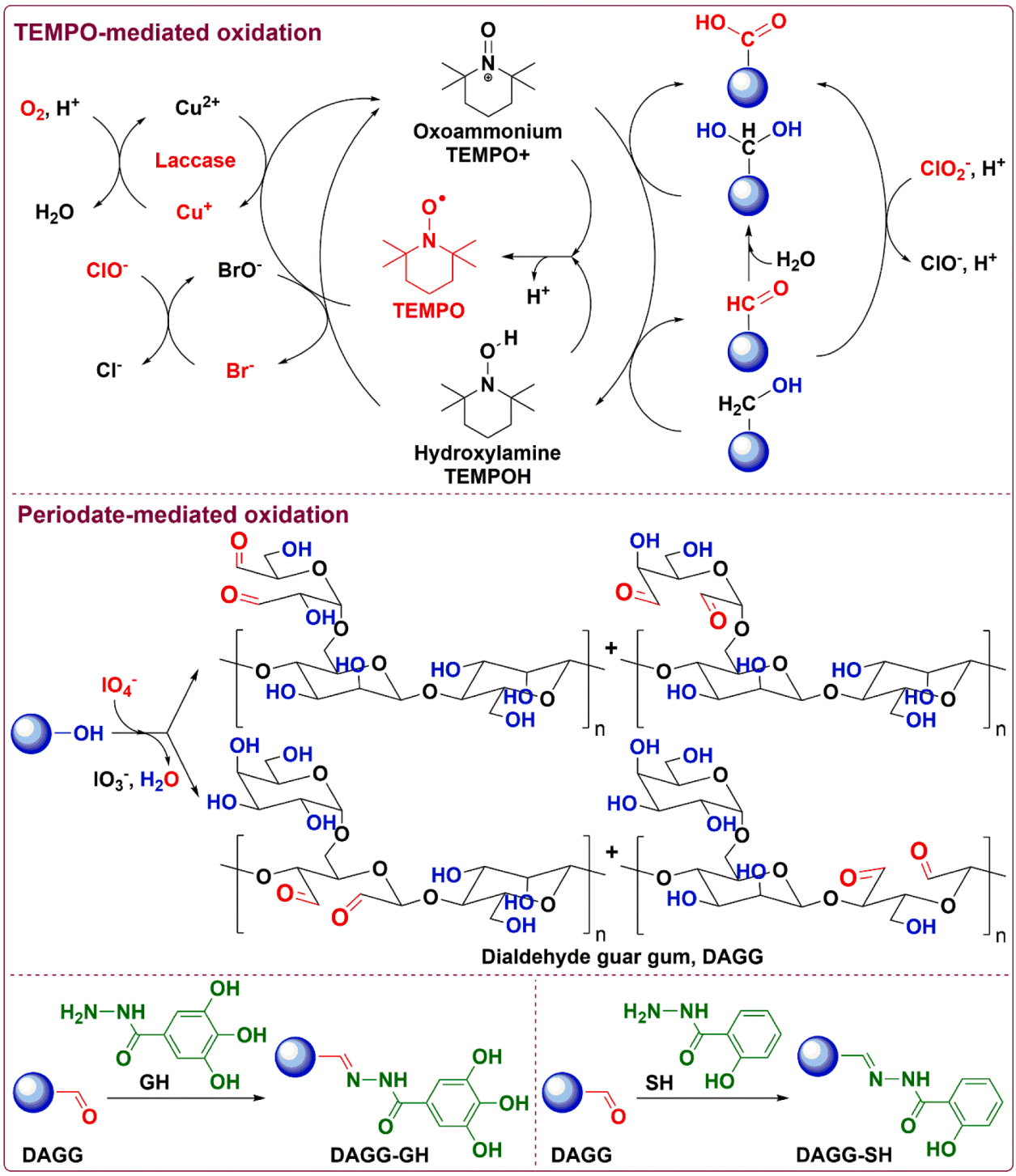

Fig. 5. Partial oxidation mechanism of GG using O_2-Laccase-TEMPO and NaOCl-NaBr-TEMPO systems (top). Regioselective oxidation of GG using periodate and further functionalization of DAGG products (bottom).

graphene oxide (GO) (Fig. 4) [190]. Nucleophilic substitution by ethylenediamine (NH_2-C_2H_4-NH_2) was first carried out to replace hydroxyl groups on GG (GG-OH to GG-NH-C_2H_4-NH_2), followed by reduction of GG-NH-C_2H_4-NH_2 by HCl to yield aminated GG-NH_2 (GG-N). GG-N was then cross-linked with GO by borax to yield borax-cross-linked GG-*N*-GO (borax-cl-GG-*N*-GO) hydrogels. The borax-cl-GG-*N*-GO hydrogel product possesses high surface area and abundant remaining -OH and -CO_2H functional groups. These contribute to the adsorption capability of pH-responsive borax-cl-GG-*N*-GO hydrogel towards inorganic and organic pollutants (e.g. Cu^{2+}, malachite green (MG), methylene blue (MB) and rhodamine B (RhB) cationic dyes).

3.2. Partial oxidation (GG-CHO, GG-CO_2H)

Over the years, partial oxidation of alcohol functional groups on polysaccharides to aldehydes has been regarded as convenient chemical synthesis approaches to diversify chemical properties of native polysaccharides [191,192]. While hydroxyl groups in general behave as nucleophiles, the presence of aldehyde and/or carboxylic acid groups on polysaccharide structures can offer electrophilic reactive sites as well as

condensation and cross-linking reaction pathways.

3.2.1. TEMPO-mediated oxidation

Oxidation of alcohol groups can be performed regioselectively on primary C6-OH groups of GG via 2,2,6,6-tetramethylpiperidine-1-oxyl radical (TEMPO)-mediated oxidation route [193,194]. In the past, TEMPO and sodium bromide (NaBr) were employed as catalysts for the oxidation of primary alcohol groups on GG derivatives to carboxylic acid groups using sodium hypochlorite (NaOCl) oxidant (NaOCl-NaBr-TEMPO system) in water [195]. C6-OH groups on Man backbone were suggested to be more accessible to TEMPO-catalyzed oxidation than C6-OH groups on Gal side chains of GG, due to possible intramolecular hydrogen bonding between C6-OH from Gal and C3-OH from adjacent Man [196,197]. In addition, enzymatic oxidation of primary alcohol groups using fungal laccase enzymes and TEMPO mediator was also reported (Fig. 5) [198].

Recently, de Seixas-Junior and coworkers prepared oxidized guar gum (OGG) by TEMPO-mediated oxidation as a reference to highlight the importance of primary alcohol groups of GG in the interaction with sodium lauryl ether sulfate anionic surfactant for the development of pharmaceutical or cosmetic products [199]. Primary alcohol groups of GG were selectively oxidized by NaOCl-NaBr-TEMPO system into carboxylic acids (1.2 mmol -CO_2H groups per g of GG). Moreover, Ponzini et al. have tested the enzymatic TEMPO-oxidation of several galactomannan polysaccharides, including GG [200]. Laccase enzyme was coupled to the catalytic oxidation of alcohol groups using O_2 oxidant and TEMPO mediator (O_2-Laccase-TEMPO system) in water [201,202]. Mass spectrometry analysis on the oxidation of primary alcohol groups based on this oxidation system indicated that both aldehyde and carboxylic acid groups are possible products from the oxidation reaction. OGG product was obtained as a hydrogel due to self-cross-linking via hemiacetal, ester bonds and could be further lyophilized to form aerogels. Interestingly, among three tested galactomannans, obtained aerogels from fenugreek gum exhibit the greatest mechanical stability comparing to aerogels from sesbania and guar gums, even though fenugreek gum has the lowest relative amount of Man comparing to Gal (Man:Gal ratios of 1:1, 1.3:1, and 1.5:1 in fenugreek, sesbania and guar gums respectively).

3.2.2. Periodate-mediated oxidation

Periodate (IO_4^-) has been well-known as an oxidizing agent for oxidative cleavage of vicinal 1,2-diols [203]. Over the years, much effort to employ periodate-mediated oxidation of vicinal alcohol groups located on equatorial-equatorial and equatorial-axial positions in polysaccharides has also been devoted [204–206]. Oxidation of galactomannan polysaccharide by periodate can be carried out on C2-OH and C3-OH of mannose backbone, as well as C2-OH, C3-OH and C4-OH of galactose side groups to yield dialdehyde products (Fig. 5) [207].

Recently, several research groups have performed periodate-mediated oxidation of GG to obtain dialdehyde GG (DAGG). Typically GG and periodate are dissolved in water solvent at room temperature and the oxidation is allowed in the dark for several hours and quenched by adding ethylene glycol. For instance, Dai and coworkers utilized this reaction pathway to prepare DAGG, followed by self-cross-linking between remaining alcohol groups and newly formed aldehyde groups via acetal bonds in DAGG, without the assistance of any external cross-linkers [208]. The obtained cross-linked-DAGG (cl-DAGG) hydrogels have great potential for oil–water separation in harsh alkaline (pH 11), salty environments (NaCl 5 wt%), with good separation efficiency (up to 99.47 %) and recyclability.

Duan et al. also carried out the oxidation and self-cross-linking of GG by periodate in the presence of Ag nanoparticles (Ag NPs) dispersed in porous iron(III) carboxylate of MIL (Materials of Institute Lavoisier, a type of metal–organic framework materials) [Ag NPs@MIL-100(Fe)] to enhance photocatalytic and antibacterial activity [209]. Photocatalytic degradation of MB dye by cl-DAGG/Ag NPs@MIL-100(Fe) hydrogel product was demonstrated with good performance (up to 100 % MB can be degraded within 100 min) and recyclability. The hydrogel also possesses injectability, self-healing, antibacterial properties against *E. coli* and can be employed in water–oil separation with a separation efficiency up to 99.1 %.

In addition, a wide range of materials has been cross-linked with DAGG to synergize properties of these materials. For instance, Maroufi et al. reported periodate-mediated oxidation of GG to yield DAGG, followed by cross-linking with amino groups in fish gelatin to form cross-linked DAGG-gelatin (cl-DAGG-gelatin) food packaging films [210]. The cl-DAGG-gelatin film products possess lower water solubility, moisture content, water vapor permeability, better tensile strength and thermal stability than GG/gelatin reference films. Green tea extract (GTE) was also incorporated into the films (cl-DAGG-gelatin/GTE) to provide antioxidant and antibacterial activities on gram-positive *S. aureus* bacteria. Moreover, DAGG was also cross-linked with amino groups from CS in the presence of pomegranate peel extract (PPE) as a chemically active component to yield antioxidant and antibacterial cross-linked DAGG-CS/PPE (cl-DAGG-CS/PPE) hydrogels for food packaging applications [211].

Pandit and coworkers recently performed Schiff-base condensation between aldehyde groups in DAGG, which were obtained from periodate-mediated oxidation of GG, and remaining amino groups on CMCS to produce cross-linked DAGG-CMCS (cl-DAGG-CMCS) hydrogels [212]. These hydrogels show good self-healing properties, injectability, biocompatibility to human embryonic kidney 293 (HEK-293) cells up to a 100 μg mL^{-1} concentration of cl-DAGG-CMCS, blood compatibility and biodegradability. These cl-DAGG-CMCS hydrogels can also be used for drug loading and delivery from their study on DOX as a model anticancer medication.

Moreover, Mokhtari et al. carried out the cross-linking between newly synthesized DAGG and amino groups in silk fibroin (SF), followed by an incorporation of curcumin (Cur)-loaded zein nanoparticles (Cur-zein NPs) to obtain a novel cross-linked DAGG-SF/Cur-zein NPs (cl-DAGG-SF/Cur-zein NPs) hydrogel scaffold [213]. Applications of SF in materials science, flexible electronics, wound dressings, drug carriers, etc. have attracted great attention recently [214–217]. Cur was added to the hydrogel scaffold to enhance anti-inflammatory, antioxidant, antimicrobial properties of the system. Due to the hydrophobic polyphenolic nature, Cur has low water-solubility, bioavailability and can be encapsulated by protein carriers to enhance the drug delivery capacity. The synthesized hydrogel scaffold can promote viability, proliferation of mouse embryonic fibroblast (NIH-3T3) cells, and possesses antimicrobial activity against gram-positive (*Bacillus*) as well as gram-negative (*E. coli*) bacteria. DAGG/SF-Cur-zein-NPs, therefore, is a promising candidate for wound dressings and healing.

In the recent time, hydrazine was used as a linker to introduce new organic functional moieties to DAGG. Schiff-base condensation between DAGG and galacylhydrazine (GH) or salicylhydrazine (SH) was carried out by Duan and Ma et al. respectively to extend applicability of GG in wastewater treatment [218,219]. While phenolic moieties in DAGG-GH can enhance the reversible adsorption of cationic dyes [bromophenol blue (BrB), methyl orange (MeO), MB, RhB] via ionic and π stacking interaction, SH moieties in DAGG-SH are efficient adsorptive sites for metal cations such as Ni^{2+}, Co^{2+} and Cr^{3+}. In addition, Wen et al. also used hydrazine to conjugate DAGG and MBAAm cross-linked copolymer of acrylic acid and methyl methacrylate [MBAAm-cl-P(AA-*co*-MMA)] to prepare a novel adsorbent [220]. Oxidation of GG was first carried out by periodate to yield DAGG with the degree of oxidation of 67.62 %. MBAAm-cl-P(AA-*co*-MMA) was prepared using KPS initiator and MBAAm cross-linker to take advantage of carboxylic acid groups from AA for interaction with cations, and ester groups of MMA for further conjugation with DAGG. Then, MBAAm-cl-P(AA-*co*-MMA) and DAGG were linked together by using hydrazine, nucleophilic acyl substitution in water and Schiff-base condensation reaction in refluxing EtOH. Hydrazine-cross-linked DAGG-MBAAm-cl-P(AA-*co*-MMA) [hydrazine-

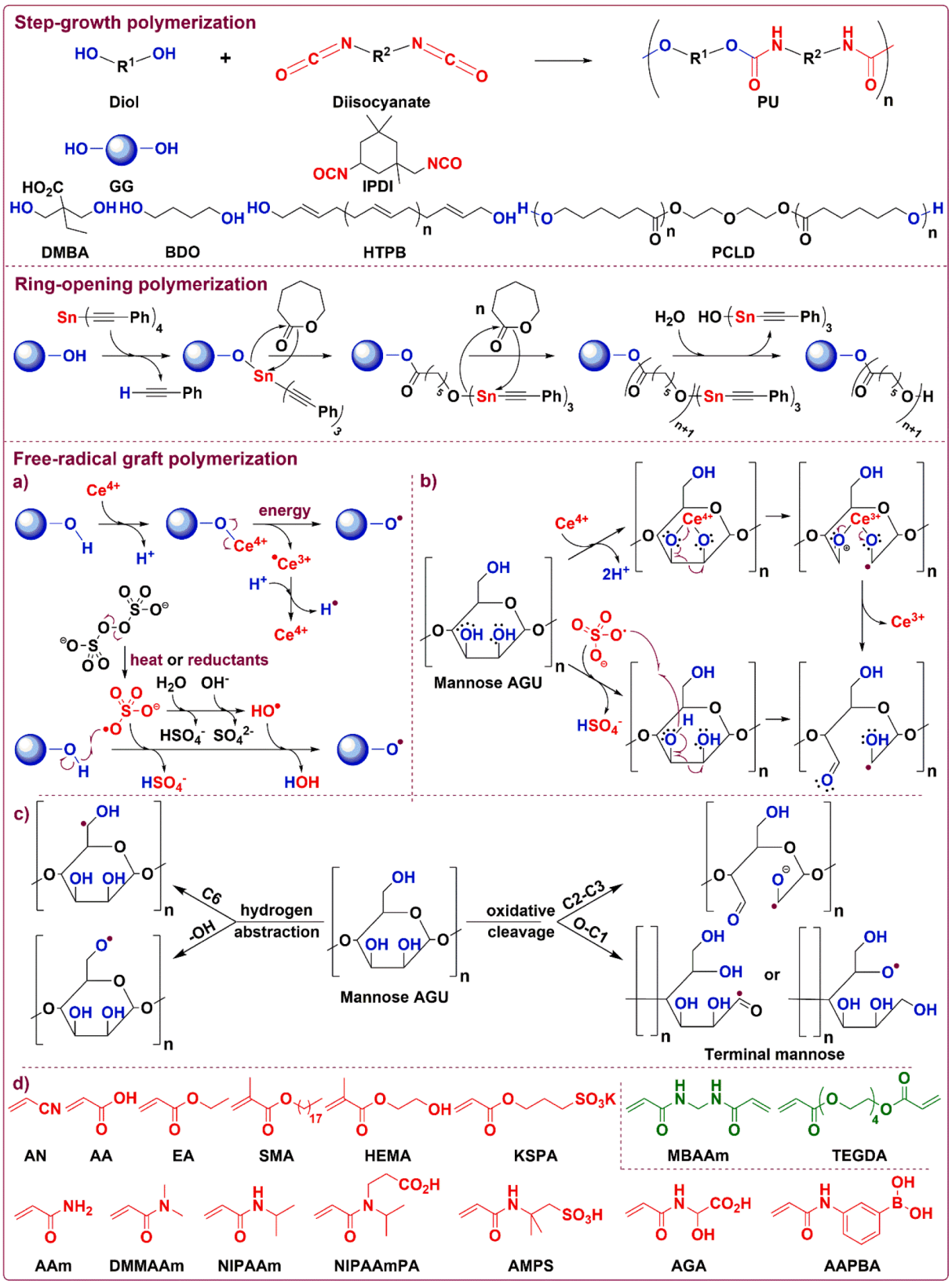

Fig. 6. Reported step-growth (top) and ring-opening (middle) polymerization of GG. Initiation mechanism of FRGP on GG and its derivatives (bottom). a) Formation of O-centered free-radicals. b) Formation of C-centered free-radicals. c) Formation of free-radicals via hydrogen abstraction and oxidative cleavage. d) Reported vinyl-containing monomers (red) and cross-linkers (green) for FRGP of GG and its derivatives. (For interpretation of the references to color in this figure legend, the reader is referred to the web version of this article.)

cl-DAGG-MBAAm-cl-P(AA-*co*-MMA)] product shows great capacity for removal of cationic organic dyes (MB, MG), Cu^{2+} metal ions from wastewater and also for water–oil separation with good efficiency and reusability.

In addition, aldehyde groups in DAGG can also be transformed into carboxylic acid groups. For instance, Ganie and coworkers used sodium chlorite ($NaClO_2$) under acidic condition [acetic acid (AcOH)] to further oxidize aldehyde groups in DAGG to dicarboxylic acid GG (DCGG) [221]. Coordination reactions between Fe^{2+} and -CO_2H groups from DCGG were employed to yield Fe^{2+}-cross-linked DCGG (Fe^{2+}-cl-DCGG), which was eventually formulated with other polymeric materials (ethyl cellulose (EC), polyvinylpyrrolidone (PVP) and PVA) to form tablets for the controlled release of Fe^{2+}. In vitro studies indicate a faster release of iron in simulated intestinal fluid (pH 4.5) than in simulated gastric fluid (pH 1.5). Antianemic activity of Fe^{2+}-cl-DCGG tablets was also tested on male albino rats to show an overall health improvement.

3.3. Graft polymerization

3.3.1. Step-growth polymerization (SGP)

Step-growth polymerization (SGP) is one of the most common synthetic approaches in polymer science. Typically, chemical reactions between bi- or multi-functional monomers are performed to fabricate step-growth polymers [222–224].

To synthesize GG-based polyurethanes (GG-PU) as potential natural polysaccharide-based stabilizer, thickener, emulsifier or binding agent, Anjum and coworkers performed SGP between -OH groups of GG, hydroxyl-terminated polybutadiene (HTPB), and isocyanate (-NCO) functional groups of isophorone diisocyanate (IPDI) (Fig. 6) [225]. Firstly, GG was mixed with HTPB as soft segments into a homogenous mixture, followed by reactions with IPDI to form GG-PU pre-polymers. Remaining -NCO groups of pre-polymers were finally allowed to react with 1,4-butanediol (BDO) as chain extender. Dibutyltin dilaurate (DBTDL) catalyst was also employed in this SGP of GG. Comparing to GG, GG-PU has better thermal stability, which was suggested due to an increase in intermolecular hydrogen bonding.

In addition, Ma et al. used -OH groups from GG and BD as chain extenders to further modify PU with -NCO terminating functional groups [226]. The synthesized PU was first fabricated from IPDI, poly(ε-caprolactone) diol (PCLD), and 2,2-dimethylolbutyric (DMBA) acid as hard, soft segments and anionic internal emulsifier respectively. Then, cross-linking of the obtained PU was carried out by GG and BD to yield GG-PU final product. The employment of GG up to 0.3 wt% results in an increase in the tensile strength, thermal stability and water resistance of GG-PU, which can be used as finishing and coating layers.

3.3.2. Ring-opening polymerization (ROP)

Over the years, ring-opening polymerization (ROP) has been of great interest to prepare and graft polymers from cyclic monomer starting materials [227–231]. Recently, El Assimi and coworkers employed ROP to prepare PCL grafted GG (GG-g-PCL) (Fig. 6) [232]. Tetra(phenylethynyl)tin [Sn(C≡CPh)$_4$ or SnAK] was used to initiate -OH groups on GG into alkoxy-tin(IV) (GG-O-Sn(C≡CPh)$_3$) moieties at room temperature in ambient atmosphere, followed by ROP of ε-caprolactone (ε-CL) onto GG. GG-g-PCL products with 1, 3 and 5 % w/w has lower hydrophilicity than native GG, which was confirmed by contact angle measurements, and can be well-dispersed in DCM solvent over a long period of time. The dispersity and reaction yield of grafted PCL was approximated of 1.75–1.86 and 92–94 % respectively. GG-g-PCL was successfully employed as a coating agent to formulate slow-release fertilizer of diammonium phosphate [233].

3.3.3. Free-radical graft polymerization (FRGP)

Free-radical polymerization is ubiquitous in polymer synthesis and modification [234,235]. The reaction is normally initiated by chemicals and/or radiation to yield free-radicals, followed by polymerization with different vinyl monomers and multifunctional cross-linkers [222].

In the recent past, a wide range of chemical initiators has been employed in free-radical graft polymerization. For instance, ceric(IV) ammonium nitrate [$(NH_4)_2[Ce(NO_3)_6]$ or CAN] is a common oxidizing agent and radical initiator in chemical synthesis. In water, CAN dissociates to hexanitratocerate(IV) [$[Ce(NO_3)_6]^{2-}$], while further dissociation and hydrolysis of Ce^{4+} ions might occur depending on pH conditions. Besides acting as a one-electron oxidant, oxo-bridged dinuclear cerium(IV) complexes [$[Ce^{IV}$-O-$Ce^{IV}]^{6+}$] can also behave as two-electron oxidizing agents [236]. Moreover, peroxydisulfate or persulfate ($S_2O_8^{2-}$) can also be used as a free-radical initiator due to the presence of peroxide O-O bond [237]. Commercially available forms of peroxydisulfate can be found with different counter-cations such as NH_4^+ [ammonium persulfate, $(NH_4)_2S_2O_8$ or APS], Na^+ (sodium persulfate, $Na_2S_2O_8$ or SPS) and K^+ (potassium persulfate, $K_2S_2O_8$ or KPS). Physical (thermal) activation of peroxydisulfate is normally carried out to yield sulfate radical anions ($SO_4^{\bullet-}$) and/or hydroxyl radicals ($HO^\bullet$) in aqueous media [Eq. (1) to (3)] [238]. In addition, chemical reactions between peroxydisulfate and reducing agents such as bisulfite (HSO_3^-) and metabisulfite [$S_2O_5^{2-}$, a precursor of HSO_3^-, Eq. (6)] also allow the formation of $SO_4^{\bullet-}$, S-centered bisulfite free radicals ($HSO_3^\bullet$) and S-centered metabisulfite radical anions ($S_2O_5^{\bullet-}$) [Eq. (4), (5)] [239]. Further reactions between $SO_4^{\bullet-}$ and excess HSO_3^- might proceed to yield $HSO_3^\bullet$, which dissociates into proton (H^+) and S-centered sulfite radical anions ($SO_3^{\bullet-}$) [Eq. (7)] [240,241]. Moreover, $SO_3^{\bullet-}$ can react with dissolved O_2 to form peroxymonosulfate radical anions ($SO_5^{\bullet-}$) [Eq. (8)], which might result in more complex free-radical reactions [242]. Organic amines, such as TMEDA or TEMED, can also be used to initiate the formation of free-radicals via chemical reactions between nucleophilic N and O from peroxide O-O bonds of persulfates [243–245]. In addition, ascorbic acid (H_2AA) might also initiate the transformation of persulfate into $SO_4^{\bullet-}$ free-radicals with ascorbic acid radical anion ($AA^{\bullet-}$) by products for graft polymerization [Eq. (9)] [246–248].

$$S_2O_{8\,(aq)}^{2-} \rightarrow 2\ SO_{4\,(aq)}^{\bullet-} \quad (1)$$

$$SO_{4\,(aq)}^{\bullet-} + H_2O_{(l)} \rightarrow HSO_{4\,(aq)}^{-} + HO_{(aq)}^{\bullet} \quad (2)$$

$$SO_{4\,(aq)}^{\bullet-} + OH_{(aq)}^{-} \rightarrow SO_{4\,(aq)}^{2-} + HO_{(aq)}^{\bullet} \quad (3)$$

$$S_2O_{8\,(aq)}^{2-} + HSO_{3\,(aq)}^{-} \rightarrow SO_{4\,(aq)}^{2-} + SO_{4\,(aq)}^{\bullet-} + HSO_{3\,(aq)}^{\bullet} \quad (4)$$

$$S_2O_{8\,(aq)}^{2-} + S_2O_{5\,(aq)}^{2-} \rightarrow SO_{4\,(aq)}^{2-} + SO_{4\,(aq)}^{\bullet-} + S_2O_{5\,(aq)}^{\bullet-} \quad (5)$$

$$S_2O_{5\,(aq)}^{2-} + H_2O_{(l)} \rightarrow 2\ HSO_{3\,(aq)}^{-} \quad (6)$$

$$SO_{4\,(aq)}^{\bullet-} + HSO_{3\,(aq)}^{-} \rightarrow SO_{4\,(aq)}^{2-} + H_{(aq)}^{+} + SO_{3\,(aq)}^{\bullet-} \quad (7)$$

$$SO_{3\,(aq)}^{\bullet-} + O_{2(g)} \rightarrow SO_{5\,(aq)}^{\bullet-} \quad (8)$$

$$S_2O_{8\,(aq)}^{2-} + H_2AA_{(aq)} \rightarrow 2H_{(aq)}^{+} + SO_{4\,(aq)}^{2-} + SO_{4\,(aq)}^{\bullet-} + AA_{(aq)}^{\bullet-} \quad (9)$$

In the presence of radical initiators, different carbon-centered and/or oxygen-centered free-radicals of polysaccharides can be formed (Fig. 6a, 6b). Electron spin resonance (ESR) studies suggest that Ce^{4+} can chelate to two adjacent -OH groups, possibly at C2 and C3 positions on AGUs of polysaccharides. Then, an electron transfer from the AGU to Ce^{4+} occurs, resulting in the reduction of Ce^{4+} to Ce^{3+}, pyranose ring opening due to C2-C3 bond cleavage and formation of a carbon-centered radical species [249,250]. Moreover, $S_2O_8^{2-}$ can be activated to yield $SO_4^{\bullet-}$ and $HO^\bullet$. These free radicals can approach -OH groups on polysaccharides and subsequently convert them into oxygen-centered radical sites for grafting polymerization [251]. In addition, other free-radical initiation pathways of polysaccharides have been proposed such as hydrogen abstraction on C6, oxidative cleavage of O-C1 bond in terminal AGU of polysaccharide chain, etc. (Fig. 6c) [252]. Once free-radicals are formed, propagation of FRGP can occur with various vinyl-containing monomers and cross-linkers (Fig. 6d).

3.3.3.1. Acrylic acid (AA) monomer. Among various polymers, poly (acrylic acid) (PAA) has been commonly used in the fabrication of numerous biocompatible and biodegradable gel systems to enhance the pH-responsiveness of materials due to numerous carboxylic acid groups on the polymer backbone [253–255].

Recently, several research groups have tried to graft AA onto GG to fabricate acrylic acid grafted guar gum (GG-g-PAA) polymers by varying the composition of GG, PAA, free-radical initiators and different cross-linkers. For instance, L-alanine (Ala) cross-linker was used by Sharma and coworkers to prepared Ala-cross-linked GG-g-PAA (Ala-cl-GG-g-PAA) in order to enhance the hydrogen bonding network, self-healing properties and to study the controlled release of levofloxacin hydrophilic medication under physiological pH and temperature [256]. Concentration of Ala was varied from 0.4 to 1 % w/v to show that Ala-cl-GG-g-PAA with 1 % w/v Ala possesses good thermal stability from 30 to 90 °C, the best mechanical and swelling properties (3350 % at pH 9). The obtained GG-g-PAA gels also show drug-loading efficiency of around 65 and 75 %, while the drug release can reach up to 98 % with varying release time up to 130 h, due to changes in the concentration of Ala.

Bifunctional MBAAm has been widely employed as a vinyl-containing cross-linker for GG and other polymeric systems [257]. Recently, Shamanta et al. studied the swelling and mechanical strength of MBAAm-cross-linked GG-g-PAA (MBAAm-cl-GG-g-PAA) hydrogels, which was prepared from an optimized system of 1 wt% APS, 1 wt% MBAAm, 25 wt% AA and 4 wt% GG [258]. Pyridoxine hydrochloride (vitamin B6) was chosen as model medication to examine the gradual drug release of the synthesized MBAAm-cl-GG-g-PAA hydrogel. Under physiological pH, carboxylic acid groups of MBAAm-cl-GG-g-PAA hydrogels get deprotonated into negatively charged carboxylates, leading to electrostatic repulsion between functional groups with the same charge, hence, swelling of the gels. This allows the physical desorption and release of vitamin B6 from the MBAAm-cl-GG-g-PAA hydrogels up to 95 % over 30 h. Moreover, MBAAm was also chosen by HaqAsif et al. to develop drug delivery systems for curcumin with the cumulative release up to 100 % over 12 h [259].

Besides using MBAAm to cross-link GG-g-PAA polymers, Singh and Dhaliwal also incorporated Ag NPs into MBAAm-cl-GG-g-PAA polymer matrix to fabricate a new MBAAm-cl-GG-g-PAA/Ag NPs adsorbent for removal of MB dye [260]. The Ag NPs with an average size of 100 nm, offer large specific surface area and surface energy to the matrix, resulting in an improvement in MB adsorption capacity of the polymer matrix. Meanwhile, Li and coworkers incorporated GG and sodium lignosulfonate (SLS) together to develop novel MBAAm-cross-linked AA grafted GG/SLS (MBAAm-cl-GG/SLS-g-PAA) hydrogel adsorbents [261]. Due to the presence of various coordinating functional groups such as alcohols, phenols, sulfonic acid and carboxylic acid, the MBAAm-cl-GG/SLS-g-PAA hydrogels show good chelating and adsorption capacity towards Cu^{2+} and Co^{2+} metal ions (709 mg g^{-1} and 601 mg g^{-1} respectively). Under neutral pH, deprotonation of acidic functional groups allows stronger adsorption of metal ions, while acidic pH can also be exploited for desorption and recovery of metal ions, resulting in good reversibility and reusability of the hydrogel adsorbents.

In the recent time, copolymers between AA and other vinyl-containing monomers have also been explored. Pal et al. reported the grafting of GG with poly(AA-*co*-acrylonitrile) [P(AA-*co*-AN)] copolymer to yield MBAAm-cross-linked AA-*co*-AN grafted GG [MBAAm-cl-GG-g-P(AA-*co*-AN)] [262]. While AA enhances pH-responsiveness of GG, AN is expected to improve physiochemical properties of the polysaccharide. Microwave was employed to initiate grafting polymerization in the absence of free-radical initiators. Different reaction parameters were optimized to achieve the best reaction conditions in terms of grafting yield (GY) (0.03 mol/L AA, 1.0 mol/L AN, 2000W microwave power under 100 s to receive 82.84 % grafting yield). Encapsulation of anti-oxidant and anti-inflammatory thymoquinone (TQ) by MBAAm-cl-GG-g-P(AA-*co*-AN) was carried out to demonstrate potential applications of the novel grafted GG, and to increase the low bioavailability of TQ in aqueous media. Under physiological pH condition, swelling of MBAAm-cl-GG-g-P(AA-*co*-AN) can be observed due to the formation of carboxylate groups from deprotonation of AA or hydrolysis of AN, resulting in the maximum release of TQ up to 78 % over 6 h. Moreover, this drug delivery system also shows hemocompatibility and no cytotoxicity against the tested monkey normal kidney Vero cell line.

In addition, grafting of AA and AAm onto GG was chosen to fabricate MBAAm-cross-linked AA-*co*-AAm grafted GG [MBAAm-cl-GG-g-P(AA-*co*-AAm)] by Karnakar and Gite for the gradual release of $ZnSO_4$ as a micronutrient for plant growth [263]. The release kinetics of $ZnSO_4$ from MBAAm-cl-GG-g-P(AA-*co*-AAm) into water fits Korsmeyer-Peppas and Peppas-Sahlin mathematical models. MBAAm-cl-GG-g-P(AA-*co*-AAm) was found degradable under hydrolytic and soil burial conditions (pH 7.4–7.5, 37 °C). Moreover, Gihar et al. also prepared GG-g-P(AA-*co*-AAm) via microwave-assisted graft polymerization for the removal of Hg^{2+} ions from aqueous solutions [264]. Hg^{2+} adsorption by the obtained GG-g-P(AA-*co*-AAm) shows best performance at pH 6, while acidic pH less than 3 reduces the adsorption capacity of GG-g-P(AA-*co*-AAm). This might be attributed to the deprotonation and protonation of carboxylic acid functional groups.

Mitra and coworkers recently prepared MBAAm-cross-linked AA-*co*-*N*-isopropylacrylamide grafted GG [MBAAm-cl-GG-g-P(AA-*co*-NIPAAm)] using AA and *N*-isopropylacrylamide (NIPAAm) [265]. The employed FRGP was initiated by chemical reaction between KPS and sodium bisulfite (SBS) at mild temperature (25 °C). Under the reported synthetic condition, in-situ reactions between grafted NIPAAm and free AA yield 3-(*N*-isopropylacrylamido)propanoic acid (NIPAAmPA) moieties also occurred, resulting in MBAAm-cross-linked AA-*co*-NIPAAm-*co*-NIPAAmPA grafted GG [MBAAm-cl-GG-g-P(AA-*co*-NIPAAm-*co*-NIPAAmPA)] as non-aromatic clusteroluminogenic polymers. MBAAm-cl-GG-g-P(AA-*co*-NIPAAm-*co*-NIPAAmPA) absorbs mainly in the UV radiation range between 200 and 350 nm depending on solvents of choice, while fluorescent emission maxima of the polymer between 400 and 450 nm were recorded. Computational studies by DFT reveal effects of NIPAAmPA moieties on electronic transitions between highest occupied molecular orbital (HOMO) and lowest unoccupied molecular orbital (LUMO). MBAAm-cl-GG-g-P(AA-*co*-NIPAAm-*co*-NIPAAmPA) shows biocompatibility to normal mammalian Madin-Darby canine kidney (MDCK) cells and a certain degree of cytotoxicity against human osteosarcoma (HOS) cancer cells. The obtained polymer can also be exploited for fluorescent sensing of Pb^{2+}, based on reversible fluorescence quenching of the polymer due to the disruption of hydrogen bonding network and breakdown of polymer aggregates in the presence of Pb^{2+} metal ions.

3.3.3.2. Acrylamide (AAm) monomer. Nonionic biocompatible polyacrylamide (PAAm) and its derivatives have been widely found in various industries, clinical and environmental systems [266–268].

Recently, AAm mononers have also been employed to fabricate new AAm grafted GG (GG-g-PAAm) materials. For instance, Sand and Vyas reported the grafting reaction in the presence of tetra(ethyleneglycol) diacrylate (TEGDA) cross-linker to yield TEGDA-cross-linked GG-g-PAAm (TEGDA-cl-GG-g-PAAm) absorbent [269]. 0.8 wt% of KPS initiator was found as an optimum concentration in terms of reaction yield and water absorbing capacity of the obtained material. Varying concentrations of TEGDA cross-linkers from 0.4 to 1.2 wt% shows no significant effect on the reaction yield but decreases the water absorbing capacity. The optimized TEGDA-cl-GG-g-PAAm has swelling capacities of 80 g g^{-1} for deionizied water and 22 g g^{-1} for 0.8 wt% sodium chloride solution.

In addition, Mahto and Mishra prepared borax-cross-linked GG-g-PAAm (borax-cl-GG-g-PAAm) with grafting yield and efficiency up to 795.6 %, 79.5 % respectively, and tested the material as an adsorbent for removal of reactive blue 19 (RB19) textile dye [270]. The optimized

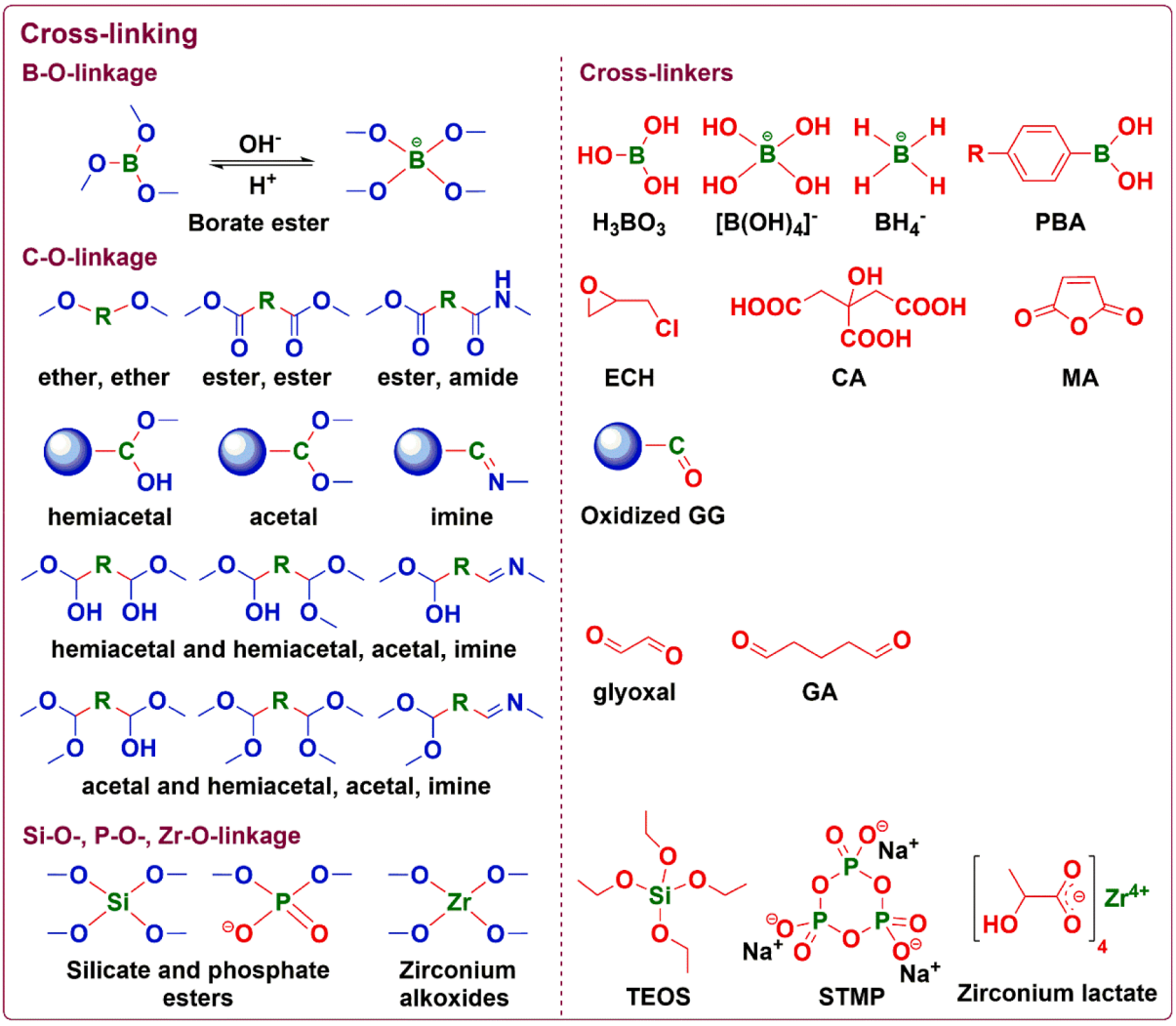

Fig. 7. Cross-linking of GG and its derivatives via B-O-, C-O-, Si-O-, P-O-, Zr-O-linkages (left) and reported cross-linkers (right).

borax-cl-GG-g-PAAm can adsorb up to 1073.84 mg g^{-1} with removal percentage of 80 %. Mildly acidic pH around 6.0 allows the best electrostatic interaction between sulfonate groups of RB19 and amide functional groups from borax-cl-GG-g-PAAm.

Meanwhile, Elsaeed and coworkers fabricated MBAAm-cross-linked AAm-*co*-2-acrylamido-2-methyl-1-propane sulfonic acid (AMPS) grafted GG [MBAAm-cl-GG-g-P(AAm-*co*-AMPS)] hydrogel and further modified this into a composite with biochar carbonic material [MBAAm-cl-GG-g-P(AAm-*co*-AMPS)/biochar] for enhanced oil recovery via polymer flooding under highly saline reservoir conditions [271]. AMPS contains both nonionic and ionic moieties, which can enhance salt tolerance, swelling capacity of the polymer and oil displacement from the sandstone surface during the secondary oil recovery process up to around 12 %, with the optimum polymer concentration of 5 g L^{-1}. Incorporating hydrophobic biochar into the polymer matrix offers high surface area and an enhancement in secondary oil recovery process of around 6 % with lower optimum polymer concentration of 2 g L^{-1}.

Recently, Palem et al. developed multifunctional nanocomposite hydrogels, which consist of MBAAm-cross-linked AAm-*co*-2-acrylamidoglycolic acid (AGA) grafted GG and Ag nanoparticles (Ag NPs) [MBAAm-cl-GG-g-P(AAm-*co*-AGA)/Ag NPs], for various applications [272]. Ag NPs were incorporated into the polymer matrix via diffusion of free Ag^+ ions, followed by reduction of Ag^+ by active components such as quinones, emodin and rhein in rhubarb-stem extract *(Rheum rhabarbarum)* bio-reductants. MBAAm-cl-GG-g-P(AAm-*co*-AGA) shows pH-responsiveness due to the presence of carboxylic acids, and better biodegradability than its nanocomposite with Ag NPs, which can be attributed to the antimicrobial activity of Ag NPs. Further confirmation on antimicrobial activity of the nanocomposites against *B. subtilis* (ATCC 6633) and *E. coli* (ATCC 25922) has also been reported. Moreover, the introduction of Ag NPs into the polymer matrix increases the matrix porosity, resulting in better drug encapsulation of 5-fluorouracil (FU), which was chosen as an anticancer model medication to study the drug release behavior of MBAAm-cl-GG-g-P(AAm-*co*-AGA)/Ag NPs. Under physiological pH, FU can be released due to the deprotonation of carboxylic acid groups and swelling of the polymer. Furthermore, the developed composite also shows catalytic potential for the reduction of p-nitrophenol to p-aminophenol using sodium borohydride ($NaBH_4$) reducing agent in aqueous solution.

3.3.3.3. Other monomers. Das and Subuddhi grafted NIPAAm, which is a thermo-responsive derivative of AAm, onto GG using APS and TEMED activator [273]. While NIPAAm has a low critical solution temperature of around 33 °C, its low mechanical stability, biocompatibility and sustained drug-releasing ability can be improved by combining with GG.

The obtained graft polymer was further cross-linked by TEOS to yield TEOS-cross-linked NIPAAm grafted GG (TEOS-cl-GG-g-PNIPAAm) hydrogel to show good biocompatibility towards L-929 rat fibroblasts. FU was also chosen to study drug release behavior of the hydrogel. By increasing weight percentage of GG comparing to NIPAAm, longer drug release time and slower drug release rate of the hydrogel can be obtained. In addition, host-guess complexation between β-cyclodextrin (β-CD) and FU was also carried out to form β-CD/FU complex, therefore, enhancing the aqueous stability, solubility and bioavailability of the medication.

Besides, AGA was grafted to GG by Palem and coworkers to obtain AGA grafted GG (GG-g-PAGA) polymer [274]. Ag^+ ions were then dispersed in the polymer system and reduced to Ag NPs of around 5.4 nm by $NaBH_4$, which also allowed the cross-linking of GG-g-PAGA to form $NaBH_4$-cross-linked GG-g-PAGA/Ag NPs ($NaBH_4$-cl-GG-g-PAGA/Ag NPs) nanocomposite. The prepared nanocomposite possesses self-healing property, stretchability, antibacterial activity against *E. coli*, *S. aureus*, *P. aeruginosa*, cytocompatibility to human skin fibroblast (CCD-986sk) cell lines and therefore, a promising candidate for wound dressing and drug release [275].

Singh et al. recently prepared MBAAm-cross-linked AMPS grafted GG (MBAAm-cl-GG-g-PAMPS) as a corrosion inhibitor for copper in NaCl media [276]. The corrosion inhibition efficiency of GG-g-PAMPS was evaluated by electrochemistry and reported up to 95 % at 600 mg L^{-1} concentration. In addition, they also fabricated ethyl acrylate (EA) grafted GG (GG-g-PEA) using KPS and H_2AA activator at mild temperature (35 °C) [277]. The obtained GG-g-PEA graft polymer was tested as a corrosion inhibitor to reduce P110 steel corrosion in acidic environment. The spontaneous adsorption of GG-EEA onto P110 steel surface was found both physical and chemical. Molecular dynamic simulations were performed and indicated an improvement in adsorption capacity of GG-g-PEA onto the steel surface, comparing to pristine GG. The corrosion inhibition efficiency of GG and GG-g-PEA for P110 steel was reported as 77.5 and 92.3 % respectively at 500 mg L^{-1} concentration.

Moreover, CAN and microwave irradiation was used by Mahto and Mishra to graft 2-hydroxyl ethyl methacrylate (HEMA) to GG (GG-g-PHEMA) via three cycles of MW irradiation and cooling in ice bath [278]. Molar ratio of GG, HEMA and CAN was optimized to obtain the grafting percentage of 1142 % and grafting efficiency (GE) of 114.22. To demonstrate the drug delivery capacity of GG-g-PHEMA, the graft polymer together with PVP binder, 5-aminosalicylic acid (ASA) medication, silicon dioxide (SiO_2) and magnesium stearate were physically mixed and formulated into GG-g-PHEMA/ASA tablets. Swelling of GG-g-PHEMA was observed under all tested pH of 1.2, 6.8, 7.4, allowing the gradual release of ASA from the tablets under these pH conditions.

3.4. Cross-linking

3.4.1. B-O-linkage

Borate esters have been widely employed as cross-linkers for polyol compounds and various polymers [279–281]. Commercially available borax [anhydrous sodium tetraborate ($Na_2B_4O_7$), sodium tetraborate pentahydrate ($Na_2B_4O_7{\cdot}5H_2O$), sodium tetraborate decahydrate [$Na_2B_4O_7{\cdot}10H_2O$ or $Na_2[B_4O_5(OH)_4]{\cdot}8H_2O$]] is normally used as a source of boron for cross-linking. In aqueous media, borax dissociates to hydrated tetraborate [$[B_4O_5(OH)_4]^{2-}_{(aq)}$, Eq. (10), (11)], followed by further hydrolysis to yield a mixture of boric acid [$B(OH)_{3(aq)}$, $pK_a \approx 9.14$] and tetrahydroxyborate conjugate base, [$[B(OH)_4]^-_{(aq)}$, Eq. (12)]. The molar ratio between boric acid and tetrahydroxyborate varies accordingly to pH of the media [Eq. (13)], and they can also react with alcohol groups to form borate ester linkages [Eq. (14), (15)]. Moreover, sodium borohydride ($NaBH_4$) is also exploited as a common source of boron. In aqueous media, $NaBH_4$ hydrolyzes to form hydrated sodium metaborate [$NaBO_2$, Eq. (16)], especially in the presence of catalysts [282,283]. Further hydrolysis of $NaBO_2$ yields $[B(OH)_4]^-$ [Eq. (17)], which allows the cross-linking with vicinal diol groups via the formation of borate ester bonds (Fig. 7).[284].

$$Na_2B_4O_{7(s)} + 2\ H_2O_{(l)} \rightarrow 2Na^+_{(aq)} + [B_4O_5(OH)_4]^{2-}_{(aq)} \quad (10)$$

$$Na_2[B_4O_5(OH)_4]{\cdot}8H_2O_{(s)} \rightarrow 2Na^+_{(aq)} + [B_4O_5(OH)_4]^{2-}_{(aq)} \quad (11)$$

$$[B_4O_5(OH)_4]^{2-}_{(aq)} + 5\ H_2O_{(l)} \rightleftharpoons 2B(OH)_{3(aq)} + 2\ [B(OH)_4]^-_{(aq)} \quad (12)$$

$$B(OH)_{3(aq)} + 2\ H_2O_{(l)} \rightleftharpoons [B(OH)_4]^-_{(aq)} + H_3O^+_{(aq)} \quad (13)$$

$$B(OH)_{3(aq)} + 3\ ROH_{(aq)} \rightarrow B(OR)_{3(aq)} + 3\ H_2O_{(l)} \quad (14)$$

$$[B(OH)_4]^-_{(aq)} + 4\ ROH_{(aq)} \rightarrow [B(OR)_4]^-_{(aq)} + 4\ H_2O_{(l)} \quad (15)$$

$$NaBH_{4(s)} + (2 + x)\ H_2O_{(l)} \rightarrow NaBO_2{\cdot}xH_2O_{(aq)} + 4\ H_{2(g)} \quad (16)$$

$$NaBO_{2(s)} + 2\ H_2O_{(l)} \rightarrow Na^+_{(aq)} + [B(OH)_4]^-_{(aq)} \quad (17)$$

Boron-based cross-linkers can be introduced to the GG polymeric structures by simple dissolution and mixing of borax, boric acid or sodium borohydride with GG in aqueous media [285–287]. Recently, Pugliese and Gelain prepared and cross-linked a self-assembly peptide (SAP) NH_2-FAQRVPPGGGLDLKLDLKLDLK-$CONH_2$ and GG using borax at pH 8.5 to form self-healing borax-cross-linked GG-SAP (borax-cl-GG-SAP) composite hydrogel [288]. GG was combined with SAP to enhance elasticity, mechanical strength and thermo-responsiveness of SAP. Meanwhile, Cao and coworkers used borax to cross-link GG in the presence of gellan gum (GelG) to form borax-cross-linked GG-GelG (borax-cl-GG-GelG) composite hydrogel [289]. At room temperature, GelG adopts hard and brittle double helix conformation with good compatibility to GG. The borax-cl-GG-GelG hydrogel exhibits electrical conductivity due to the presence of borate ions, as well as self-healing properties because of dynamic borate and hydrogen bonds. Mechanical deformation of the hydrogel can produce electrical signals, allowing the fabrication of flexible hydrogel-based strain sensors for detecting and monitoring human motions with good repeatability and reliability.

Additionally, a wide range of inorganic particles has been incorporated into GG-based polymeric matrices to form composites. For example, Dassanayake et al. recently cross-linked GG by borax to yield borax-cross-linked GG (borax-cl-GG) [290]. Then, permanganate(VII) (MnO_4^-) precursor ions were allowed to diffuse into the borax-cl-GG polymeric structure and oxidize -OH groups of GG. Meanwhile, MnO_4^- was reduced into manganate(VI) (MnO_4^{2-}) ions, and eventually to manganese dioxide (MnO_2) nanoparticles under alkaline pH, resulting in the formation of borax-cl-GG/MnO_2 brownish nanocomposite. Potential applications of B-cl-GG/MnO_2 were demonstrated based on oxidative decolorization of MB dye. Comparing to MnO_2 nanoparticle reference, the borax-cl-GG/MnO_2 photocatalyst has a much better oxidative decolorization capacity under the tested pH of 4, 7 and 10.

Moreover, Wang and coworkers employed $NaBH_4$ to cross-link GG with a composite of Pd heterogeneous catalyst nanoparticles (Pd NPs) and cellulose nanocrystal (CNC) system (CNC/Pd NPs) [291]. A homogeneous mixture of $PdCl_2$ and CNC was firstly prepared, followed by the reduction of Pd^{2+} to Pd NPs by $NaBH_4$ reducing agent to form CNC/Pd NPs nanocomposite. Then, the obtained CNC/Pd NPs nanocomposite was mixed with GG and $NaBH_4$ to yield $NaBH_4$-cross-linked GG/CNC/Pd NPs ($NaBH_4$-cl-GG/CNC/Pd NPs) nanocomposite. The boron-based cross-linkers are temperature-sensitive, which allows the sol–gel transition by changing the temperature of $NaBH_4$-cl-GG/CNC/Pd NPs, hence, the catalytic reactions and recycling of Pd NPs. The catalytic activity of $NaBH_4$-cl-GG/CNC/Pd NPs was tested on Suzuki cross coupling reactions between various aryl halides and aryl boronic acids

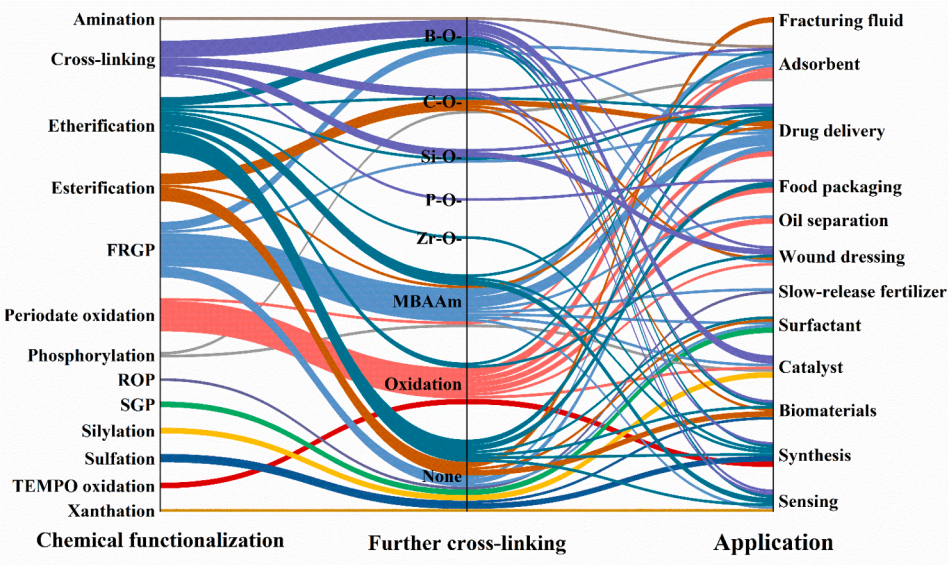

Fig. 8. Summary on different chemical functionalization, further cross-linking approaches and potential applications of GG and its derivatives.

and showed promising efficiency and recyclability.

Recently, Talodthaisong and coworkers cross-linked Cur-stabilized Ag NPs (Cur-Ag NPs) and GG to develop borax-cross-linked GG/Cur-Ag NPs (borax-cl-GG/Cur-Ag NPs) nanocomposite [292]. Borax was used to cross-link GG in the presence of Cur-stabilized Ag NPs, which were obtained from thermal decomposition of $AgNO_3$, resulting in injectable self-healing borax-cl-GG/Cur-Ag NPs hydrogel. The hydrogel is also pH- and temperature-responsive due to the responsiveness of borate ester cross-linkers present in the hydrogel structure. In addition, borax-cl-GG/Cur-Ag NPs also possesses antibacterial activity, with greater inhibition capacity against gram-positive bacteria (*E. coli, P. aeruginosa*) compared to gram-negative bacteria (*S. Aureus*).

Meanwhile, Deka et al. employed $NaBH_4$ as a reducing agent for the preparation of Ag NPs from $AgNO_3$, and a cross-linker for GG and PVA polymeric matrix [293]. The fabricated $NaBH_4$-cross-linked GG/PVA/Ag NPs ($NaBH_4$-cl-GG-PVA/Ag NPs) nanocomposite also shows pH-responsiveness, injectability, improved mechanical strength and antibacterial activity against *E. coli*. Moreover, $NaBH_4$-cl-GG-PVA/Ag NPs is a promising catalyst for reduction of nitrobenzene to aniline using $NaBH_4$ reductant.

3.4.2. C-O-linkage

Various C-based functional groups have been employed in the cross-linking of GG and its derivatives (Fig. 7). For example, epoxide and chloro groups on ECH can easily form ether groups for cross-linking [180]. Moreover, carboxylic acid anhydrides can be used for cross-linking via the formation of ester, amide bonds, and/or aza-Michael addition reaction [85,142]. Aldehyde functional groups, which might be found directly on oxidized GG and its derivatives, or from external cross-linkers such as GA, have also shown efficient cross-linking with other polysaccharides via the formation of hemiacetal, acetal and/or imine linkages [122,123,136,137,149,200,208–213,294].

Additionally, Bag and coworkers employed GA to cross-link GG into a polymeric structure in the presence of iron oxide nanoparticles (Fe_3O_4 NPs) for the fabrication of GA-cross-linked GG/Fe_3O_4 NPs (GA-cl-GG/Fe_3O_4 NPs) nanocomposite [295]. Firstly, Fe_3O_4 NPs were synthesized by coprecipitation method with an assistance of citric acid surfactant. Then, GG was cross-linked in the presence of the Fe_3O_4 NPs to obtain the nanocomposite final product, which shows no genotoxic effects on Drosophila melanogaster fruit flies.

To enhance mechanical strength and self-healing properties of natural polysaccharide-based hydrogels, Rao et al. combined two self-healing mechanisms, namely, covalent cross-linking between GG, sodium alginate (SAL) by GA, and coordination bonds between SAL, dopamine (DA) and Fe^{3+} [296]. Stellate mesoporous silica (STMS) nanoparticles with high specific surface area and large pore volume, were chosen to store GA cross-linking agent for its gradual release, and to offer a surface for the preparation of polydopamine. The obtained PDA-coated GA-loaded STMS (PDA-STMS/GA) nanoparticles were dispersed in a mixture of Fe^{3+}, GG and SAL to fabricate GA, Fe^{3+}-cross-linked GG/SAL/DA-STMS/GA (GA, Fe^{3+}-cl-GG/SAL/DA-STMS/GA) nanocomposite. The nanocomposite product possesses excellent self-healing properties, tensile strength (up to 7.0 MPa) and can also be used to develop strain electronic sensors.

Besides GA, glyoxal can also be employed as a cross-linker and was used by Gupta et al. to develop glyoxal-cross-linked GG/activated C (glyoxal-cl-GG/activated C) nanocomposite [297]. The obtained nanocomposite has been found as a promising dye adsorbent for wastewater treatment, with adsorption capacity of 831.82 mg g^{-1} at 30 °C and good recyclability.

3.4.3. Si-O-linkage

TEOS is a typical Si-containing precursor for cross-linking GG and its derivatives [81,86,273]. Recently, Butt el al. blended a mixture of GG, CS, polyethylene glycol (PEG), cephradine (CED) antibiotic medication in water and chemically cross-linked these polymers by TEOS to develop a novel pH-sensitive TEOS-cross-linked GG-CS-PEG/CED (TEOS-cl-GG-CS-PEG/CED) hydrogel for controlled drug release of CED [298]. Better swelling behavior of the prepared hydrogels was recorded under acidic environment (pH around 4), comparing to neutral and alkaline pH. This might be attributed to the protonation of -NH_2 functional groups in CS, resulting in electrostatic repulsion and swelling of the polymeric matrix. The loaded CED can be released from the hydrogels in a controlled manner, up to 85 % in PBS and 82.4 % in simulated intestinal fluid (SIF) over 130 min.

Meanwhile, Khan and coworkers also used TEOS in cross-linking GG and arabinoxylan (ARX) to fabricate TEOS-cross-linked GG-ARX (TEOS-cl-GG-ARX) hydrogels, as well as GG, CS and PVA to prepare TEOS-cross-linked GG-CS-PVA (TEOS-cl-GG-CS-PVA) hydrogels for wound dressing [299,300]. Maximum swelling of TEOS-cl-GG-ARX and TEOS-cl-GG-CS-PVA hydrogels were reported at pH 7 and 4 respectively. Silver sulfadiazine (SSD) antibiotic was incorporated into TEOS-cl-GG-ARX (TEOS-cl-GG-ARX/SSD) hydrogel. This drug release hydrogel shows antimicrobial activity against skin disease-causing bacteria such as

gram-negative *P. aeruginosa*, gram-positive *S. aureus*, and noncytotoxic responses towards mouse MC3T3-E1 cell line. Besides, paracetamol was loaded into TEOS-cl-GG-CS-PVA (TEOS-cl-GG-CS-PVA/paracetamol) and could be released up to 98 % in PBS medium at pH 7.4. The TEOS-cl-GG-CS-PVA/paracetamol hydrogels also possess antibacterial activity against gram-negative (*E. coli*, *P. aeruginosa*) and gram-positive (*B. cereus*, *S. aureus*) bacteria.

3.4.4. P-O-linkage

Aydogdu and coworkers recently demonstrated the cross-linking of GG in the presence of SL emulsion stabilizer, glycerol plasticizer, orange oil, using non-toxic, FDA-approved STMP cross-linker under alkaline condition (pH 12) [301]. The fabricated STMP-cross-linked GG/orange oil (STMP-cl-GG/orange oil) films were tested for food packaging. Incorporation of orange oil into the films and crosslinking of GG decrease the water dissolvability and surface water wettability of these films, hence, enhancing their hydrophobicity. In addition, the films also show antimicrobial activity against gram-negative (*E. coli*) and gram-positive (*B. subtilis*) bacteria.

4. Conclusions

In the recent past, various chemical modification approaches of natural GG polysaccharide and its derivatives have been explored to alter their properties and extend their applicability in numerous fields (Fig. 8). Among the reported functionalization methods, etherification, esterification, FRGP, periodate-mediated oxidation and cross-linking have been ones of the most commonly used chemical reactions, while other reaction pathways such as amination, phosphorylation, ROP, SGP, silylation, sulfation, TEMPO-mediated oxidation and xanthation are also promising for future research. Moreover, further cross-linking of chemically modified GG has also been of profound interest and can be done by employing different chemical cross-linking methods. Chemical derivatives of natural GG are versatile polysaccharides that can be used in numerous fields, from biomedicine, wound dressing, drug delivery, to catalysis, sensing, food packaging, surfactant, slow-release fertilizer, metal corrosion inhibition, waste treatment, oil separation and recovery. With a fascinating increase in the amount of published work on GG, this review can be used as a library of choice for readers who are searching for chemical modification approaches of GG and its derivatives to develop and explore novel properties and applications of GG-based advanced materials (Table 2).

CRediT authorship contribution statement

Trung-Anh Le: Conceptualization, Methodology, Investigation, Writing – original draft, Writing – review & editing. **Tan-Phat Huynh:** Conceptualization, Supervision, Writing – review & editing.

Declaration of Competing Interest

The authors declare the following financial interests/personal relationships which may be considered as potential competing interests: Tan-Phat Huynh reports financial support was provided by Abo Akademi University Faculty of Science and Engineering. Tan-Phat Huynh reports financial support was provided by Academy of Finland. Trung-Anh Le reports was provided by Magnus Ehrnrooth foundation. Tan-Phat Huynh reports financial support was provided by Liv och Hälsa Foundation.

Data availability

The authors do not have permission to share data.

Acknowledgment

T.-A. Le acknowledges the DNMR doctoral fellowship from Åbo Akademi University, Magnus Ehrnrooth foundation and Finnish Society of Sciences & Letters; T.-P. Huynh acknowledges the starting fund from the Liv och Hälsa Foundation and the Academy of Finland (Grant No. 323240) for financial support.

References

[1] J. Rogelj, O. Geden, A. Cowie, A. Reisinger, Net-zero emissions targets are vague: three ways to fix, Nature 591 (2021) 365–368, https://doi.org/10.1038/d41586-021-00662-3.
[2] L. Jeffry, M.Y. Ong, S. Nomanbhay, M. Mofijur, M. Mubashir, P.L. Show, Greenhouse gases utilization: A review, Fuel 301 (2021), 121017, https://doi.org/10.1016/j.fuel.2021.121017.
[3] J. González-Martín, N.J.R. Kraakman, C. Pérez, R. Lebrero, R. Muñoz, A state–of–the-art review on indoor air pollution and strategies for indoor air pollution control, Chemosphere 262 (2021), 128376, https://doi.org/10.1016/j.chemosphere.2020.128376.
[4] P. Li, X. Wang, M. Su, X. Zou, L. Duan, H. Zhang, Characteristics of Plastic Pollution in the Environment: A Review, Bull. Environ. Contam. Toxicol. 107 (2021) 577–584, https://doi.org/10.1007/s00128-020-02820-1.
[5] T. Le, T. Huynh, The Combination of Hydrogen and Methanol Production through Artificial Photosynthesis—Are We Ready Yet? ChemSusChem 11 (2018) 2654–2672, https://doi.org/10.1002/cssc.201800731.
[6] R.K. Goswami, S. Mehariya, P.K. Obulisamy, P. Verma, Advanced microalgae-based renewable biohydrogen production systems: A review, Bioresour. Technol. 320 (2021), 124301, https://doi.org/10.1016/j.biortech.2020.124301.
[7] A.-E.-L. Hesham, T. Kaur, R. Devi, D. Kour, S. Prasad, N. Yadav, et al., Current Trends in Microbial Biotechnology for Agricultural Sustainability: Conclusion and Future, Challenges (2021) 555–572, https://doi.org/10.1007/978-981-15-6949-4_22.
[8] P. Horton, S.P. Long, P. Smith, S.A. Banwart, D.J. Beerling, Technologies to deliver food and climate security through agriculture, Nat. Plants 7 (2021) 250–255, https://doi.org/10.1038/s41477-021-00877-2.
[9] Jana S, Maiti S, Jana S, Sen KK, Nayak AK. Guar gum in drug delivery applications. Natural Polysaccharides in Drug Delivery and Biomedical Applications, Elsevier; 2019, p. 187–201. 10.1016/B978-0-12-817055-7.00007-8.
[10] A. George, P.A. Shah, P.S. Shrivastav, Guar gum: Versatile natural polymer for drug delivery applications, Eur. Polym. J. 112 (2019) 722–735, https://doi.org/10.1016/j.eurpolymj.2018.10.042.
[11] Q. Huang, S. Liu, G. Wang, B. Wu, Y. Zhang, Coalbed methane reservoir stimulation using guar-based fracturing fluid: A review, J. Nat. Gas Sci. Eng. 66 (2019) 107–125, https://doi.org/10.1016/j.jngse.2019.03.027.
[12] A.K. Nayak, M.S. Hasnain, K. Pal, I. Banerjee, D. Pal, Gum-based hydrogels in drug deliveryBiopolymer-Based Formulations, Elsevier (2020) 605–645, https://doi.org/10.1016/B978-0-12-816897-4.00025-4.
[13] M. Dehghani Soltani, H. Meftahizadeh, M. Barani, A. Rahdar, S.M. Hosseinikhah, M. Hatami, et al., Guar (Cyamopsis tetragonoloba L.) plant gum: From biological applications to advanced nanomedicine, Int. J. Biol. Macromol. 193 (2021) 1972–1985, https://doi.org/10.1016/j.ijbiomac.2021.11.028.
[14] L. Saya, V. Malik, A. Singh, S. Singh, G. Gambhir, W.R. Singh, et al., Guar gum based nanocomposites: Role in water purification through efficient removal of dyes and metal ions, Carbohydr. Polym. 261 (2021), 117851, https://doi.org/10.1016/j.carbpol.2021.117851.
[15] D. Verma, S.K. Sharma, Recent advances in guar gum based drug delivery systems and their administrative routes, Int. J. Biol. Macromol. 181 (2021) 653–671, https://doi.org/10.1016/j.ijbiomac.2021.03.087.
[16] M.-E.-S. Abdel-raouf, A. Sayed, M. Mostafa, Application of Guar Gum and Its Derivatives in, Agriculture (2022) 1–17, https://doi.org/10.1007/978-3-030-76523-1_5-1.
[17] V. Adimule, S.S. Kerur, S. Chinnam, B.C. Yallur, S.S. Nandi, Guar Gum and its Nanocomposites as Prospective Materials for Miscellaneous Applications: A Short Review, Top. Catal. (2022), https://doi.org/10.1007/s11244-022-01587-5.
[18] S. Kaur, S. Santra, Recent Progress in Chemical Modification of the Natural Polysaccharide Guar Gum, Curr. Org. Synth. 19 (2022) 197–219, https://doi.org/10.2174/1570179418666211109105416.
[19] G. Sharma, S. Sharma, A. Kumar, A.H. Al-Muhtaseb, M.u. Naushad, A.A. Ghfar, et al., Guar gum and its composites as potential materials for diverse applications: A review, Carbohydr. Polym. 199 (2018) 534–545, https://doi.org/10.1016/j.carbpol.2018.07.053.
[20] S. Thakur, B. Sharma, A. Verma, J. Chaudhary, S. Tamulevicius, V.K. Thakur, Recent approaches in guar gum hydrogel synthesis for water purification, Int. J. Polym. Anal. Charact. 23 (2018) 621–632, https://doi.org/10.1080/1023666X.2018.1488661.
[21] A.M.A. Hasan, M.E. Abdel-Raouf, Applications of guar gum and its derivatives in petroleum industry: A review, Egypt. J. Pet. 27 (2018) 1043–1050, https://doi.org/10.1016/j.ejpe.2018.03.005.
[22] R.J. Chudzikowski, Guar gum and its applications, J. Soc. Cosmet. Chem. 22 (1971) 43–60.

[23] E.R. Sujatha, S. Saisree, Geotechnical behaviour of guar gum-treated soil, Soils Found. 59 (2019) 2155–2166, https://doi.org/10.1016/j.sandf.2019.11.012.
[24] S. Anandha Kumar, E.R. Sujatha, A. Pugazhendi, M.T. Jamal, Guar gum-stabilized soil: a clean, sustainable and economic alternative liner material for landfills, Clean Techn. Environ. Policy (2021), https://doi.org/10.1007/s10098-021-02032-z.
[25] A.A.B. Moghal, K.V. Vydehi, State-of-the-art review on efficacy of xanthan gum and guar gum inclusion on the engineering behavior of soils, Innov. Infrastr. Sol. 6 (2021) 108, https://doi.org/10.1007/s41062-021-00462-8.
[26] T. Radvand, V. Toufigh, Properties of concrete containing Guar gum, Eur. J. Environ. Civ. Eng. 26 (2022) 2736–2752, https://doi.org/10.1080/19648189.2020.1767217.
[27] G. Palumbo, K. Berent, E. Proniewicz, J. Banaś, Guar Gum as an Eco-Friendly Corrosion Inhibitor for Pure Aluminium in 1-M HCl Solution, Materials 12 (2019) 2620, https://doi.org/10.3390/ma12162620.
[28] K.O. Shamsheera, A.R. Prasad, P.K. Jaseela, A. Joseph, Effect of surfactant addition to Guar Gum and protection of mild steel in hydrochloric acid at high temperatures: Experimental and theoretical studies, J. Mol. Liq. 331 (2021), 115807, https://doi.org/10.1016/j.molliq.2021.115807.
[29] S.E. Atakoohi, P. Naeiji, K. Peyvandi, S.S. Mollashahi, The experimental study and molecular dynamic simulation of THF hydrate growth kinetics in the presence of Arabic and Guar gum: New approaches in promotion of THF hydrate formation, J. Mol. Liq. 325 (2021), 115249, https://doi.org/10.1016/j.molliq.2020.115249.
[30] S. Mollashahi Sanatgar, K. Peyvandi, New edible additives as green inhibitors for preventing methane hydrate formation, J. Environ. Chem. Eng. 7 (2019), 103172, https://doi.org/10.1016/j.jece.2019.103172.
[31] P. Gupta, V.C. Nair, J.S. Sangwai, Phase Equilibrium of Methane Hydrate in Aqueous Solutions of Polyacrylamide, Xanthan Gum, and Guar Gum, J. Chem. Eng. Data 64 (2019) 1650–1661, https://doi.org/10.1021/acs.jced.8b01194.
[32] S.K. Bajpai, A. D'Souza, B. Suhail, Carbon dots from Guar Gum: Synthesis, characterization and preliminary in vivo application in plant cells, Mater. Sci. Eng. B 241 (2019) 92–99, https://doi.org/10.1016/j.mseb.2019.02.014.
[33] Y. Cheng, H. Guo, X. Li, X. Wu, X. Xu, L. Zheng, et al., Rational design of ultrahigh loading metal single-atoms (Co, Ni, Mo) anchored on in-situ pre-crosslinked guar gum derived N-doped carbon aerogel for efficient overall water splitting, Chem. Eng. J. 410 (2021), 128359, https://doi.org/10.1016/j.cej.2020.128359.
[34] L.-H. Huang, C.-C. Li, Effects of interactions between binders and different-sized silicons on dispersion homogeneity of anodes and electrochemistry of lithium-silicon batteries, J. Power Sources 409 (2019) 38–47, https://doi.org/10.1016/j.jpowsour.2018.10.087.
[35] Z.-W. Yin, T. Zhang, S.-J. Zhang, Y.-P. Deng, X.-X. Peng, J.-Q. Wang, et al., Understanding the role of water-soluble guar gum binder in reducing capacity fading and voltage decay of Li-rich cathode for Li-ion batteries, Electrochim. Acta 351 (2020), 136401, https://doi.org/10.1016/j.electacta.2020.136401.
[36] S. Kaur, S. Santra, Application of Guar Gum and its Derivatives as Green Binder/Separator for Advanced Lithium-Ion Batteries, ChemistryOpen 11 (2022), https://doi.org/10.1002/open.202100209.
[37] Y. Huang, J. Zhang, J. Liu, Z. Li, S. Jin, Z. Li, et al., Flexible and stable quasi-solid-state zinc ion battery with conductive guar gum electrolyte, Mater. Today Energy 14 (2019), 100349, https://doi.org/10.1016/j.mtener.2019.100349.
[38] R. Xu, J. Zhou, H. Gong, L. Qiao, Y. Li, D. Li, et al., Environment-friendly degradable zinc-ion battery based on guar gum-cellulose aerogel electrolyte, Biomater. Sci. 10 (2022) 1476–1485, https://doi.org/10.1039/D1BM01747K.
[39] U. Bhardwaj, A. Sharma, A. Mathur, A. Halder, H.S. Kushwaha, Novel guar-gum electrolyte to aggrandize the performance of $LaMnO_3$ perovskite-based zinc-air batteries. Electrochem.Sci.Adv. 2 (2022) https://doi.org/10.1002/elsa.202100056.
[40] A. Gunasekaran, A. Sorrentino, A.M. Asiri, S. Anandan, Guar gum-based polymer gel electrolyte for dye-sensitized solar cell applications, Sol. Energy 208 (2020) 160–165, https://doi.org/10.1016/j.solener.2020.07.084.
[41] D. Mudgil, S. Barak, B.S. Khatkar, Guar gum: processing, properties and food applications—A Review, J. Food Sci. Technol. 51 (2014) 409–418, https://doi.org/10.1007/s13197-011-0522-x.
[42] Gupta S, Variyar PS. Guar Gum: A Versatile Polymer for the Food Industry. Biopolymers for Food Design, Elsevier; 2018, p. 383–407. 10.1016/B978-0-12-811449-0.00012-8.
[43] F. Liu, W. Chang, M. Chen, F. Xu, J. Ma, F. Zhong, Film-forming properties of guar gum, tara gum and locust bean gum, Food Hydrocoll. 98 (2020), 105007, https://doi.org/10.1016/j.foodhyd.2019.03.028.
[44] E. Kirtil, A. Aydogdu, T. Svitova, C.J. Radke, Assessment of the performance of several novel approaches to improve physical properties of guar gum based biopolymer films, Food Packag. Shelf Life 29 (2021), 100687, https://doi.org/10.1016/j.fpsl.2021.100687.
[45] T. Gasti, V.D. Hiremani, S.S. Kesti, V.N. Vanjeri, N. Goudar, S.P. Masti, et al., Physicochemical and Antibacterial Evaluation of Poly (Vinyl Alcohol)/Guar Gum/Silver Nanocomposite Films for Food Packaging Applications, J. Polym. Environ. 29 (2021) 3347–3363, https://doi.org/10.1007/s10924-021-02123-4.
[46] R.K. Deshmukh, K. Akhila, D. Ramakanth, K.K. Gaikwad, Guar gum/carboxymethyl cellulose based antioxidant film incorporated with halloysite nanotubes and litchi shell waste extract for active packaging, Int. J. Biol. Macromol. 201 (2022) 1–13, https://doi.org/10.1016/j.ijbiomac.2021.12.198.
[47] A. Theocharidou, I. Mourtzinos, C. Ritzoulis, The role of guar gum on sensory perception, on food function, and on the development of dysphagia supplements – A review, Food Hydrocolloid Health 2 (2022), 100053, https://doi.org/10.1016/j.fhfh.2022.100053.
[48] A. Indurkar, P. Bangde, M. Gore, P. Reddy, R. Jain, P. Dandekar, Optimization of guar gum-gelatin bioink for 3D printing of mammalian cells, Bioprinting 20 (2020) e00101.
[49] M.Y. Rezk, M. Zeitoun, A.N. El-Shazly, M.M. Omar, N.K. Allam, Robust photoactive nanoadsorbents with antibacterial activity for the removal of dyes, J. Hazard. Mater. 378 (2019), 120679, https://doi.org/10.1016/j.jhazmat.2019.05.072.
[50] J. Balachandramohan, T. Sivasankar, M. Sivakumar, Facile sonochemical synthesis of Ag_2O-guar gum nanocomposite as a visible light photocatalyst for the organic transformation reactions, J. Hazard. Mater. 385 (2020), 121621, https://doi.org/10.1016/j.jhazmat.2019.121621.
[51] J. Balachandramohan, R. Singh, T. Sivasankar, S. Manickam, Sonochemical synthesis of highly efficient Ag_3PO_4-Guar gum nanocomposite with photo-oxidation property under visible light irradiation, Chem. Eng. Process. - Process Intesif. 168 (2021), 108549, https://doi.org/10.1016/j.cep.2021.108549.
[52] T.M. Aminabhavi, M.N. Nadagouda, S.D. Joshi, U.A. More, Guar gum as platform for the oral controlled release of therapeutics, Expert Opin. Drug Deliv. 11 (2014) 753–766, https://doi.org/10.1517/17425247.2014.897326.
[53] Seeli DS, Prabaharan M. Prospects of Guar Gum and its Derivatives as Biomaterials. Handbook of Polymers for Pharmaceutical Technologies, Hoboken, NJ, USA: John Wiley & Sons, Inc.; 2015, p. 413–31. 10.1002/9781119041375.ch13.
[54] D.S. Seeli, M. Prabaharan, Guar Gum and Its Derivatives: Versatile Materials for Controlled Drug Delivery, in: Handbook of Sustainable Polymers, Jenny Stanford Publishing, 2016, pp. 261–287, https://doi.org/10.1201/b19948-11.
[55] A. Martín-Illana, R. Cazorla-Luna, F. Notario-Pérez, L.M. Bedoya, R. Ruiz-Caro, M. D. Veiga, Freeze-dried bioadhesive vaginal bigels for controlled release of Tenofovir, Eur. J. Pharm. Sci. 127 (2019) 38–51, https://doi.org/10.1016/j.ejps.2018.10.013.
[56] S. Das, D. Bera, K. Pal, D. Mondal, P. Karmakar, S. Das, et al., Guar gum micro-vehicle mediated delivery strategy and synergistic activity of thymoquinone and piperine: An in vitro study on bacterial and hepatocellular carcinoma cells, J. Drug Delivery Sci. Technol. 60 (2020), 101994, https://doi.org/10.1016/j.jddst.2020.101994.
[57] H.D. Jhundoo, T. Siefen, A. Liang, C. Schmidt, J. Lokhnauth, B. Moulari, et al., Anti-inflammatory effects of acacia and guar gum in 5-amino salicylic acid formulations in experimental colitis, Int. J. Pharm.: X 3 (2021), 100080, https://doi.org/10.1016/j.ijpx.2021.100080.
[58] B. Mukherjee, L. Kumari, I. Ehsan, P. Ghosh, S. Banerjee, S. Chakraborty, et al., Guar gum-based nanomaterials in drug delivery and biomedical applicationsBiopolymer-Based Nanomaterials in Drug Delivery and Biomedical Applications, Elsevier (2021) 143–164, https://doi.org/10.1016/B978-0-12-820874-8.00016-6.
[59] S. Das, U. Subuddhi, Potential of guar gum hydrogels in drug deliveryPlant and Algal Hydrogels for Drug Delivery and Regenerative Medicine, Elsevier (2021) 143–180, https://doi.org/10.1016/B978-0-12-821649-1.00006-4.
[60] M. Caldera-Villalobos, D.A. Cabrera-Munguía, J.J. Becerra-Rodríguez, J. A. Claudio-Rizo, Tailoring biocompatibility of composite scaffolds of collagen/guar gum with metal–organic frameworks, RSC Adv. 12 (2022) 3672–3686, https://doi.org/10.1039/D1RA08824F.
[61] Z.H. Ghauri, A. Islam, M.A. Qadir, N. Gull, B. Haider, R.U. Khan, et al., Development and evaluation of pH-sensitive biodegradable ternary blended hydrogel films (chitosan/guar gum/PVP) for drug delivery application, Sci. Rep. 11 (2021) 21255, https://doi.org/10.1038/s41598-021-00452-x.
[62] J. Wang, Y. Huang, B. Liu, Z. Li, J. Zhang, G. Yang, et al., Flexible and anti-freezing zinc-ion batteries using a guar-gum/sodium-alginate/ethylene-glycol hydrogel electrolyte, Energy Storage Mater. 41 (2021) 599–605, https://doi.org/10.1016/j.ensm.2021.06.034.
[63] M. Mofradi, H. Karimi, K. Dashtian, M. Ghaedi, Processing Guar Gum into polyester fabric based promising mixed matrix membrane for water treatment, Carbohydr. Polym. 254 (2021), 116806, https://doi.org/10.1016/j.carbpol.2020.116806.
[64] J.L. Slavin, N.A. Greenberg, Partially hydrolyzed guar gum, Nutrition 19 (2003) 549–552, https://doi.org/10.1016/S0899-9007(02)01032-8.
[65] D. Mudgil, Partially Hydrolyzed Guar Gum: Preparation and Properties. Polymers for Food Applications, Springer International Publishing, Cham, 2018, pp. 529–549.
[66] A.I. Bourbon, A.C. Pinheiro, C. Ribeiro, C. Miranda, J.M. Maia, J.A. Teixeira, et al., Characterization of galactomannans extracted from seeds of Gleditsia triacanthos and Sophora japonica through shear and extensional rheology: Comparison with guar gum and locust bean gum, Food Hydrocoll. 24 (2010) 184–192, https://doi.org/10.1016/j.foodhyd.2009.09.004.
[67] M. Prabaharan, Prospective of guar gum and its derivatives as controlled drug delivery systems, Int. J. Biol. Macromol. 49 (2011) 117–124, https://doi.org/10.1016/j.ijbiomac.2011.04.022.
[68] M.D. Torres, R. Moreira, F. Chenlo, M.J. Vázquez, Water adsorption isotherms of carboxymethyl cellulose, guar, locust bean, tragacanth and xanthan gums, Carbohydr. Polym. 89 (2012) 592–598, https://doi.org/10.1016/j.carbpol.2012.03.055.
[69] N. Thombare, U. Jha, S. Mishra, M.Z. Siddiqui, Guar gum as a promising starting material for diverse applications: A review, Int. J. Biol. Macromol. 88 (2016) 361–372, https://doi.org/10.1016/j.ijbiomac.2016.04.001.
[70] G. Dodi, D. Hritcu, M.I. Popa, Carboxymethylation of guar gum: synthesis and characterization, Cellul. Chem. Technol. 45 (2011) 171–176.
[71] K.P. Chandrika, A. Singh, A. Rathore, A. Kumar, Novel cross linked guar gum-g-poly(acrylate) porous superabsorbent hydrogels: Characterization and swelling

behaviour in different environments, Carbohydr. Polym. 149 (2016) 175–185, https://doi.org/10.1016/j.carbpol.2016.04.077.
[72] N. Thombare, U. Jha, S. Mishra, M.Z. Siddiqui, Borax cross-linked guar gum hydrogels as potential adsorbents for water purification, Carbohydr. Polym. 168 (2017) 274–281, https://doi.org/10.1016/j.carbpol.2017.03.086.
[73] N. Thombare, S. Mishra, M.Z. Siddiqui, U. Jha, D. Singh, G.R. Mahajan, Design and development of guar gum based novel, superabsorbent and moisture retaining hydrogels for agricultural applications, Carbohydr. Polym. 185 (2018) 169–178, https://doi.org/10.1016/j.carbpol.2018.01.018.
[74] S. Pal, Carboxymethyl guar: Its synthesis and macromolecular characterization, J. Appl. Polym. Sci. 111 (2009) 2630–2636, https://doi.org/10.1002/app.29338.
[75] S. Kundu, A. Das, A. Basu, D. Ghosh, P. Datta, A. Mukherjee, Carboxymethyl guar gum synthesis in homogeneous phase and macroporous 3D scaffolds design for tissue engineering, Carbohydr. Polym. 191 (2018) 71–78, https://doi.org/10.1016/j.carbpol.2018.03.007.
[76] H. Gong, M. Liu, J. Chen, F. Han, C. Gao, B. Zhang, Synthesis and characterization of carboxymethyl guar gum and rheological properties of its solutions, Carbohydr. Polym. 88 (2012) 1015–1022, https://doi.org/10.1016/j.carbpol.2012.01.057.
[77] R.T. Thimma, S. Tammishetti, Barium chloride crosslinked carboxymethyl guar gum beads for gastrointestinal drug delivery, J. Appl. Polym. Sci. 82 (2001) 3084–3090, https://doi.org/10.1002/app.2164.
[78] R.T. Thimma, S. Tammishetti, Study of complex coacervation of gelatin with sodium carboxymethyl guar gum: Microencapsulation of clove oil and sulphamethoxazole, J. Microencapsul. 20 (2003) 203–210, https://doi.org/10.3109/02652040309178062.
[79] S.K. Ghosh, A. Das, A. Basu, A. Halder, S. Das, S. Basu, et al., Semi-interpenetrating hydrogels from carboxymethyl guar gum and gelatin for ciprofloxacin sustained release, Int. J. Biol. Macromol. 120 (2018) 1823–1833, https://doi.org/10.1016/j.ijbiomac.2018.09.212.
[80] G. Dalei, S. Das, Carboxymethyl guar gum: A review of synthesis, properties and versatile applications, Eur. Polym. J. 176 (2022), 111433, https://doi.org/10.1016/j.eurpolymj.2022.111433.
[81] G. Dalei, S. Das, S.P. Das, Non-thermal plasma assisted surface nano-textured carboxymethyl guar gum/chitosan hydrogels for biomedical applications, RSC Adv. 9 (2019) 1705–1716, https://doi.org/10.1039/C8RA09161G.
[82] A.M.A. Hasan, M. Keshawy, M.-E.-S. Abdel-Raouf, Atomic force microscopy investigation of smart superabsorbent hydrogels based on carboxymethyl guar gum: Surface topography and swelling properties, Mater. Chem. Phys. 278 (2022), 125521, https://doi.org/10.1016/j.matchemphys.2021.125521.
[83] D. Chauhan, A. Kumar, S.G. Warkar, Synthesis, characterization and metal ions sensing applications of *meta* -benziporphodimethene-embedded polyacrylamide/carboxymethyl guargum polymeric hydrogels in water, Environ. Technol. 43 (2022) 991–1002, https://doi.org/10.1080/09593330.2020.1812730.
[84] W. Chen, Y. Bu, D. Li, Y. Liu, G. Chen, X. Wan, et al., Development of high-strength, tough, and self-healing carboxymethyl guar gum-based hydrogels for human motion detection, J. Mater. Chem. C 8 (2020) 900–908, https://doi.org/10.1039/C9TC05797H.
[85] P. Orsu, S. Matta, Fabrication and characterization of carboxymethyl guar gum nanocomposite for application of wound healing, Int. J. Biol. Macromol. 164 (2020) 2267–2276, https://doi.org/10.1016/j.ijbiomac.2020.07.322.
[86] G. Dalei, S. Das, S.P. Das, Low-pressure nitrogen and ammonia plasma treatment on carboxymethyl guar gum/PVA hydrogels: impact on drug delivery, biocompatibility and biodegradability, Int. J. Polym. Mater. Polym. Biomater. 70 (2021) 75–89, https://doi.org/10.1080/00914037.2019.1695204.
[87] M.A. Shenoy, D.J. D'Melo, Evaluation of mechanical properties of unsaturated polyester-guar gum/hydroxypropyl guar gum composites, Express Polym. Lett. 1 (2007) 622–628, https://doi.org/10.3144/expresspolymlett.2007.85.
[88] H. Fan, Z. Gong, Z. Wei, H. Chen, H. Fan, J. Geng, et al., Understanding the temperature–resistance performance of a borate cross-linked hydroxypropyl guar gum fracturing fluid based on a facile evaluation method, RSC Adv. 7 (2017) 53290–53300, https://doi.org/10.1039/C7RA11687J.
[89] L. Qiu, Y. Shen, T. Wang, C. Wang, Rheological and fracturing characteristics of a novel sulfonated hydroxypropyl guar gum, Int. J. Biol. Macromol. 117 (2018) 974–982, https://doi.org/10.1016/j.ijbiomac.2018.05.072.
[90] Y. Li, S. Wang, J. Guo, R. Chen, F. Zhao, Y. Liu, Reducing adsorption of hydroxypropyl guar gum on sandstone by silicon nanoparticles, Carbohydr. Polym. 219 (2019) 21–28, https://doi.org/10.1016/j.carbpol.2019.05.016.
[91] C. Berlangieri, G. Poggi, S. Murgia, M. Monduzzi, L. Dei, E. Carretti, Structural, rheological and dynamics insights of hydroxypropyl guar gel-like systems, Colloids Surf. BBiointerfaces 168 (2018) 178–186, https://doi.org/10.1016/j.colsurfb.2018.02.025.
[92] Q. Shi, B. Qin, Q. Bi, B. Qu, Fly ash suspensions stabilized by hydroxypropyl guar gum and xanthan gum for retarding spontaneous combustion of coal, Combust. Sci. Technol. 190 (2018) 2097–2110, https://doi.org/10.1080/00102202.2018.1491845.
[93] D. Carvalho, N. Loeffler, G.-T. Kim, S. Passerini, High Temperature Stable Separator for Lithium Batteries Based on SiO2 and Hydroxypropyl Guar Gum, Membranes (Basel) 5 (2015) 632–645, https://doi.org/10.3390/membranes5040632.
[94] Y. Meng, H. Luo, C. Dong, C. Zhang, Z. He, Z. Long, et al., Hydroxypropyl Guar/Cellulose Nanocrystal Film with Ionic Liquid and Anthocyanin for Real-Time and Visual Detection of NH $_3$, ACS Sustain. Chem. Eng. 8 (2020) 9731–9741, https://doi.org/10.1021/acssuschemeng.0c01833.
[95] J. Gao, B.P. Grady, Hydroxypropylation of Guar Splits: Kinetics and Rheology, Ind. Eng. Chem. Res. 58 (2019) 11673–11679, https://doi.org/10.1021/acs.iecr.9b01674.
[96] L. Ray, R. Karthik, V. Srivastava, S.P. Singh, A.B. Pant, N. Goyal, et al., Efficient antileishmanial activity of amphotericin B and piperine entrapped in enteric coated guar gum nanoparticles, Drug Deliv. Transl. Res. 11 (2021) 118–130, https://doi.org/10.1007/s13346-020-00712-9.
[97] X. Lu, Y. Li, W. Feng, S. Guan, P. Guo, Self-healing hydroxypropyl guar gum/poly (acrylamide-co-3-acrylamidophenyl boronic acid) composite hydrogels with yield phenomenon based on dynamic PBA ester bonds and H-bond, Colloids Surf. A Physicochem. Eng. Asp. 561 (2019) 325–331, https://doi.org/10.1016/j.colsurfa.2018.10.071.
[98] Z. Sun, L. Wang, X. Jiang, L. Bai, W. Wang, H. Chen, et al., Self-healing, sensitive and antifreezing biomass nanocomposite hydrogels based on hydroxypropyl guar gum and application in flexible sensors, Int. J. Biol. Macromol. 155 (2020) 1569–1577, https://doi.org/10.1016/j.ijbiomac.2019.11.134.
[99] D. Risica, M. Dentini, V. Crescenzi, Guar gum methyl ethers. Part I., Synthesis and macromolecular characterization, Polymer (Guildf) 46 (2005) 12247–12255, https://doi.org/10.1016/j.polymer.2005.10.083.
[100] J. Tripathi, R. Ambolikar, S. Gupta, D. Jain, J. Bahadur, P.S. Variyar, Methylation of guar gum for improving mechanical and barrier properties of biodegradable packaging films, Sci. Rep. 9 (2019) 14505, https://doi.org/10.1038/s41598-019-50991-7.
[101] J. Tripathi, R. Ambolikar, S. Gupta, P.S. Variyar, Preparation and characterization of methylated guar gum based nano-composite films, Food Hydrocoll. 124 (2022), 107312, https://doi.org/10.1016/j.foodhyd.2021.107312.
[102] H.J. Prado, M.C. Matulewicz, Cationization of polysaccharides: A path to greener derivatives with many industrial applications, Eur. Polym. J. 52 (2014) 53–75, https://doi.org/10.1016/j.eurpolymj.2013.12.011.
[103] S. Pal, D. Mal, R.P. Singh, Synthesis and characterization of cationic guar gum: A high performance flocculating agent, J. Appl. Polym. Sci. 105 (2007) 3240–3245, https://doi.org/10.1002/app.26440.
[104] Y. Huang, H. Yu, C. Xiao, pH-sensitive cationic guar gum/poly (acrylic acid) polyelectrolyte hydrogels: Swelling and in vitro drug release, Carbohydr. Polym. 69 (2007) 774–783, https://doi.org/10.1016/j.carbpol.2007.02.016.
[105] C. Banerjee, S. Ghosh, G. Sen, S. Mishra, P. Shukla, R. Bandopadhyay, Study of algal biomass harvesting using cationic guar gum from the natural plant source as flocculant, Carbohydr. Polym. 92 (2013) 675–681, https://doi.org/10.1016/j.carbpol.2012.09.022.
[106] X. Wan, C. Guo, J. Feng, T. Yu, X.-S. Chai, G. Chen, et al., Determination of the Degree of Substitution of Cationic Guar Gum by Headspace-Based Gas Chromatography during Its Synthesis, J. Agric. Food Chem. 65 (2017) 7012–7016, https://doi.org/10.1021/acs.jafc.7b03144.
[107] T. Bujak, Z. Nizioł-Łukaszewska, A. Ziemlewska, Amphiphilic cationic polymers as effective substances improving the safety of use of body wash gels, Int. J. Biol. Macromol. 147 (2020) 973–979, https://doi.org/10.1016/j.ijbiomac.2019.10.064.
[108] R.L. McMullen, D. Laura, G. Zhang, B. Kroon, Investigation of the interactions of cationic guar with human hair by electrokinetic analysis, Int. J. Cosmet. Sci. 43 (2021) 375–390, https://doi.org/10.1111/ics.12704.
[109] L. Dai, T. Cheng, Y. Wang, H. Lu, S. Nie, H. He, et al., Injectable all-polysaccharide self-assembling hydrogel: a promising scaffold for localized therapeutic proteins, Cellulose 26 (2019) 6891–6901, https://doi.org/10.1007/s10570-019-02579-7.
[110] C. Pu, W. Tang, X. Li, M. Li, Q. Sun, Stability enhancement efficiency of surface decoration on curcumin-loaded liposomes: Comparison of guar gum and its cationic counterpart, Food Hydrocoll. 87 (2019) 29–37, https://doi.org/10.1016/j.foodhyd.2018.07.039.
[111] H. Yagoub, L. Zhu, M.H.M.A. Shibraen, X. Xu, D.M.D. Babiker, J. Xu, et al., Complex membrane of cellulose and chitin nanocrystals with cationic guar gum for oil/water separation, J. Appl. Polym. Sci. 136 (2019) 47947, https://doi.org/10.1002/app.47947.
[112] M.F. Abdullah, S.K. Ghosh, S. Basu, A. Mukherjee, Cationic guar gum orchestrated environmental synthesis for silver nano-bio-composite films, Carbohydr. Polym. 134 (2015) 30–37, https://doi.org/10.1016/j.carbpol.2015.06.029.
[113] M. Chu, N. Feng, H. An, G. You, C. Mo, H. Zhong, et al., Design and validation of antibacterial and pH response of cationic guar gum film by combining hydroxyethyl cellulose and red cabbage pigment, Int. J. Biol. Macromol. 162 (2020) 1311–1322, https://doi.org/10.1016/j.ijbiomac.2020.06.198.
[114] M.H.M.A. Shibraen, O.M. Ibrahim, R.A.M. Asad, S. Yang, M.R. El-Aassar, Interpenetration of metal cations into polyelectrolyte-multilayer-films via layer-by-layer assembly: Selective antibacterial functionality of cationic guar gum/polyacrylic acid- Ag+ nanofilm against resistant E. coli, Colloids Surf. A Physicochem. Eng. Asp. 610 (2021), 125921, https://doi.org/10.1016/j.colsurfa.2020.125921.
[115] X. Tan, Y. Zhu, C. Sun, X. Zhang, J. Su, Adding cationic guar gum after collector: A novel investigation in flotation separation of galena from sphalerite, Miner. Eng. 157 (2020), 106542, https://doi.org/10.1016/j.mineng.2020.106542.
[116] E. Grządka, J. Matusiak, E. Godek, U. Maciołek, Mixtures of cationic guar gum and anionic surfactants as stabilizers of zirconia suspensions, J. Mol. Liq. 343 (2021), 117677, https://doi.org/10.1016/j.molliq.2021.117677.
[117] W. Zou, S. Tang, Q. Li, G. Hu, L. Liu, Y. Jin, et al., Addition of cationic guar-gum and oleic acid improved the stability of plasma emulsions prepared with enzymatically hydrolyzed egg yolk, Food Hydrocoll. 105 (2020), 105827, https://doi.org/10.1016/j.foodhyd.2020.105827.
[118] A. Nakamura, M. Ozaki, K. Murakami, Elucidation of the aggregation mechanism of bentonite with cationic guar gum as flocculant and application to filtration,

Colloids Surf. A Physicochem. Eng. Asp. 596 (2020), 124660, https://doi.org/10.1016/j.colsurfa.2020.124660.
[119] R. Tyagi, P. Sharma, R. Nautiyal, A.K. Lakhera, V. Kumar, Synthesis of quaternised guar gum using Taguchi L(16) orthogonal array, Carbohydr. Polym. 237 (2020), 116136, https://doi.org/10.1016/j.carbpol.2020.116136.
[120] R. Jeyapaul, P. Shahabudeen, K. Krishnaiah, Quality management research by considering multi-response problems in the Taguchi method – a review, Int. J. Adv. Manuf. Technol. 26 (2005) 1331–1337, https://doi.org/10.1007/s00170-004-2102-y.
[121] H. Jing, J. Feng, J. Shi, L. He, P. Guo, S. Guan, et al., Ultra-stretchable, self-recovering, self-healing cationic guar gum/poly(stearyl methacrylate-co-acrylic acid) hydrogels, Carbohydr. Polym. 256 (2021), 117563, https://doi.org/10.1016/j.carbpol.2020.117563.
[122] L. Dai, Y. Wang, Z. Li, X. Wang, C. Duan, W. Zhao, et al., A multifunctional self-crosslinked chitosan/cationic guar gum composite hydrogel and its versatile uses in phosphate-containing water treatment and energy storage, Carbohydr. Polym. 244 (2020), 116472, https://doi.org/10.1016/j.carbpol.2020.116472.
[123] X. Yu, C. Cheng, X. Peng, K. Zhang, X. Yu, A self-healing and injectable oxidized quaternized guar gum/carboxymethyl chitosan hydrogel with efficient hemostatic and antibacterial properties for wound dressing, Colloids Surf. BBiointerfaces 209 (2022), 112207, https://doi.org/10.1016/j.colsurfb.2021.112207.
[124] E.A. Kamoun, E.-R.-S. Kenawy, X. Chen, A review on polymeric hydrogel membranes for wound dressing applications: PVA-based hydrogel dressings, J. Adv. Res. 8 (2017) 217–233, https://doi.org/10.1016/j.jare.2017.01.005.
[125] D. Simões, S.P. Miguel, M.P. Ribeiro, P. Coutinho, A.G. Mendonça, I.J. Correia, Recent advances on antimicrobial wound dressing: A review, Eur. J. Pharm. Biopharm. 127 (2018) 130–141, https://doi.org/10.1016/j.ejpb.2018.02.022.
[126] A. Gupta, M. Kowalczuk, W. Heaselgrave, S.T. Britland, C. Martin, I. Radecka, The production and application of hydrogels for wound management: A review, Eur. Polym. J. 111 (2019) 134–151, https://doi.org/10.1016/j.eurpolymj.2018.12.019.
[127] Y. Liang, J. He, B. Guo, Functional Hydrogels as Wound Dressing to Enhance Wound Healing, ACS Nano 15 (2021) 12687–12722, https://doi.org/10.1021/acsnano.1c04206.
[128] Q. Zeng, X. Qi, G. Shi, M. Zhang, H. Haick, Wound Dressing: From Nanomaterials to Diagnostic Dressings and Healing Evaluations, ACS Nano 16 (2022) 1708–1733, https://doi.org/10.1021/acsnano.1c08411.
[129] M.C. Jennings, K.P.C. Minbiole, W.M. Wuest, Quaternary Ammonium Compounds: An Antimicrobial Mainstay and Platform for Innovation to Address Bacterial Resistance, ACS Infect. Dis. 1 (2015) 288–303, https://doi.org/10.1021/acsinfecdis.5b00047.
[130] P. Jana, S. Ghosh, K. Sarkar, Low molecular weight polyethyleneimine conjugated guar gum for targeted gene delivery to triple negative breast cancer, Int. J. Biol. Macromol. 161 (2020) 1149–1160, https://doi.org/10.1016/j.ijbiomac.2020.06.090.
[131] T.-A. Le, Y. Guo, J.-N. Zhou, J. Yan, H. Zhang, T.-P. Huynh, Synthesis, characterization and biocompatibility of guar gum-benzoic acid, Int. J. Biol. Macromol. 194 (2022) 110–116, https://doi.org/10.1016/j.ijbiomac.2021.11.180.
[132] A.C. Reis, L.v. dos Santos, K.R. Santos, M.K. Lima-Tenório, K.S. Paludo, M. R. Maurício, et al., Chemically crosslinked guar gum hydrogels: An investigation on the water transport and its relationship with hydrocortisone release, Int. J. Pharm. 617 (2022), 121626, https://doi.org/10.1016/j.ijpharm.2022.121626.
[133] S. Sarkar, R.S. Singhal, Esterification of guar gum hydrolysate and gum Arabic with n-octenyl succinic anhydride and oleic acid and its evaluation as wall material in microencapsulation, Carbohydr. Polym. 86 (2011) 1723–1731, https://doi.org/10.1016/j.carbpol.2011.07.003.
[134] H. Kono, F. Otaka, M. Ozaki, Preparation and characterization of guar gum hydrogels as carrier materials for controlled protein drug delivery, Carbohydr. Polym. 111 (2014) 830–840, https://doi.org/10.1016/j.carbpol.2014.05.050.
[135] C. Lacroix, E. Sultan, E. Fleury, A. Charlot, Functional galactomannan platform from convenient esterification in imidazolium-based ionic liquids, Polym. Chem. 3 (2012) 538–546, https://doi.org/10.1039/C2PY00512C.
[136] V. Raj, A. Bajpai, Synthesis of hydrophobically modified guar gum film for packaging materials, Mater. Today: Proc. 29 (2020) 1132–1142, https://doi.org/10.1016/j.matpr.2020.05.339.
[137] A. Bajpai, V. Raj, Hydrophobically modified guar gum films for wound dressing, Polym. Bull. 78 (2021) 4109–4128, https://doi.org/10.1007/s00289-020-03302-4.
[138] S. r, m. p., Multi-functional FITC-silica@gold nanoparticles conjugated with guar gum succinate, folic acid and doxorubicin for CT/fluorescence dual imaging and combined chemo/PTT of cancer, Colloids Surf. BBiointerfaces 186 (2020), 110701, https://doi.org/10.1016/j.colsurfb.2019.110701.
[139] S. Kunjiappan, P. Pavadai, S. Vellaichamy, S. Ram Kumar Pandian, V. Ravishankar, P. Palanisamy, et al., Surface receptor-mediated targeted drug delivery systems for enhanced cancer treatment: A state-of-the-art review, Drug Dev. Res. 82 (2021) 309–340, https://doi.org/10.1002/ddr.21758.
[140] N. Soni, N.N. Shah, R.S. Singhal, Dodecenyl succinylated guar gum hydrolysate as a wall material for microencapsulation: Synthesis, characterization and evaluation, J. Food Eng. 242 (2019) 133–140, https://doi.org/10.1016/j.jfoodeng.2018.08.030.
[141] Z. Zhang, J. Mao, B. Yang, X. Yang, W. Zhang, C. Zhang, et al., Experimental evaluation of a novel modification of anionic guar gum with maleic anhydride for fracturing fluid, Rheol. Acta 58 (2019) 173–181, https://doi.org/10.1007/s00397-019-01131-5.
[142] X. Yuan, R. Amarnath Praphakar, M.A. Munusamy, A.A. Alarfaj, S. Suresh Kumar, M. Rajan, Mucoadhesive guargum hydrogel inter-connected chitosan-g-polycaprolactone micelles for rifampicin delivery, Carbohydr. Polym. 206 (2019) 1–10, https://doi.org/10.1016/j.carbpol.2018.10.098.
[143] M. Zhang, J. He, M. Deng, P. Gong, X. Zhang, M. Fan, et al., Rheological behaviours of guar gum derivatives with hydrophobic unsaturated long-chains, RSC Adv. 10 (2020) 32050–32057, https://doi.org/10.1039/D0RA04322B.
[144] A. Das, S. Kundu, S.K. Ghosh, A. Basu, M. Gupta, A. Mukherjee, Guar gum cinnamate ouzo nanoparticles for bacterial contact killing in water environment, Carbohydr. Res. 491 (2020), 107983, https://doi.org/10.1016/j.carres.2020.107983.
[145] L. Petruš, D.G. Gray, J.N. BeMiller, Homogeneous alkylation of cellulose in lithium chloride/dimethyl sulfoxide solvent with dimsyl sodium activation. A proposal for the mechanism of cellulose dissolution in LiCl/Me2SO, Carbohydr. Res. 268 (1995) 319–323, https://doi.org/10.1016/0008-6215(94)00330-I.
[146] Z. Liu, C. Zhang, R. Liu, W. Zhang, H. Kang, P. Li, et al., Dissolution of cellobiose in the aqueous solutions of chloride salts: Hofmeister series consideration, Cellulose 23 (2016) 295–305, https://doi.org/10.1007/s10570-015-0827-4.
[147] S. Kundu, A. Das, A. Basu, M.F. Abdullah, A. Mukherjee, Guar gum benzoate nanoparticle reinforced gelatin films for enhanced thermal insulation, mechanical and antimicrobial properties, Carbohydr. Polym. 170 (2017) 89–98, https://doi.org/10.1016/j.carbpol.2017.04.056.
[148] E. Lepeltier, C. Bourgaux, P. Couvreur, Nanoprecipitation and the “Ouzo effect”: Application to drug delivery devices, Adv. Drug Deliv. Rev. 71 (2014) 86–97, https://doi.org/10.1016/j.addr.2013.12.009.
[149] A. Das, A. Das, A. Basu, P. Datta, M. Gupta, A. Mukherjee, Newer guar gum ester/chicken feather keratin interact films for tissue engineering, Int. J. Biol. Macromol. 180 (2021) 339–354, https://doi.org/10.1016/j.ijbiomac.2021.03.034.
[150] R. Bhattacharyya, P. Chowdhury, Hydrogels of Acryloyl guar gum-g-(acrylic acid-co-3sulfopropylacrylate) for high-performance adsorption and release of gentamicin sulphate, J. Polym. Res. 28 (2021) 286, https://doi.org/10.1007/s10965-021-02633-8.
[151] R.G. Pearson, Hard and soft acids and bases, HSAB, part 1: Fundamental principles, J. Chem. Educ. 45 (1968) 581, https://doi.org/10.1021/ed045p581.
[152] X. Li, W. Ma, H. Li, Q. Zhang, H. Liu, Sulfur-functionalized metal-organic frameworks: Synthesis and applications as advanced adsorbents, Coord. Chem. Rev. 408 (2020), 213191, https://doi.org/10.1016/j.ccr.2020.213191.
[153] A. Pohl, Removal of Heavy Metal Ions from Water and Wastewaters by Sulfur-Containing Precipitation Agents, Water Air Soil Pollut. 231 (2020) 503, https://doi.org/10.1007/s11270-020-04863-w.
[154] J. Chen, The interaction of flotation reagents with metal ions in mineral surfaces: A perspective from coordination chemistry, Miner. Eng. 171 (2021), 107067, https://doi.org/10.1016/j.mineng.2021.107067.
[155] Y. Qin, S. Liu, R. Xing, H. Yu, K. Li, X. Meng, et al., Synthesis and characterization of dithiocarbamate chitosan derivatives with enhanced antifungal activity, Carbohydr. Polym. 89 (2012) 388–393, https://doi.org/10.1016/j.carbpol.2012.03.018.
[156] V.N. Mehta, H. Basu, R.K. Singhal, S.K. Kailasa, Simple and sensitive colorimetric sensing of Cd2+ ion using chitosan dithiocarbamate functionalized gold nanoparticles as a probe, Sens. Actuators B 220 (2015) 850–858, https://doi.org/10.1016/j.snb.2015.05.105.
[157] E. Doustkhah, S. Rostamnia, B. Gholipour, B. Zeynizadeh, A. Baghban, R. Luque, Design of chitosan-dithiocarbamate magnetically separable catalytic nanocomposites for greener aqueous oxidations at room temperature, Mol. Catal. 434 (2017) 7–15, https://doi.org/10.1016/j.mcat.2017.01.031.
[158] J. Hao, J. Liu, D. Yang, X. Qin, H. Gao, X. Bai, et al., Application of a new depressant dithiocarbamate chitosan in separation of chalcopyrite and molybdenite, Colloids Surf. A Physicochem. Eng. Asp. 634 (2022), 127920, https://doi.org/10.1016/j.colsurfa.2021.127920.
[159] B.M. Córdova, T. Venâncio, M. Olivera, R.G. Huamani-Palomino, A. C. Valderrama, Xanthation of alginate for heavy metal ions removal. Characterization of xanthate-modified alginates and its metal derivatives, Int. J. Biol. Macromol. 169 (2021) 130–142, https://doi.org/10.1016/j.ijbiomac.2020.12.022.
[160] A.D. Gupta, K.P. Rawat, V. Bhadauria, H. Singh, Recent trends in the application of modified starch in the adsorption of heavy metals from water: A review, Carbohydr. Polym. 269 (2021), 117763, https://doi.org/10.1016/j.carbpol.2021.117763.
[161] T.-A. Le, M. Zouheir, K. Nikiforow, M. Khatib, O. Zohar, H. Haick, et al., Synthesis, characterization, and humidity-responsiveness of guar gum xanthate and its nanocomposite with copper sulfide covellite, Int. J. Biol. Macromol. 206 (2022) 105–114, https://doi.org/10.1016/j.ijbiomac.2022.02.132.
[162] S.C. Richter, M. Oestreich, Emerging Strategies for C-H Silylation, Trends in Chemistry 2 (2020) 13–27, https://doi.org/10.1016/j.trechm.2019.07.003.
[163] A. Tyagi, N. Yadav, J. Khan, S. Singh, H.C. Kumar, Transition-Metal-Free C−H Silylation: An Emerging Strategy, Asian J. Org. Chem. 10 (2021) 334–354, https://doi.org/10.1002/ajoc.202000584.
[164] M.A. Ashraf, Z. Liu, C. Li, D. Zhang, Recent advances in catalytic silylation of hydroxyl-bearing compounds: A green technique for protection of alcohols using Si–O bond formations, Appl. Organomet. Chem. 35 (2021), https://doi.org/10.1002/aoc.6131.
[165] S. Ghosh, D. Lai, A. Hajra, Visible-light-induced silylation: an update, Org. Biomol. Chem. 19 (2021) 2399–2415, https://doi.org/10.1039/D1OB00082A.

[166] F. Yan, Y. Jiang, X. Sun, Z. Bai, Y. Zhang, X. Zhou, Surface modification and chemical functionalization of carbon dots: a review, Microchim. Acta 185 (2018) 424, https://doi.org/10.1007/s00604-018-2953-9.
[167] S.-L. Bee, M.A.A. Abdullah, S.-T. Bee, L.T. Sin, A.R. Rahmat, Polymer nanocomposites based on silylated-montmorillonite: A review, Prog. Polym. Sci. 85 (2018) 57–82, https://doi.org/10.1016/j.progpolymsci.2018.07.003.
[168] K. Kuciński, H. Stachowiak-Dłużyńska, G. Hreczycho, Catalytic silylation of O–nucleophiles via Si–H or Si–C bond cleavage: A route to silyl ethers, silanols and siloxanes, Coord. Chem. Rev. 459 (2022), 214456, https://doi.org/10.1016/j.ccr.2022.214456.
[169] T. Baran, N. Yılmaz Baran, A. Menteş, Highly active and recyclable heterogeneous palladium catalyst derived from guar gum for fabrication of biaryl compounds, Int. J. Biol. Macromol. 132 (2019) 1147–1154, https://doi.org/10.1016/j.ijbiomac.2019.04.042.
[170] KumariS. Krishna, D. Yadav, S.K.Cu Sharma, (II), Schiff base complex grafted guar gum: Catalyst for benzophenone derivatives synthesis, Appl. Catal. A: Gen. 601 (117529) (2020), https://doi.org/10.1016/j.apcata.2020.117529.
[171] F.H. Westheimer, Why Nature Chose Phosphates, Science 1987 (235) (1979) 1173–1178, https://doi.org/10.1126/science.2434996.
[172] T. Hunter, Why nature chose phosphate to modify proteins, Philos. Trans. R. Soc., B 367 (2012) 2513–2516, https://doi.org/10.1098/rstb.2012.0013.
[173] S.C.L. Kamerlin, P.K. Sharma, R.B. Prasad, A. Warshel, Why nature really chose phosphate, Q. Rev. Biophys. 46 (2013) 1–132, https://doi.org/10.1017/S0033583512000157.
[174] C.-P. Li, H. Enomoto, Y. Hayashi, H. Zhao, T. Aoki, Recent advances in phosphorylation of food proteins: A review, LWT Food Sci. Technol. 43 (2010) 1295–1300, https://doi.org/10.1016/j.lwt.2010.03.016.
[175] N. Sbei, G.M. Martins, B. Shirinfar, N. Ahmed, Electrochemical Phosphorylation of Organic Molecules, Chem. Rec. 20 (2020) 1530–1552, https://doi.org/10.1002/tcr.202000096.
[176] K.W. Knouse, D.T. Flood, J.C. Vantourout, M.A. Schmidt, I.M. Mcdonald, M. D. Eastgate, et al., Nature Chose Phosphates and Chemists Should Too: How Emerging P(V) Methods Can Augment Existing Strategies, ACS Cent. Sci. 7 (2021) 1473–1485, https://doi.org/10.1021/acscentsci.1c00487.
[177] S. Xia, Y. Zhai, X. Wang, Q. Fan, X. Dong, M. Chen, et al., Phosphorylation of polysaccharides: A review on the synthesis and bioactivities, Int. J. Biol. Macromol. 184 (2021) 946–954, https://doi.org/10.1016/j.ijbiomac.2021.06.149.
[178] G. Sharma, A. Kumar, S. Sharma, A.H. Al-Muhtaseb, M.u. Naushad, A.A. Ghfar, et al., Fabrication and characterization of novel Fe0@Guar gum-crosslinked-soya lecithin nanocomposite hydrogel for photocatalytic degradation of methyl violet dye, Sep. Purif. Technol. 211 (2019) 895–908, https://doi.org/10.1016/j.seppur.2018.10.028.
[179] J. Wang, S. Zhuang, Extraction and adsorption of U(VI) from aqueous solution using affinity ligand-based technologies: an overview, Rev. Environ. Sci. Bio/Technol. 18 (2019) 437–452, https://doi.org/10.1007/s11157-019-09507-y.
[180] M.F. Hamza, A. Fouda, K.Z. Elwakeel, Y. Wei, E. Guibal, N.A. Hamad, Phosphorylation of Guar Gum/Magnetite/Chitosan Nanocomposites for Uranium (VI) Sorption and Antibacterial Applications, Molecules 26 (2021) 1920, https://doi.org/10.3390/molecules26071920.
[181] D. Belosinschi, A. Benkaddour, B.-M. Tofanica, T. Ngo, Phosphorylation of Cellulose in the Presence of Urea, Mech. React. Reagent Impact. (2022), https://doi.org/10.21203/rs.3.rs-862264/v1.
[182] Y. Xu, Y. Wu, P. Sun, F. Zhang, R.J. Linhardt, A. Zhang, Chemically modified polysaccharides: Synthesis, characterization, structure activity relationships of action, Int. J. Biol. Macromol. 132 (2019) 970–977, https://doi.org/10.1016/j.ijbiomac.2019.03.213.
[183] L. Xie, M. Shen, Y. Hong, H. Ye, L. Huang, J. Xie, Chemical modifications of polysaccharides and their anti-tumor activities, Carbohydr. Polym. 229 (2020), 115436, https://doi.org/10.1016/j.carbpol.2019.115436.
[184] H.P. de Oliveira Barddal, F.A.M. Faria, A.V. Nogueira, M. Iacomini, T.R. Cipriani, Anticoagulant and antithrombotic effects of chemically sulfated guar gum, Int. J. Biol. Macromol. 145 (2020) 604–610, https://doi.org/10.1016/j.ijbiomac.2019.12.210.
[185] A.S. Kazachenko, F. Akman, A. Sagaama, N. Issaoui, Y.N. Malyar, N.Y. Vasilieva, et al., Theoretical and experimental study of guar gum sulfation, J. Mol. Model. 27 (5) (2021), https://doi.org/10.1007/s00894-020-04645-5.
[186] A.S. Kazachenko, Y.N. Malyar, N.Y. Vasilyeva, V.S. Borovkova, N. Issaoui, Optimization of guar gum galactomannan sulfation process with sulfamic acid, Biomass Convers. Biorefin. (2021), https://doi.org/10.1007/s13399-021-01895-y.
[187] M. Simsek, T.T. Asiyanbi-Hammed, N. Rasaq, A.M. Hammed, Progress in Bioactive Polysaccharide-Derivatives: A Review, Food Rev. Intl. (2021) 1–16, https://doi.org/10.1080/87559129.2021.1935998.
[188] P. Jana, T. Mitra, T.K.R. Selvaraj, A. Gnanamani, Kundu pp., Preparation of guar gum scaffold film grafted with ethylenediamine and fish scale collagen, cross-linked with ceftazidime for wound healing application, Carbohydr. Polym. 153 (2016) 573–581, https://doi.org/10.1016/j.carbpol.2016.07.053.
[189] Y. Zhang, M. Chen, J. Zhang, J. Li, S.Q. Shi, Q. Gao, A High-Performance Bio-Adhesive Using Hyperbranched Aminated Soybean Polysaccharide and Bio-Based Epoxide, Adv. Mater. Interfaces 7 (2020) 2000148, https://doi.org/10.1002/admi.202000148.
[190] E. Jsc, S. Gopi, A, R, G, S, A. Pius, Highly crosslinked 3-D hydrogels based on graphene oxide for enhanced remediation of multi contaminant wastewater, J. Water Proc. Eng. 31 (2019), https://doi.org/10.1016/j.jwpe.2019.100850.
[191] I. Cumpstey, Chemical Modification of Polysaccharides, ISRN Org. Chem. 2013 (2013) 1–27, https://doi.org/10.1155/2013/417672.
[192] S. Coseri, G. Biliuta, B.C. Simionescu, K. Stana-Kleinschek, V. Ribitsch, V. Harabagiu, Oxidized cellulose—Survey of the most recent achievements, Carbohydr. Polym. 93 (2013) 207–215, https://doi.org/10.1016/j.carbpol.2012.03.086.
[193] G. Pierre, C. Punta, C. Delattre, L. Melone, P. Dubessay, A. Fiorati, et al., TEMPO-mediated oxidation of polysaccharides: An ongoing story, Carbohydr. Polym. 165 (2017) 71–85, https://doi.org/10.1016/j.carbpol.2017.02.028.
[194] A. Isogai, TEMPO-catalyzed oxidation of polysaccharides, Polym. J. 54 (2022) 387–402, https://doi.org/10.1038/s41428-021-00580-1.
[195] B. Ding, Y. Ye, qing, J. Cheng, K. Wang, J. Luo, B. Jiang, TEMPO-mediated selective oxidation of substituted polysaccharides—an efficient approach for the determination of the degree of substitution at C-6, Carbohydr. Res. 343 (2008) 3112–3116, https://doi.org/10.1016/j.carres.2008.09.005.
[196] C.N. Sakakibara, M.R. Sierakowski, N. Lucyszyn, R.A. de Freitas, TEMPO-mediated oxidation on galactomannan: Gal/Man ratio and chain flexibility dependence, Carbohydr. Polym. 153 (2016) 371–378, https://doi.org/10.1016/j.carbpol.2016.07.114.
[197] C.L.O. Petkowicz, F. Reicher, K. Mazeau, Conformational analysis of galactomannans: from oligomeric segments to polymeric chains, Carbohydr. Polym. 37 (1998) 25–39, https://doi.org/10.1016/S0144-8617(98)00051-4.
[198] M. Lavazza, C. Formantici, V. Langella, D. Monti, U. Pfeiffer, Y.M. Galante, Oxidation of galactomannan by laccase plus TEMPO yields an elastic gel, J. Biotechnol. 156 (2011) 108–116, https://doi.org/10.1016/j.jbiotec.2011.08.029.
[199] C.H. de Seixas-Junior, M.M. de Carvalho, J. Jacumazo, R.D. Piazza, G.P. Parchen, R.A. de Freitas, Interaction of guar gum galactomannans with the anionic surfactant sodium lauryl ether sulphate, Int. J. Biol. Macromol. 165 (2020) 713–721, https://doi.org/10.1016/j.ijbiomac.2020.09.216.
[200] E. Ponzini, A. Natalello, F. Usai, M. Bechmann, F. Peri, N. Müller, et al., Structural characterization of aerogels derived from enzymatically oxidized galactomannans of fenugreek, sesbania and guar gums, Carbohydr. Polym. 207 (2019) 510–520, https://doi.org/10.1016/j.carbpol.2018.11.100.
[201] S. Witayakran, A.J. Ragauskas, Synthetic Applications of Laccase in Green Chemistry, Adv. Synth. Catal. 351 (2009) 1187–1209, https://doi.org/10.1002/adsc.200800775.
[202] S.A. Tromp, I. Matijošytė, R.A. Sheldon, I.W.C.E. Arends, G. Mul, M.T. Kreutzer, et al., Mechanism of Laccase-TEMPO-Catalyzed Oxidation of Benzyl Alcohol, ChemCatChem 2 (2010) 827–833, https://doi.org/10.1002/cctc.201000068.
[203] A. Sudalai, A. Khenkin, R. Neumann, Sodium periodate mediated oxidative transformations in organic synthesis, Org. Biomol. Chem. 13 (2015) 4374–4394, https://doi.org/10.1039/C5OB00238A.
[204] K.A. Kristiansen, A. Potthast, B.E. Christensen, Periodate oxidation of polysaccharides for modification of chemical and physical properties, Carbohydr. Res. 345 (2010) 1264–1271, https://doi.org/10.1016/j.carres.2010.02.011.
[205] T. Nypelö, B. Berke, S. Spirk, J.A. Sirviö, Review: Periodate oxidation of wood polysaccharides—Modulation of hierarchies, Carbohydr. Polym. 252 (2021), 117105, https://doi.org/10.1016/j.carbpol.2020.117105.
[206] L. Münster, M. Fojtů, Z. Capáková, M. Muchová, L. Musilová, T. Vaculovič, et al., Oxidized polysaccharides for anticancer-drug delivery: What is the role of structure? Carbohydr. Polym. 257 (2021), 117562 https://doi.org/10.1016/j.carbpol.2020.117562.
[207] W. Ding, Y. Wu, Sustainable dialdehyde polysaccharides as versatile building blocks for fabricating functional materials: An overview, Carbohydr. Polym. 248 (2020), 116801, https://doi.org/10.1016/j.carbpol.2020.116801.
[208] L. Dai, T. Cheng, Y. Wang, B. Wang, C. Duan, H. Ke, et al., A self-assembling guar gum hydrogel for efficient oil/water separation in harsh environments, Sep. Purif. Technol. 225 (2019) 129–135, https://doi.org/10.1016/j.seppur.2019.05.070.
[209] C. Duan, C. Liu, X. Meng, K. Gao, W. Lu, Y. Zhang, et al., Facile synthesis of Ag NPs@ MIL-100(Fe)/ guar gum hybrid hydrogel as a versatile photocatalyst for wastewater remediation: Photocatalytic degradation, water/oil separation and bacterial inactivation, Carbohydr. Polym. 230 (2020), 115642, https://doi.org/10.1016/j.carbpol.2019.115642.
[210] L. Yavari Maroufi, M. Ghorbani, M. Tabibiazar, A Gelatin-Based Film Reinforced by Covalent Interaction with Oxidized Guar Gum Containing Green Tea Extract as an Active Food Packaging System, Food Bioproc. Tech. 13 (2020) 1633–1644, https://doi.org/10.1007/s11947-020-02509-7.
[211] L.Y. Maroufi, M. Tabibiazar, M. Ghorbani, A. Jahanban-Esfahlan, Fabrication and characterization of novel antibacterial chitosan/dialdehyde guar gum hydrogels containing pomegranate peel extract for active food packaging application, Int. J. Biol. Macromol. 187 (2021) 179–188, https://doi.org/10.1016/j.ijbiomac.2021.07.126.
[212] A.H. Pandit, S. Nisar, K. Imtiyaz, M. Nadeem, N. Mazumdar, M.M.A. Rizvi, et al., Injectable, Self-Healing, and Biocompatible *N*, *O* -Carboxymethyl Chitosan/Multialdehyde Guar Gum Hydrogels for Sustained Anticancer Drug Delivery, Biomacromolecules 22 (2021) 3731–3745, https://doi.org/10.1021/acs.biomac.1c00537.
[213] P. Nezhad-Mokhtari, M. Ghorbani, N. Abdyazdani, Reinforcement of hydrogel scaffold using oxidized-guar gum incorporated with curcumin-loaded zein nanoparticles to improve biological performance, Int. J. Biol. Macromol. 167 (2021) 59–65, https://doi.org/10.1016/j.ijbiomac.2020.11.103.
[214] L.-D. Koh, Y. Cheng, C.-P. Teng, Y.-W. Khin, X.-J. Loh, S.-Y. Tee, et al., Structures, mechanical properties and applications of silk fibroin materials, Prog. Polym. Sci. 46 (2015) 86–110, https://doi.org/10.1016/j.progpolymsci.2015.02.001.

[215] D.-L. Wen, D.-H. Sun, P. Huang, W. Huang, M. Su, Y. Wang, et al., Recent progress in silk fibroin-based flexible electronics, Microsyst. Nanoeng. 7 (2021) 35, https://doi.org/10.1038/s41378-021-00261-2.
[216] M. Farokhi, F. Mottaghitalab, Y. Fatahi, A. Khademhosseini, D.L. Kaplan, Overview of Silk Fibroin Use in Wound Dressings, Trends Biotechnol. 36 (2018) 907–922, https://doi.org/10.1016/j.tibtech.2018.04.004.
[217] M. Farokhi, F. Mottaghitalab, R.L. Reis, S. Ramakrishna, S.C. Kundu, Functionalized silk fibroin nanofibers as drug carriers: Advantages and challenges, J. Control. Release 321 (2020) 324–347, https://doi.org/10.1016/j.jconrel.2020.02.022.
[218] M. Duan, J. Ma, S. Fang, Synthesis of hydrazine-grafted guar gum material for the highly effective removal of organic dyes, Carbohydr. Polym. 211 (2019) 308–314, https://doi.org/10.1016/j.carbpol.2019.01.112.
[219] J. Ma, S. Fang, P. Shi, M. Duan, Hydrazine-Functionalized guar-gum material capable of capturing heavy metal ions, Carbohydr. Polym. 223 (2019), 115137, https://doi.org/10.1016/j.carbpol.2019.115137.
[220] Y. Wen, Z. Xie, S. Xue, W. Li, H. Ye, W. Shi, et al., Functionalized polymethyl methacrylate-modified dialdehyde guar gum containing hydrazide groups for effective removal and enrichment of dyes, ion, and oil/water separation, J. Hazard. Mater. 426 (2022), 127799, https://doi.org/10.1016/j.jhazmat.2021.127799.
[221] S.A. Ganie, R.A. Naik, A. Ali, T.A. Mir, N. Mazumdar, Preparation, characterization, release and antianemic studies of guar gum functionalized Iron complexes, Int. J. Biol. Macromol. 183 (2021) 1495–1504, https://doi.org/10.1016/j.ijbiomac.2021.05.125.
[222] T.-P. Huynh, T.-A. Le, CHAPTER 2, Synthetic Chemistry for Molecular Imprinting (2018) 28–64, https://doi.org/10.1039/9781788010474-00028.
[223] A. Bossion, K.v. Heifferon, L. Meabe, N. Zivic, D. Taton, J.L. Hedrick, et al., Opportunities for organocatalysis in polymer synthesis via step-growth methods, Prog. Polym. Sci. 90 (2019) 164–210, https://doi.org/10.1016/j.progpolymsci.2018.11.003.
[224] G. Yilmaz, Y. Yagci, Light-induced step-growth polymerization, Prog. Polym. Sci. 100 (2020), 101178, https://doi.org/10.1016/j.progpolymsci.2019.101178.
[225] A. Anjum, M. Zuber, K.M. Zia, M.N. Anjum, W. Aftab, Preparation and characterization of guar gum based polyurethanes, Int. J. Biol. Macromol. 183 (2021) 2174–2183, https://doi.org/10.1016/j.ijbiomac.2021.06.025.
[226] J. Ma, J. Zhou, G. Liu, Z. Luo, K. Yan, H. Yao, et al., Synthesis and Properties of Waterborne Polyurethane Modified with Guar Gum Polysaccharide, ChemistrySelect 5 (2020) 2348–2353, https://doi.org/10.1002/slct.201904054.
[227] J. Gao, D. Zhu, W. Zhang, G.A. Solan, Y. Ma, W.-H. Sun, Recent progress in the application of group 1, 2 & 13 metal complexes as catalysts for the ring opening polymerization of cyclic esters, Inorg. Chem. Front. 6 (2019) 2619–2652, https://doi.org/10.1039/C9QI00855A.
[228] D.M. Lyubov, A.O. Tolpygin, A.A. Trifonov, Rare-earth metal complexes as catalysts for ring-opening polymerization of cyclic esters, Coord. Chem. Rev. 392 (2019) 83–145, https://doi.org/10.1016/j.ccr.2019.04.013.
[229] A. Rasines Mazo, S. Allison-Logan, F. Karimi, N.-J.-A. Chan, W. Qiu, W. Duan, et al., Ring opening polymerization of α-amino acids: advances in synthesis, architecture and applications of polypeptides and their hybrids, Chem. Soc. Rev. 49 (2020) 4737–4834, https://doi.org/10.1039/C9CS00738E.
[230] H. Li, R.M. Shakaroun, S.M. Guillaume, J. Carpentier, Recent Advances in Metal-Mediated Stereoselective Ring-Opening Polymerization of Functional Cyclic Esters towards Well-Defined Poly(hydroxy acid)s: From Stereoselectivity to Sequence-Control. Chemistry – A, Eur. J. 26 (2020) 128–138, https://doi.org/10.1002/chem.201904108.
[231] S.A. Kedzior, J.O. Zoppe, R.M. Berry, E.D. Cranston, Recent advances and an industrial perspective of cellulose nanocrystal functionalization through polymer grafting, Curr. Opin. Solid State Mater. Sci. 23 (2019) 74–91, https://doi.org/10.1016/j.cossms.2018.11.005.
[232] T. el Assimi, R. Blažic, A. el Kadib, M. Raihane, R. Beniazza, G.A. Luinstra, et al., Synthesis of poly(ε-caprolactone)-grafted guar gum by surface-initiated ring-opening polymerization, Carbohydr. Polym. 220 (2019) 95–102, https://doi.org/10.1016/j.carbpol.2019.05.049.
[233] T. el Assimi, M. Chaib, M. Raihane, A. el Meziane, M. Khouloud, R. Benhida, et al., Poly(ε-caprolactone)-g-Guar Gum and Poly(ε-caprolactone)-g-Halloysite Nanotubes as Coatings for Slow-Release DAP Fertilizer, J. Polym. Environ. 28 (2020) 2078–2090, https://doi.org/10.1007/s10924-020-01750-7.
[234] R. Kumar, R.K.r. Sharma, A.P. Singh, Grafted cellulose: a bio-based polymer for durable applications, Polym. Bull. 75 (2018) 2213–2242, https://doi.org/10.1007/s00289-017-2136-6.
[235] D. Kumar, S. Gihar, M.K. Shrivash, P. Kumar, P.P. Kundu, A review on the synthesis of graft copolymers of chitosan and their potential applications, Int. J. Biol. Macromol. 163 (2020) 2097–2112, https://doi.org/10.1016/j.ijbiomac.2020.09.060.
[236] T.J. Demars, M.K. Bera, S. Seifert, M.R. Antonio, R.J. Ellis, Revisiting the Solution Structure of Ceric Ammonium Nitrate, Angew. Chem. Int. Ed. 54 (2015) 7534–7538, https://doi.org/10.1002/anie.201502336.
[237] J. Lee, U. von Gunten, J.-H. Kim, Persulfate-Based Advanced Oxidation: Critical Assessment of Opportunities and Roadblocks, Environ. Sci. Tech. 54 (2020) 3064–3081, https://doi.org/10.1021/acs.est.9b07082.
[238] S. Wacławek, H.v. Lutze, K. Grübel, V.V.T. Padil, M. Černík, D. Dionysiou Dionysios, Chemistry of persulfates in water and wastewater treatment: A review, Chem. Eng. J. 330 (2017) 44–62, https://doi.org/10.1016/j.cej.2017.07.132.
[239] A.S. Sarac, Redox polymerization, Prog. Polym. Sci. 24 (1999) 1149–1204, https://doi.org/10.1016/S0079-6700(99)00026-X.
[240] C.G. Gutierrez, G. Cáceres Montenegro, R.J. Minari, J.R. Vega, L.M. Gugliotta, Scale Inhibitor and Dispersant Based on Poly(Acrylic Acid) Obtained by Redox-Initiated Polymerization, Macromol. React. Eng. 13 (2019) 1900007, https://doi.org/10.1002/mren.201900007.
[241] M. Bühl, T. Hutson, A. Missio, J.C. Walton, Sulfur and Phosphorus Oxyacid Radicals, J. Phys. Chem. A 126 (2022) 760–771, https://doi.org/10.1021/acs.jpca.1c10455.
[242] D. Zhou, L. Chen, J. Li, F. Wu, Transition metal catalyzed sulfite auto-oxidation systems for oxidative decontamination in waters: A state-of-the-art minireview, Chem. Eng. J. 346 (2018) 726–738, https://doi.org/10.1016/j.cej.2018.04.016.
[243] X.D. Feng, X.Q. Guo, K.Y. Qiu, Studies on the initiation mechanism of persulfate/aliphatic secondary amine system in vinyl polymerization, Polym. Bull. (1987) 18, https://doi.org/10.1007/BF00255817.
[244] X.-D. Feng, The role of amine in vinyl radical polymerization, Makromol. Chem. Macromol. Sympos. 63 (1992) 1–18, https://doi.org/10.1002/masy.19920630105.
[245] V. Nikolic, S. Velickovic, A. Popovic, Amine activators influence on grafting reaction between methacrylic acid and starch, Carbohydr. Polym. 88 (2012) 1407–1413, https://doi.org/10.1016/j.carbpol.2012.02.027.
[246] U.D.N. Bajpai, V. Mishra, S. Rai, Grafting of poly(acrylonitrile) onto guar gum using potassium persulfate/ascorbic acid redox initiating system, J. Appl. Polym. Sci. 47 (1993) 717–722, https://doi.org/10.1002/app.1993.070470415.
[247] Y.-J. Tu, D. Njus, H.B. Schlegel, A theoretical study of ascorbic acid oxidation and HOO/O_2^- radical scavenging, Org. Biomol. Chem. 15 (2017) 4417–4431, https://doi.org/10.1039/C7OB00791D.
[248] X. Hou, G. Zhan, X. Huang, N. Wang, Z. Ai, L. Zhang, Persulfate activation induced by ascorbic acid for efficient organic pollutants oxidation, Chem. Eng. J. 382 (2020), 122355, https://doi.org/10.1016/j.cej.2019.122355.
[249] J.C. Arthur, P.J. Baugh, O. Hinojosa, ESR study of reactions of cellulose initiated by the ceric ion method, J. Appl. Polym. Sci. 10 (1966) 1591–1606, https://doi.org/10.1002/app.1966.070101015.
[250] M.S. Bains, Inorganic redox systems in graft polymerization onto cellulosic materials, J. Polym. Sci., Part C: Polym. Symp. 37 (2007) 125–151, https://doi.org/10.1002/polc.5070370108.
[251] S. Iftekhar, V. Srivastava, A. Casas, M. Sillanpää, Synthesis of novel GA-g-PAM/SiO_2 nanocomposite for the recovery of rare earth elements (REE) ions from aqueous solution, J. Clean. Prod. 170 (2018) 251–259, https://doi.org/10.1016/j.jclepro.2017.09.166.
[252] M. Kumar, P.S. Gehlot, D. Parihar, P.K. Surolia, G. Prasad, Promising grafting strategies on cellulosic backbone through radical polymerization processes – A review, Eur. Polym. J. 152 (2021), 110448, https://doi.org/10.1016/j.eurpolymj.2021.110448.
[253] S.S. Halacheva, D.J. Adlam, E.K. Hendow, T.J. Freemont, J. Hoyland, B. R. Saunders, Injectable Biocompatible and Biodegradable pH-Responsive Hollow Particle Gels Containing Poly(acrylic acid): The Effect of Copolymer Composition on Gel Properties, Biomacromolecules 15 (2014) 1814–1827, https://doi.org/10.1021/bm5002069.
[254] S. Bazban-Shotorbani, M.M. Hasani-Sadrabadi, A. Karkhaneh, V. Serpooshan, K. I. Jacob, A. Moshaverinia, et al., Revisiting structure-property relationship of pH-responsive polymers for drug delivery applications, J. Control. Release 253 (2017) 46–63, https://doi.org/10.1016/j.jconrel.2017.02.021.
[255] G. Sennakesavan, M. Mostakhdemin, L.K. Dkhar, A. Seyfoddin, S.J. Fatihhi, Acrylic acid/acrylamide based hydrogels and its properties - A review, Polym. Degrad. Stab. 180 (2020), 109308, https://doi.org/10.1016/j.polymdegradstab.2020.109308.
[256] S. Sharma, S. Afgan, K.A. Deepak, R. Kumar, l-Alanine induced thermally stable self-healing guar gum hydrogel as potential drug vehicle for sustained release of hydrophilic drug, Mater. Sci. Eng. C 99 (2019) 1384–1391, https://doi.org/10.1016/j.msec.2019.02.074.
[257] M. Dinari, M.A. Shirani, M.H. Maleki, R. Tabatabaeian, Green cross-linked bionanocomposite of magnetic layered double hydroxide/guar gum polymer as an efficient adsorbent of Cr(VI) from aqueous solution, Carbohydr. Polym. 236 (2020), 116070, https://doi.org/10.1016/j.carbpol.2020.116070.
[258] H.S. Samanta, S.K. Ray, Synthesis of interpenetrating network (IPN) hydrogels based on acrylic acid (AAc) and guar gum and its application as drug delivery for pyridoxine hydrochloride (vitamin B6), J. Polym. Res. 28 (2021) 479, https://doi.org/10.1007/s10965-021-02848-9.
[259] A. HaqAsif, R.R. Karnakar, N. Sreeharsha, V. Gite, N. Borane, B.E. Al-Dhubiab, et al., pH and Salt Responsive Hydrogel based on Guar Gum as a Renewable Material for Delivery of Curcumin: A Natural Anti-Cancer Drug, J. Polym. Environ. 29 (2021) 1978–1989, https://doi.org/10.1007/s10924-020-01934-1.
[260] J. Singh, A.S. Dhaliwal, Effective Removal of Methylene Blue Dye Using Silver Nanoparticles Containing Grafted Polymer of Guar Gum/Acrylic Acid as Novel Adsorbent, J. Polym. Environ. 29 (2021) 71–88, https://doi.org/10.1007/s10924-020-01859-9.
[261] X. Li, X. Wang, T. Han, C. Hao, S. Han, X. Fan, Synthesis of sodium lignosulfonate-guar gum composite hydrogel for the removal of Cu2+ and Co2+, Int. J. Biol. Macromol. 175 (2021) 459–472, https://doi.org/10.1016/j.ijbiomac.2021.02.018.
[262] R.R. Pal, D. Kumar, V. Raj, V. Rajpal, P. Maurya, S. Singh, et al., Synthesis of pH-sensitive crosslinked guar gum-g-poly(acrylic acid-co-acrylonitrile) for the delivery of thymoquinone against inflammation, Int. J. Biol. Macromol. 182 (2021) 1218–1228, https://doi.org/10.1016/j.ijbiomac.2021.05.072.
[263] R.R. Karnakar, V. Gite, v., Eco-friendly slow release of $ZnSO_4$ as a micronutrient from poly (acrylic acid: acrylamide) and guar gum based crosslinked

biodegradable hydrogels, Polymer-Plastics Technology and Materials 61 (2022) 691–708.
[264] S. Gihar, D. Kumar, P. Kumar, Facile synthesis of novel pH-sensitive grafted guar gum for effective removal of mercury (II) ions from aqueous solution, Carbohyd. Polym. Technol. Appl. 2 (2021), 100110, https://doi.org/10.1016/j.carpta.2021.100110.
[265] M. Mitra, M. Mahapatra, A. Dutta, M. Deb, S. Dutta, P.K. Chattopadhyay, et al., Fluorescent Guar Gum- *g* -Terpolymer via In Situ Acrylamido-Acid Fluorophore-Monomer in Cell Imaging, Pb(II) Sensor, and Security Ink, ACS Appl. Bio Mater. 3 (2020) 1995–2006, https://doi.org/10.1021/acsabm.9b01146.
[266] S. Awasthi, J.K. Gaur, M.S. Bobji, C. Srivastava, Nanoparticle-reinforced polyacrylamide hydrogel composites for clinical applications: a review, J. Mater. Sci. 57 (2022) 8041–8063, https://doi.org/10.1007/s10853-022-07146-3.
[267] J.K. Koh, C.W. Lai, M.R. Johan, S.S. Gan, W.W. Chua, Recent advances of modified polyacrylamide in drilling technology, J. Pet. Sci. Eng. 215 (2022), 110566, https://doi.org/10.1016/j.petrol.2022.110566.
[268] B. Xiong, R.D. Loss, D. Shields, T. Pawlik, R. Hochreiter, A.L. Zydney, et al., Polyacrylamide degradation and its implications in environmental systems, Npj Clean Water 1 (2018) 17, https://doi.org/10.1038/s41545-018-0016-8.
[269] A. Sand, A. Vyas, Superabsorbent polymer based on guar gum-graft-acrylamide: synthesis and characterization, J. Polym. Res. 27 (2020) 43, https://doi.org/10.1007/s10965-019-1951-x.
[270] A. Mahto, S. Mishra, The removal of textile industrial Dye-RB-19 using Guar gum-based adsorbent with thermodynamic and kinetic evaluation parameters, Polym. Bull. 79 (2022) 3353–3378, https://doi.org/10.1007/s00289-021-03663-4.
[271] E. ShimaaM, E.G. Zaki, W.A.E. Omar, A. Ashraf Soliman, A.M. Attia, Guar Gum-Based Hydrogels as Potent Green Polymers for Enhanced Oil Recovery in High-Salinity Reservoirs. ACS, Omega 6 (2021) 23421–23431, https://doi.org/10.1021/acsomega.1c03352.
[272] R.R. Palem, G. Shimoga, T.J. Kang, S.-H. Lee, Fabrication of multifunctional Guar gum-silver nanocomposite hydrogels for biomedical and environmental applications, Int. J. Biol. Macromol. 159 (2020) 474–486, https://doi.org/10.1016/j.ijbiomac.2020.05.041.
[273] S. Das, U. Subuddhi, Guar gum–poly(N-isopropylacrylamide) smart hydrogels for sustained delivery of 5-fluorouracil, Polym. Bull. 76 (2019) 2945–2963, https://doi.org/10.1007/s00289-018-2526-4.
[274] R.R. Palem, K. Madhusudana Rao, T.J. Kang, Self-healable and dual-functional guar gum-grafted-polyacrylamidoglycolic acid-based hydrogels with nano-silver for wound dressings, Carbohydr. Polym. 223 (2019), 115074, https://doi.org/10.1016/j.carbpol.2019.115074.
[275] R.R. Palem, G. Shimoga, K.S.V.K. Rao, S.-H. Lee, T.J. Kang, Guar gum graft polymer-based silver nanocomposite hydrogels: synthesis, characterization and its biomedical applications, J. Polym. Res. 27 (2020) 68, https://doi.org/10.1007/s10965-020-2026-8.
[276] A. Singh, M. Liu, E. Ituen, Y. Lin, Anti-Corrosive Properties of an Effective Guar Gum Grafted 2-Acrylamido-2-Methylpropanesulfonic Acid (GG-AMPS) Coating on Copper in a 3.5% NaCl Solution, Coatings (2020;10:241.), https://doi.org/10.3390/coatings10030241.
[277] A. Singh, K.R. Ansari, M.A. Quraishi, S. Kaya, S. Erkan, Chemically modified guar gum and ethyl acrylate composite as a new corrosion inhibitor for reduction in hydrogen evolution and tubular steel corrosion protection in acidic environment, Int. J. Hydrogen Energy 46 (2021) 9452–9465, https://doi.org/10.1016/j.ijhydene.2020.12.103.
[278] A. Mahto, S. Mishra, Design, development and validation of guar gum based pH sensitive drug delivery carrier via graft copolymerization reaction using microwave irradiations, Int. J. Biol. Macromol. 138 (2019) 278–291, https://doi.org/10.1016/j.ijbiomac.2019.07.063.
[279] B. Marco-Dufort, M.W. Tibbitt, Design of moldable hydrogels for biomedical applications using dynamic covalent boronic esters, Mater. Today Chem. 12 (2019) 16–33, https://doi.org/10.1016/j.mtchem.2018.12.001.
[280] J.A.L. da Silva, Borate esters of polyols: Occurrence, applications and implications, Inorg. Chim. Acta 520 (2021), 120307, https://doi.org/10.1016/j.ica.2021.120307.
[281] M. Maseda, Y. Miyazaki, T. Takamuku, Thermodynamics for complex formation of boric acid and borate with hydroxy acids and diols, J. Mol. Liq. 341 (2021), 117343, https://doi.org/10.1016/j.molliq.2021.117343.
[282] U.B. Demirci, O. Akdim, J. Andrieux, J. Hannauer, R. Chamoun, P. Miele, Sodium Borohydride Hydrolysis as Hydrogen Generator: Issues, State of the Art and Applicability Upstream from a Fuel Cell, Fuel Cells 10 (2010) 335–350, https://doi.org/10.1002/fuce.200800171.
[283] H.N. Abdelhamid, A review on hydrogen generation from the hydrolysis of sodium borohydride, Int. J. Hydrogen Energy 46 (2021) 726–765, https://doi.org/10.1016/j.ijhydene.2020.09.186.
[284] L. Dai, B. Nadeau, X. An, D. Cheng, Z. Long, Y. Ni, Silver nanoparticles-containing dual-function hydrogels based on a guar gum-sodium borohydride system, Sci. Rep. 6 (2016) 36497, https://doi.org/10.1038/srep36497.
[285] H. Wei, H. Gao, X. Wang, Development of novel guar gum hydrogel based media for abrasive flow machining: Shear-thickening behavior and finishing performance, Int. J. Mech. Sci. 157–158 (2019) 758–772, https://doi.org/10.1016/j.ijmecsci.2019.05.022.
[286] Y. Cheng, K. Pang, X. Xu, P. Yuan, Z. Zhang, X. Wu, et al., Borate crosslinking synthesis of structure tailored carbon-based bifunctional electrocatalysts directly from guar gum hydrogels for efficient overall water splitting, Carbon N Y 157 (2020) 153–163, https://doi.org/10.1016/j.carbon.2019.10.024.
[287] J. Liu, S. Wang, C. Wang, F. Zhao, S. Lei, H. Yi, et al., Influence of nanomaterial morphology of guar-gum fracturing fluid, physical and mechanical properties, Carbohydr. Polym. 234 (2020), 115915, https://doi.org/10.1016/j.carbpol.2020.115915.
[288] R. Pugliese, F. Gelain, Characterization of elastic, thermo-responsive, self-healable supramolecular hydrogel made of self-assembly peptides and guar gum, Mater. Des. 186 (2020), 108370, https://doi.org/10.1016/j.matdes.2019.108370.
[289] D. Cao, Y. Lv, Q. Zhou, Y. Chen, X. Qian, Guar gum/gellan gum interpenetrating-network self-healing hydrogels for human motion detection, Eur. Polym. J. 151 (2021), 110371, https://doi.org/10.1016/j.eurpolymj.2021.110371.
[290] R.S. Dassanayake, E. Rajakaruna, N. Abidi, Borax-Cross-Linked Guar Gum-Manganese Dioxide Composites for Oxidative Decolorization of Methylene Blue, J. Nanomater. 2019 (2019) 1–11, https://doi.org/10.1155/2019/7232715.
[291] B. Wang, L. Dai, G. Yang, G. Bendrich, Y. Ni, G. Fang, A highly efficient thermo responsive palladium nanoparticles incorporated guar gum hydrogel for effective catalytic reactions, Carbohydr. Polym. 226 (2019), 115289, https://doi.org/10.1016/j.carbpol.2019.115289.
[292] C. Talodthaisong, W. Boonta, S. Thammawithan, R. Patramanon, N. Kamonsutthipaijit, J.A. Hutchison, et al., Composite guar gum-silver nanoparticle hydrogels as self-healing, injectable, and antibacterial biomaterials, Mater. Today Commun. 24 (2020), 100992, https://doi.org/10.1016/j.mtcomm.2020.100992.
[293] R. Deka, S. Sarma, P. Patar, P. Gogoi, J.K. Sarmah, Highly stable silver nanoparticles containing guar gum modified dual network hydrogel for catalytic and biomedical applications, Carbohydr. Polym. 248 (2020), 116786, https://doi.org/10.1016/j.carbpol.2020.116786.
[294] A. Indurkar, P. Bangde, M. Gore, A.K. Agrawal, R. Jain, P. Dandekar, Fabrication of guar gum-gelatin scaffold for soft tissue engineering, Carbohyd. Polym. Technol. Appl. 1 (2020), 100006, https://doi.org/10.1016/j.carpta.2020.100006.
[295] J. Bag, S. Mukherjee, S.K. Ghosh, A. Das, A. Mukherjee, J.K. Sahoo, et al., Fe_3O_4 coated guargum nanoparticles as non-genotoxic materials for biological application, Int. J. Biol. Macromol. 165 (2020) 333–345, https://doi.org/10.1016/j.ijbiomac.2020.09.144.
[296] Z. Rao, S. Liu, R. Wu, G. Wang, Z. Sun, L. Bai, et al., Fabrication of dual network self-healing alginate/guar gum hydrogels based on polydopamine-type microcapsules from mesoporous silica nanoparticles, Int. J. Biol. Macromol. 129 (2019) 916–926, https://doi.org/10.1016/j.ijbiomac.2019.02.089.
[297] V.K. Gupta, S. Agarwal, R. Ahmad, A. Mirza, J. Mittal, Sequestration of toxic congo red dye from aqueous solution using ecofriendly guar gum/ activated carbon nanocomposite, Int. J. Biol. Macromol. 158 (2020) 1310–1318, https://doi.org/10.1016/j.ijbiomac.2020.05.025.
[298] A. Butt, S. Jabeen, N. Nisar, A. Islam, N. Gull, S.S. Iqbal, et al., Controlled release of cephradine by biopolymers based target specific crosslinked hydrogels, Int. J. Biol. Macromol. 121 (2019) 104–112, https://doi.org/10.1016/j.ijbiomac.2018.10.018.
[299] M.U.A. Khan, M.A. Raza, S.I.A. Razak, M.R. Abdul Kadir, A. Haider, S.A. Shah, et al., Novel functional antimicrobial and biocompatible arabinoxylan/guar gum hydrogel for skin wound dressing applications, J. Tissue Eng. Regen. Med. 14 (2020) 1488–1501, https://doi.org/10.1002/term.3115.
[300] M.U.A. Khan, I. Iqbal, M.N.M. Ansari, S.I.A. Razak, M.A. Raza, A. Sajjad, et al., Development of Antibacterial, Degradable and pH-Responsive Chitosan/Guar Gum/Polyvinyl Alcohol Blended Hydrogels for Wound Dressing, Molecules 26 (2021) 5937, https://doi.org/10.3390/molecules26195937.
[301] A. Aydogdu, C.J. Radke, S. Bezci, E. Kirtil, Characterization of curcumin incorporated guar gum/orange oil antimicrobial emulsion films, Int. J. Biol. Macromol. 148 (2020) 110–120, https://doi.org/10.1016/j.ijbiomac.2019.12.255.